

**LITHOLOGY,
MICROSTRUCTURES,
FLUID INCLUSIONS, AND
GEOCHEMISTRY OF ROCK SALT
AND OF THE CAP-ROCK CONTACT
IN OAKWOOD DOME, EAST TEXAS:
SIGNIFICANCE FOR NUCLEAR WASTE STORAGE**

Owen R. Dix and
M. P. A. Jackson



1982



Bureau of Economic Geology
The University of Texas at Austin
Austin, Texas 78712

W. L. Fisher, Director

Report of Investigations No. 120

Project funded by
U. S. Department of Energy
under Contract No. DE-AC97-80ET-46617
(formerly Contract No. DE-AC97-79ET-46605)

**LITHOLOGY,
MICROSTRUCTURES,
FLUID INCLUSIONS, AND
GEOCHEMISTRY OF ROCK SALT
AND OF THE CAP-ROCK CONTACT
IN OAKWOOD DOME, EAST TEXAS:
SIGNIFICANCE FOR NUCLEAR WASTE STORAGE**

Owen R. Dix and
M. P. A. Jackson



1982



Bureau of Economic Geology
The University of Texas at Austin
Austin, Texas 78712

W. L. Fisher, Director

Cover photograph: Brine inclusions in recrystallized rock salt of Oakwood Dome.

CONTENTS

	Page
ABSTRACT	1
INTRODUCTION	1
GEOLOGY OF OAKWOOD DOME	4
LITHOLOGY AND MICROSTRUCTURES	5
Foliated rock salt (R-1 zone)	5
Unfoliated rock salt	11
Medium-grained R-2 zone	11
Coarse-grained R-3 zone	13
Contact between rock salt and cap rock	14
Lamination in the contact zone	20
FLUID INCLUSIONS	26
Brine inclusions	26
Origin of brine inclusions	28
Compressed-gas inclusions	31
Pressures and temperatures during halite recrystallization	31
GEOCHEMISTRY	33
ORIGIN OF ANHYDRITE CAP ROCK	35
SUMMARY	38
SIGNIFICANCE FOR STORAGE OF NUCLEAR WASTES	38
ACKNOWLEDGMENTS	40
REFERENCES	40
APPENDIX: Oakwood Salt-Core Log	43

Figures

1. Map showing the East Texas Basin and location of Oakwood Dome	2
2. Northwest-southeast cross section of Oakwood Dome	3
3. Profile of the TOG-1 rock-salt core showing the three zones	4
4. Mesoscopic open folding of disseminated-anhydrite layer in foliated rock salt	5
5. Dismembered and contorted anhydrite-rich layers in pale, medium-grained rock salt	6
6. Mesoscopic structure in the interval containing anhydrite-rich layers	6
7. Coarse-to-medium grained rock salt containing dark, medium-grained disseminated-anhydrite layer	7
8. Halite grain boundaries in the R-1 and R-2 zones	8
9. Intercrystalline network of liquid along halite grain boundaries in foliated rock salt	9
10. Anhydrite crystal showing pitted and unpitted areas	9
11. Irregular network of unpitted areas on an anhydrite crystal	10
12. Preferred orientation in anhydrite-rich layer on the limb of a microfold	10
13. Contact between the foliated R-1 zone and the unfoliated R-2 zone	11
14. Millimeter-scale transposition of a disseminated-anhydrite layer in the medium-grained unfoliated R-2 zone	11
15. Schematic diagram showing inferred anhydrite and halite microstructure in a disseminated-anhydrite layer during successive stages of transposition	12
16. Abrupt contact between medium-grained unfoliated rock salt from the R-2 zone and coarse-grained unfoliated rock salt from the R-3 zone	13
17. Possible evolution of the R-2 and R-3 zones of unfoliated rock salt	15
18. Abrupt contact between cap rock and rock salt of the R-3 zone	16
19. Schematic diagram of the rock-salt - cap-rock contact zone, showing the transition zones	17
20. Anhydrite grains surrounded by halite in the transition zones	18
21. Base of the cap rock consisting of equant anhydrite grains	19
22. Percentage of idioblastic anhydrite, mean anhydrite grain size, and anhydrite axial ratios across the rock-salt - cap-rock contact	19
23. Contact between rock salt and cap rock	20
24. Explanatory diagram of specimen in figure 23	21

25. Block diagram of the drip hypothesis, illustrating formation of splash crater and accretion of anhydrite.....	22
26. Two different thicknesses of layers at the base of the anhydrite cap.....	23
27. Solution cleavage cutting across contorted laminae in the base of the anhydrite cap rock.....	24
28. Undulating upper contact of a rock-salt layer enclosed in anhydrite cap rock.....	25
29. Brine inclusions within a halite grain of recrystallized R-3 rock salt.....	26
30. Irregular brine inclusion in halite grain from the R-3 zone.....	27
31. Graph showing the concentration of cuboid brine inclusions in R-3 rock salt.....	28
32. Irregular film of liquid on an anhydrite crystal enclosed in halite.....	30
33. Elongate fillet of brine between two anhydrite crystals in halite.....	30
34. Anhydrite grain containing a bubble-bearing fluid inclusion.....	31
35. Bubbles of decompressed gas released from anhydrite-halite grain boundaries during experimental dissolution of halite in water.....	32
36. Compressed-gas inclusions in rock salt isolated within the anhydrite cap rock.....	32
37. Laminae in lowermost cap rock from Oakwood and Hockley Domes.....	36

Tables

1. Grain-size data for laminae at the base of the anhydrite cap rock.....	23
2. Fluid-inclusion data and anhydrite percentage for R-3 rock salt.....	29
3. Anhydrite contents of rock salt and bromine contents of halite.....	34
4. Sequence of events in rock salt and base of cap rock.....	37
5. Processes detrimental to nuclear-waste storage.....	39
6. Processes favorable for nuclear-waste storage.....	39

ABSTRACT

Oakwood salt dome in Leon and Freestone Counties, Texas, has a core composed of a diapiric salt stock at a depth of 355 m. A vertical borehole in the center of the salt stock yielded 57.3 m of continuous rock-salt core overlain by 137 m of anhydrite-calcite cap rock. The lower 55.3 m of rock salt exhibits a strong, penetrative schistosity and parallel cleavage dipping at 30° to 40° and more than 60 variably dipping layers of disseminated anhydrite. Anhydrite constitutes 1.3 ± 0.7 percent of the rock-salt core. The upper 2 m of rock salt is unfoliated, comprising a lower 1.4-m interval of medium-grained granoblastic rock salt and an upper 0.6-m interval of coarse-grained granoblastic rock salt. An abrupt, cavity-free contact separates rock salt from laminated cap rock consisting of granoblastic-polygonal anhydrite virtually devoid of halite or pore space.

Microstructures and concentration gradients of fluid inclusions suggest that the unfoliated rock salt at the crest of the salt stock was once strongly foliated, but that this fabric was destroyed by

solid-state recrystallization. Downward movement of brine from the rock-salt - cap-rock contact was apparently accompanied by two recrystallization fronts. Dissolution of halite at the contact released disseminated anhydrite that presumably accumulated as sand on the floor of the dissolution cavity. Renewed rise of the salt stock closed the cavity, and the anhydrite sand was accreted against the base of the cap rock. Much, if not all, of the lamination in the 80 m of anhydrite cap rock may result from cycles of dissolution, recrystallization, and upward movement in the salt stock, followed by accretion of anhydrite residuum as laminae against the base of the cap rock.

These processes, which are strongly influenced by fluids, act both to breach waste repositories and to geologically isolate them. Despite repeated attrition and uplift of the salt stock, the geologic system has the ability to offset, at least partially, these negative processes by self-sealing and recovery.

INTRODUCTION

Oakwood salt dome is located on the Freestone/Leon county line in the East Texas Basin (fig. 1). Oakwood is one of several salt domes in East Texas that have been studied since 1977 by Bureau of Economic Geology researchers to evaluate the suitability of using these and other domes for storing high-level nuclear wastes (Kreitler and others, 1978).

Salt deposits of the Gulf Coast are of Jurassic age and constitute two discrete units: the offshore Challenger Formation and the largely onshore Louann Formation. The latter unit is located within the Gulf Coast Basin and the South Texas, East Texas, North Louisiana, and Mississippi interior salt basins (Martin, 1978, 1980).

More than 400 salt domes have been identified in the Gulf Coast region (Halbouty, 1979, p. 5). Oakwood Dome is one of more than 20 diapirs in the East Texas Basin (fig. 1). The East Texas Basin is a structural and depositional depression bounded by the Angelina Flexure, the Mexia-Talco Fault Zone, and the Sabine Arch. Louann Salt within this basin lies at depths of 3,000 m to 6,000 m and is overlain by a succession of clastic and carbonate strata. The Jurassic evaporites have undergone considerable internal deformation during the formation of a variety of salt structures, which range in shape from low-amplitude salt pillows to conical mounds and vertical

cylindrical stocks. A pipelike salt body is referred to as a "salt stock," whereas the envelope of uplifted strata and the central stock constitute a salt dome (Kupfer, 1970). If the adjacent strata are absent over the crest of the salt stock, the stock has pierced its overburden and is termed a "diapir." Interior domes of the East Texas Basin underwent maximum uplift during the Early Cretaceous, followed by a gradual reduction in growth rates to the present (Seni and Kreitler, 1981).

Despite more than 100 years of interest in salt domes of the Gulf Coastal region, remarkably little literature has appeared on lithology and structure of diapiric rock salt. This inadequacy was noted nearly 50 years ago by Hanna (1934). The problem is economic: oil is present in cap rock and within sediments above and adjacent to the salt domes. In contrast, the only resource in the salt stock itself is rock salt, so there is little incentive for petroleum companies to drill farther than a few meters below the cap rock. Furthermore, on domes mined for sulfur, drilling of rock salt would have been disastrous because the hot, high-pressure water used to extract sulfur would rapidly dissolve halite and cause collapse of the sulfurous cap rock.

Many early papers described the lithology of the cap rock, but not the rock salt or the most critical zone—the rock-salt - cap-rock contact. Detailed petrographic studies of cap rock were

undertaken by Brown (1931) and Goldman (1933, 1952). Balk (1949, 1953), Muehlberger (1959), and Kupfer (1963) provided comprehensive information on the microstructure of rock salt.

This study of rock salt from Oakwood Dome was designed:

(1) To determine the nature of the contact between rock salt and cap rock with respect to structural stability and hydrologic integrity of the stock, and to determine the origin of the cap rock.

(2) To determine the stratigraphy and microstructure of the diapiric crest by means of petrographic studies, geochemical analyses, and fluid-inclusion studies.

(3) To determine the macrostructure of the diapiric crest by means of geometric analysis.

(4) To determine the variations in shortening of the rock salt by means of strain analysis and to assess the implications for structural stability of the salt stock.

The latter two aspects (3 and 4) of the study will be dealt with in a forthcoming Bureau publication.

A vertical borehole (TOG-1) was drilled into rock salt near the axis of the dome (fig. 2). A continuous core 10 cm in diameter intersected cap rock at a depth of 217.3 m and rock salt at 354.5 m. The hole ended at a depth of 411.8 m, yielding 57.3 m of rock-salt core. A detailed log of the rock salt (Appendix) provides petrographic details, locations referred to in the text, and localities of specimens used for thin sections, thick sections, geochemical analysis, strain analysis, and magnetic-anisotropy analysis.

This study demonstrates that:

(1) The upper 2 m of rock salt has recrystallized in the presence of brines, probably during dissolution of the diapiric crest.

(2) Anhydrite in the cap rock was concentrated partly or entirely by accretion of layers against the base of the cap rock.

(3) Where intersected by the borehole, Oakwood Dome appears at present to be structurally and hydrologically stable.

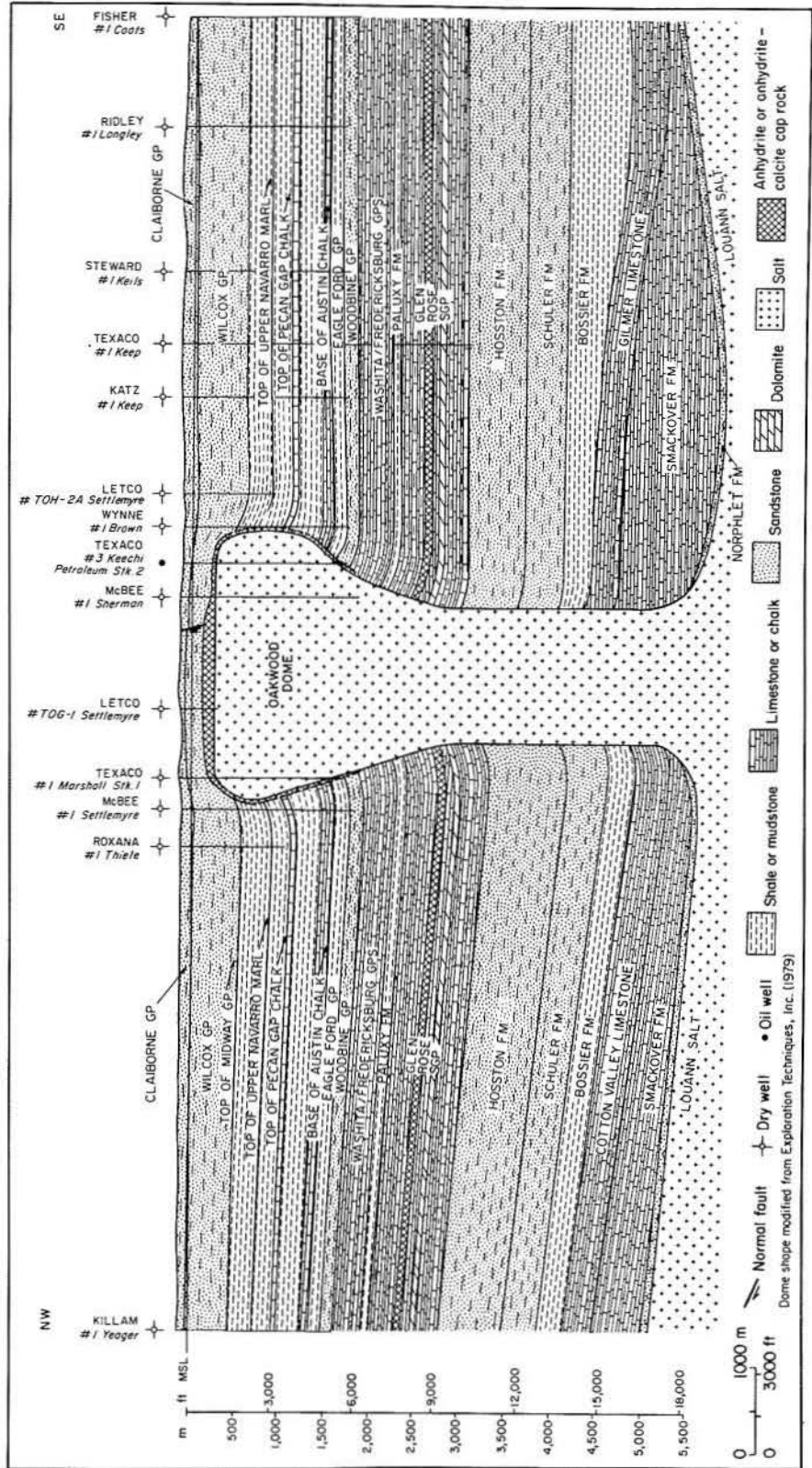


Figure 2. Northwest-southeast cross section of Oakwood Dome based on seismic and well data (from Giles and Wood, in preparation). Location of LETCO TOG-1 well is shown.

GEOLOGY OF OAKWOOD DOME

The salt stock in the center of Oakwood Dome extends from a depth of 355 m (measured from borehole log) to approximately 5,880 m (measured from depth-converted seismic section). The piercing stock is pear shaped in plan view and has maximum lateral dimensions of 4.6 by 3.7 km; maximum cross-sectional area is 13 km². A planar horizontal crest passes downward into a broad symmetrical overhang at an elevation of -600 m, below which the sides of the stock are vertical (fig. 2). The salt stock has a vertical axis and overall monoclinic structural symmetry; its crest is overlain by approximately 10 to 200 m of cap rock.

Diapiric salt has pierced the entire post-Louann Jurassic, Cretaceous, and lower Tertiary stratigraphic section up to the Wilcox Group. The salt stock is overlain by a deformed envelope of lower Tertiary clastic strata comprising the Wilcox and Claiborne Groups. Domal structure of the surrounding strata varies with depth and includes homoclines, monoclines, and synclines at different levels.

Interpretation of seismic sections suggests that Oakwood Dome began growing as a low-amplitude salt pillow by the end of Smackover time about 150 Ma ago (Giles and Wood, in preparation). Salt pierced diapirically during the major Schuler-Hosston clastic influx originating about 140 Ma ago. Subsidence rates ("sedimentary downbuilding" of Barton, 1933) around the Oakwood stock declined from a peak of 0.07 mm/yr in the Early Cretaceous to 0.03 mm/yr about 50 Ma ago in the Eocene (Seni and Jackson, in preparation). Subsidence rates provide a measure of the rate of relative salt uplift.

Cap rock intersected by borehole TOG-1 is 137.2 m thick and comprises:

- (1) an upper 57.6-m-thick zone consisting predominantly of calcium carbonate;
- (2) a 1.8-m-thick transition zone consisting of calcium carbonate and anhydrite; and
- (3) a lower 77.8-m-thick zone of predominantly anhydrite cap rock (Dutton and Kreitler, 1981).

The borehole intersects rock salt at 354.5 m and ends at a depth of 411.8 m (fig. 3). This 57.3-m section of core comprises two distinct zones. A lower 55.3-m interval of rock salt contains strong, moderately dipping, penetrative schistosity and numerous moderately to steeply dipping layers of disseminated anhydrite (Appendix). An upper 2.0-m interval of unfoliated rock salt directly beneath the cap rock comprises a lower 1.4-m interval of medium-grained granoblastic rock salt and an upper 0.6-m interval of coarse-grained granoblastic rock salt (fig. 3). The contact between rock salt and the overlying anhydrite cap rock is abrupt.

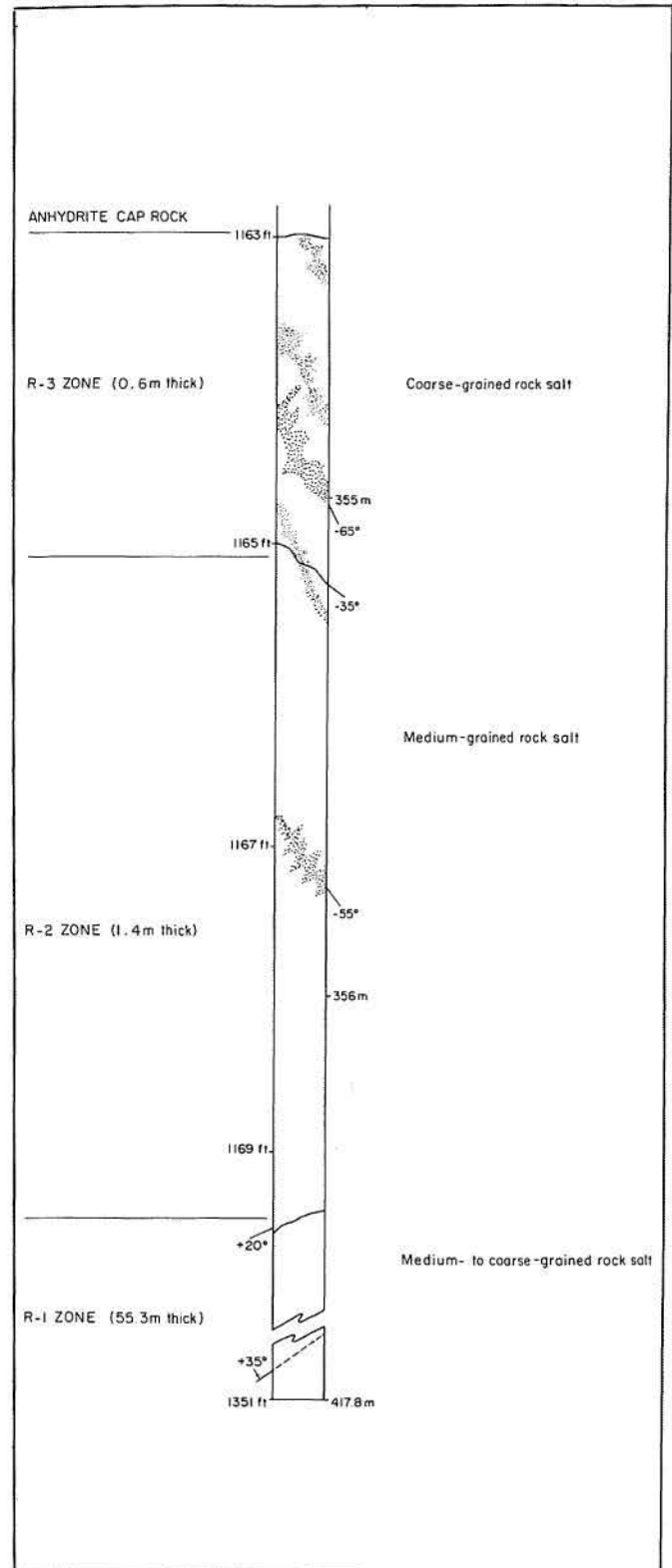


Figure 3. Profile of the TOG-1 rock-salt core showing the three zones (R-1, R-2, and R-3), the dip of the foliation in the R-1 zone (dashed line), and the disseminated-anhydrite layers (stippled). Horizontal and vertical scales are equal.

LITHOLOGY AND MICROSTRUCTURES

Because of the highly translucent nature of the rock salt, the core was studied by both transmitted and reflected light. Either thick sections or thin sections were prepared, depending on the translucence of the samples and the size of the structures in the core. Thick sections range from 1 to 10 mm thick, whereas thin sections are less than 1 mm thick. The thick sections, mounted on Plexiglas, are 15 to 30 cm long and 10 cm wide, the same as the diameter of the core. The thick sections were more rewarding for study than the smaller thin sections because of the coarse-grained texture and transparency of the halite and the wide dissemination of inclusions.

Dip angles measured from the core axis represent true dip because the hole is vertical to within 2° throughout its depth. The core is not oriented with respect to azimuth, but because the dip of the foliation is uniform, it is probable that the dip direction is also fairly uniform. For this reason, the core log (Appendix) portrays the foliation dipping toward the left, and provides a useful reference direction for other structural elements. The foliation was arbitrarily assigned positive dip angles; layering that has a dip azimuth of more than 90° from the foliation dip azimuth was assigned negative angles of dip.

Foliated Rock Salt (R-1 Zone)

The lower 55.3 m of rock salt making up the R-1 zone contains a strong penetrative schistosity defined by preferred orientation of disclike halite crystals having a mean axial ratio of 1.4:1.0:0.5 (Jackson, in preparation). This zone contains more than 60 layers of disseminated anhydrite ranging from 2 to 50 cm thick (fig. 4 and Appendix). Mean anhydrite content of the entire rock-salt core is calculated to be less than 2 percent (see section entitled "Geochemistry"). Disseminated-anhydrite layers alternate with zones of pure rock salt 5 to 600 cm thick. Pure rock salt is translucent and consists of medium- to coarse-grained halite and less than 0.5 percent anhydrite.

Disseminated-anhydrite layers appear gray in reflected light. In transmitted light they commonly consist of a dark-gray center bounded by pale-gray margins. These tonal variations reflect changes in the anhydrite content, ranging from 5 to 15 percent in the dark-gray zones to 2 to 5 percent in the pale-gray zones. Darkening of rock salt containing anhydrite results from increased absorption of light as the result of internal

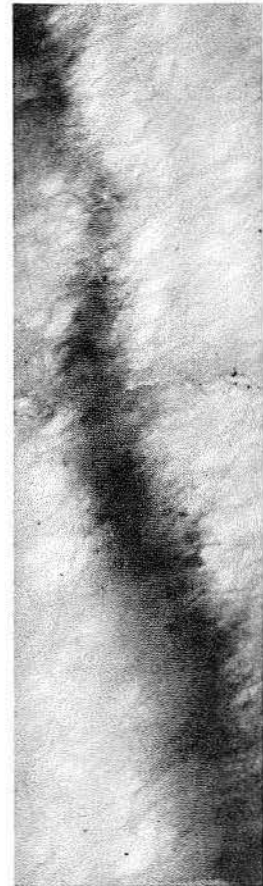


Figure 4. Mesoscopic open folding of disseminated-anhydrite layer in foliated rock salt (5 to 10 percent anhydrite). Darkness of layer is due to internal reflection. 10-cm-wide unslabbed core, transmitted light, depth 362.6 m.

reflection; the anhydrite itself is colorless (compare Balk, 1949; Kupfer, 1963). Layers are generally planar within the width of the core, although mesoscopic folds (fig. 4) and irregular, diffuse forms are also present. Anhydrite content of the layers ranges from less than 2 percent to about 15 percent. A single 90-cm-thick zone consisting of more than 50 percent anhydrite contains opaque anhydrite layers 1 to 5 cm thick that have undergone microfolding, refolding, and boudinage (figs. 5 and 6). These anhydrite layers contain black laminae 1 mm thick that are enriched in organic carbon; anhydrite within these black laminae has 0.08 percent total organic carbon (TOC), as compared with 0.05 percent TOC in the pure anhydrite and rock salt.

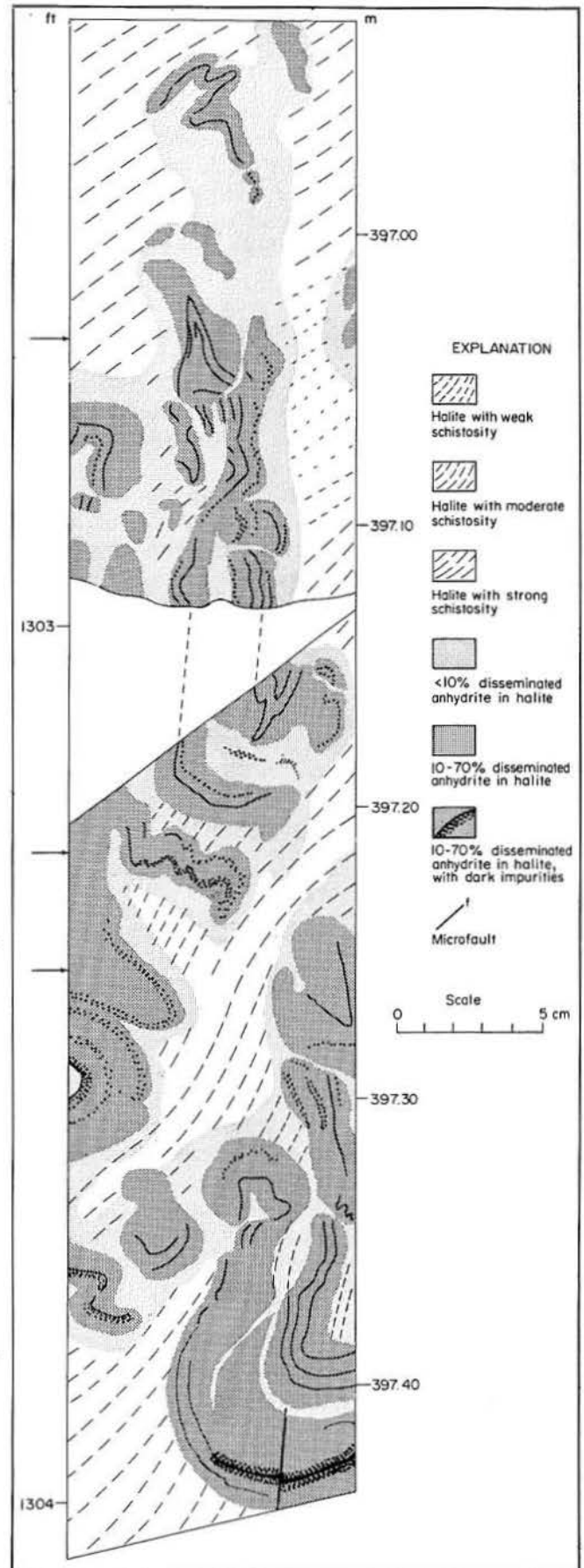
Associated with variations in anhydrite content is a change in halite grain size. In pure rock salt (fig. 7), the mean halite grain size is about 23 by 7 mm (determined from measurements of 150 grains visible to the naked eye in sections parallel to the XZ principal plane of strain). In rock salt containing more than about 5 percent anhydrite, halite has about half this mean grain size (fig. 7). This phenomenon has been noted in other salt domes (Balk, 1949; Nance and Wilcox, 1979). It could be the result of primary variations in grain



Figure 5. (above) Dismembered and contorted anhydrite-rich (>50 percent anhydrite) layers in pale, medium-grained rock salt. 10-cm-wide thick section, transmitted light, depth 397.2 m.

size, but such variations are unlikely to have survived the complex history of repeated deformation and recrystallization that rock salt undergoes during growth of a diapir. Alternatively, immobilization of halite grain boundaries by disseminated anhydrite crystals during normal grain growth could inhibit grain enlargement. This latter process, known as "pinning," is more plausible and is commonly invoked to explain grain-size changes in metamorphic rocks such as metaquartzite and marble (Spry, 1969, p. 127; Hobbs and others, 1976, p. 113; Vernon, 1976, p. 137-138). By analogy with

Figure 6. (right) Mesoscopic structure in the interval containing anhydrite-rich layers. Schistosity (dashed lines) in the halite transects older isoclinal folds at arrowed localities: thin, anhydrite-rich layers containing dark laminae (each shown as a solid line) have been boudinaged in numerous places. Traced from contiguous thick sections.



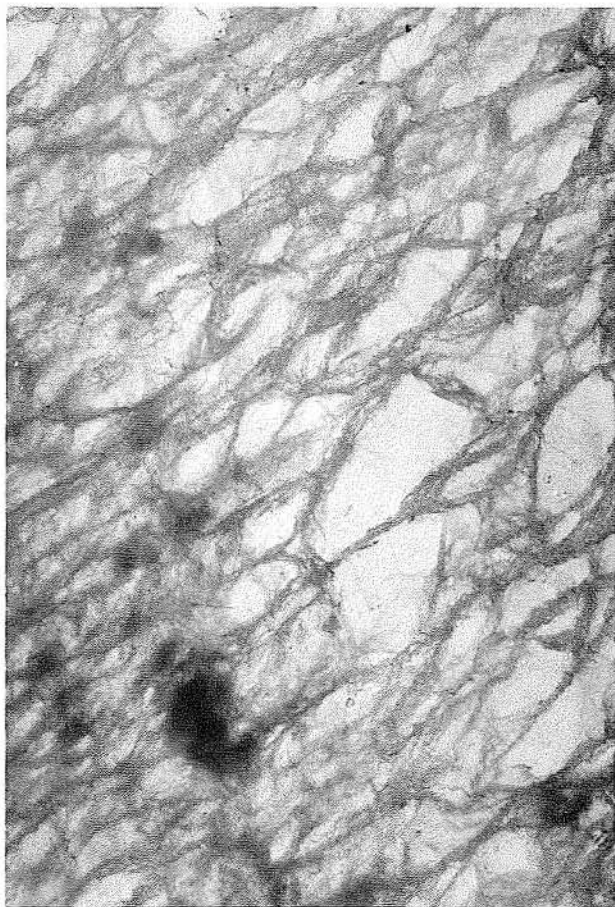


Figure 7. Coarse- to medium-grained rock salt containing dark, medium-grained, disseminated-anhydrite layer at lower left dipping at -60° ; schistosity dips at $+40^\circ$. 10-cm-wide thick section, transmitted light, depth 365.8 m.

other crystalline rocks (Flinn, 1969), anhydrite grains are more likely to be scattered on the surface of halite crystals than to group together in aggregates; this is because the interfacial energy of contacts between unlike phases is less than that between similar phases (Smith, 1948).

Halite grain boundaries in this zone are very irregular (fig. 8A), a high-energy, unstable boundary configuration (Vernon, 1976, p. 136). Postdeformational recrystallization, which would have reduced strain and interfacial energy of the crystals, has therefore been minimal.

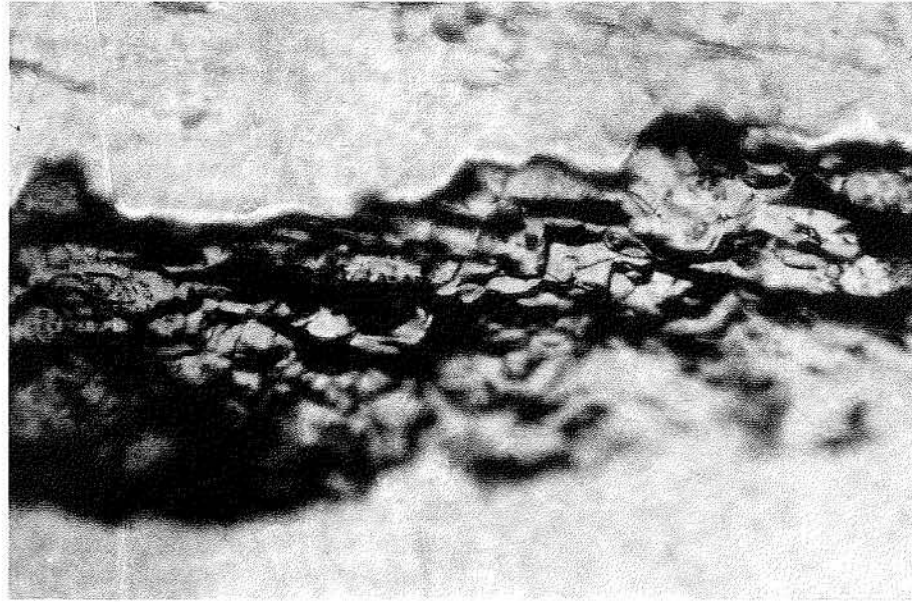
A network of fluid inclusions is commonly present along halite grain boundaries (fig. 9). The liquid is mobile when the rock is elastically flexed and will migrate out of the rock salt when mildly

heated by warm air. Hence, it is probable that at least some of this intercrystalline liquid was introduced during drilling, sample preparation, or storage.

Anhydrite generally consists of idioblastic to subidioblastic prismatic crystals having a mean grain size of less than 0.5 mm. Opaque inclusions, possibly consisting of iron oxide, sulfide, or organic matter, are abundant. Small, transparent, unidentified crystal inclusions with a relatively high refractive index and rare fluid inclusions are also present (see section entitled "Fluid Inclusions"). The (100) crystallographic plane of anhydrite is commonly pitted (figs. 10 and 11). This fine pitting is displayed by less than 20 percent of anhydrite from the foliated rock salt and by more than 80 percent of anhydrite from the unfoliated R-2 and R-3 zones. Minor dissolution of anhydrite by intercrystalline brine films may have caused the pitting. Roedder and Belkin (1979) reported the presence of brine films along many anhydrite-halite grain boundaries in rock salt from Rayburn's and Vacherie Domes in northern Louisiana. In rock salt from Oakwood Dome, either the brine was preferentially trapped on the (100) crystal face of anhydrite, or the mineral may be more susceptible to dissolution along this plane. Where a crystal of anhydrite was formerly in partial contact with the (100) plane of a second anhydrite grain, the area of contact on the (100) plane is generally unpitted (fig. 10). It is possible, therefore, that brines are not trapped between the (100) crystal faces of adjoining anhydrite grains because of the close fit of similar lattice structures; this would account for the lack of pitting at crystal junctions. However, none of the other faces of anhydrite crystals became pitted after two weeks of experimental immersion in fresh water. We therefore conclude that either this etching process is extremely slow or the (100) faces are more susceptible to dissolution.

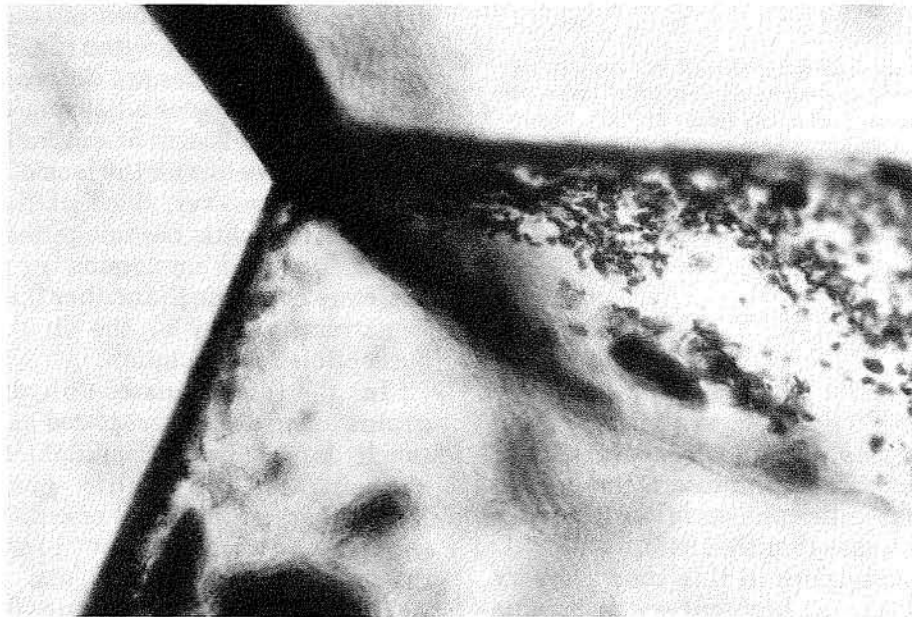
In the disseminated-anhydrite layers, the grains are generally scattered as inclusions in the much larger halite poikiloblasts and weakly concentrated on halite grain boundaries. Morphological preferred orientation of anhydrite (unlike halite) is not prominent in the disseminated-anhydrite layers.

Anhydrite within the anhydrite-rich layer is xenoblastic to idioblastic (fig. 12). Unlike the anhydrite-rich cap rock, recrystallization in this layer has not produced a granoblastic texture with 120° dihedral angles between grains (compare Vernon, 1970). Folding created a fabric defined by alignment of anhydrite long axes in fold limbs (fig. 12). Undulose extinction in anhydrite grains is weak to moderate.



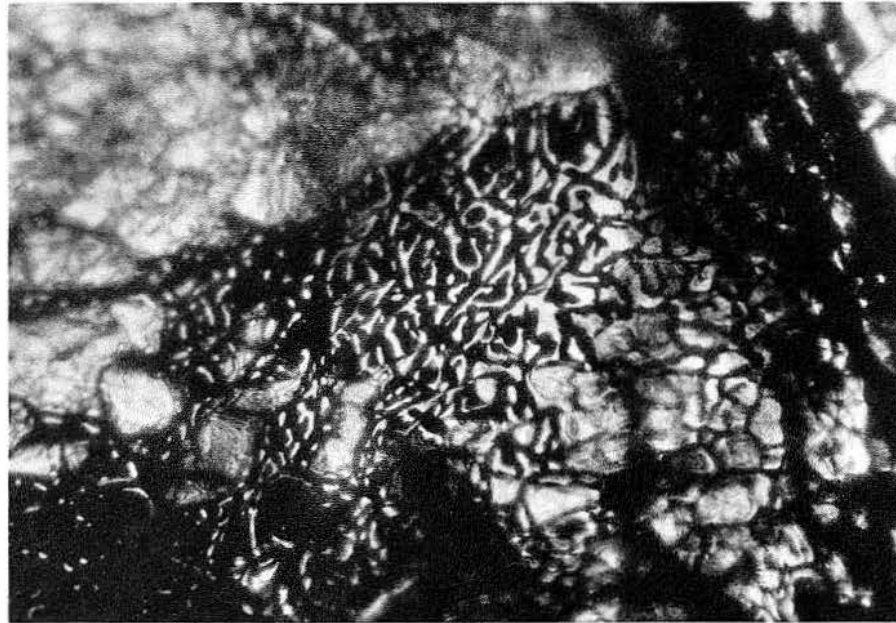
0 1 2 3 mm

Figure 8A. Photomicrograph of inclined halite boundary (dark) showing steplike irregular surface typical of the R-1 foliated rock salt. These grain boundaries have high interfacial free energy and are thermodynamically unstable. Thin section, plane-polarized light, depth 356.5 m.



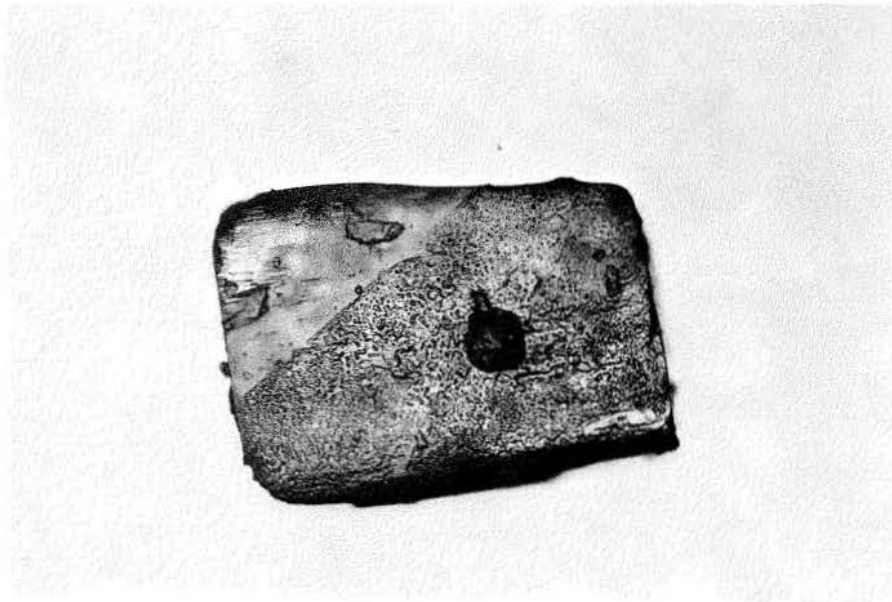
0 1 2 3 mm

Figure 8B. Photomicrograph of inclined halite boundaries (dark) with smooth surfaces in the unfoliated R-2 rock salt. These grain boundaries are characterized by lower interfacial free energy and more-advanced recrystallization than in A. Thin section, plane-polarized light, depth 356.4 m.



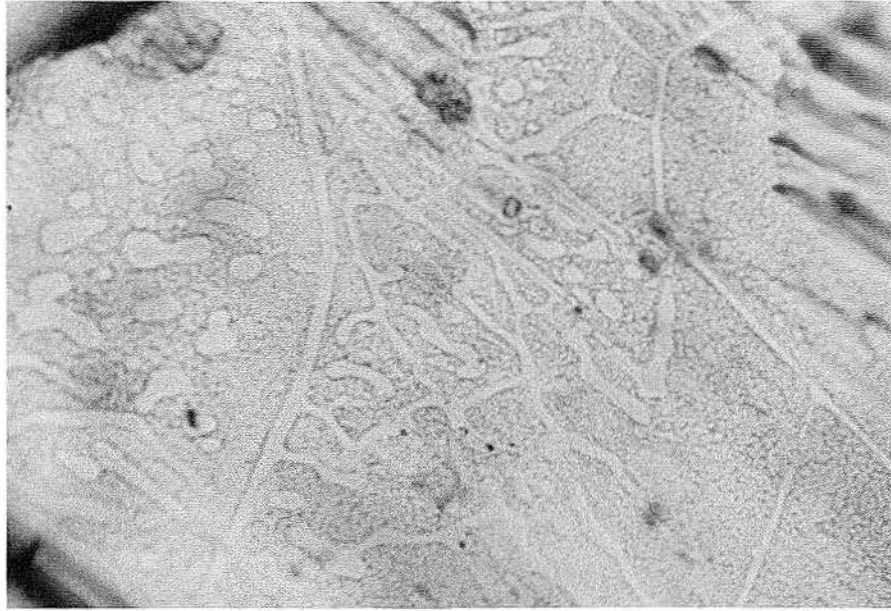
0 1 2 3 mm

Figure 9. Photomicrograph showing intercrystalline network of liquid along halite grain boundaries in foliated rock salt. Darkness of liquid is due to internal reflection. Thick section, plane-polarized light, depth 384.3 m.



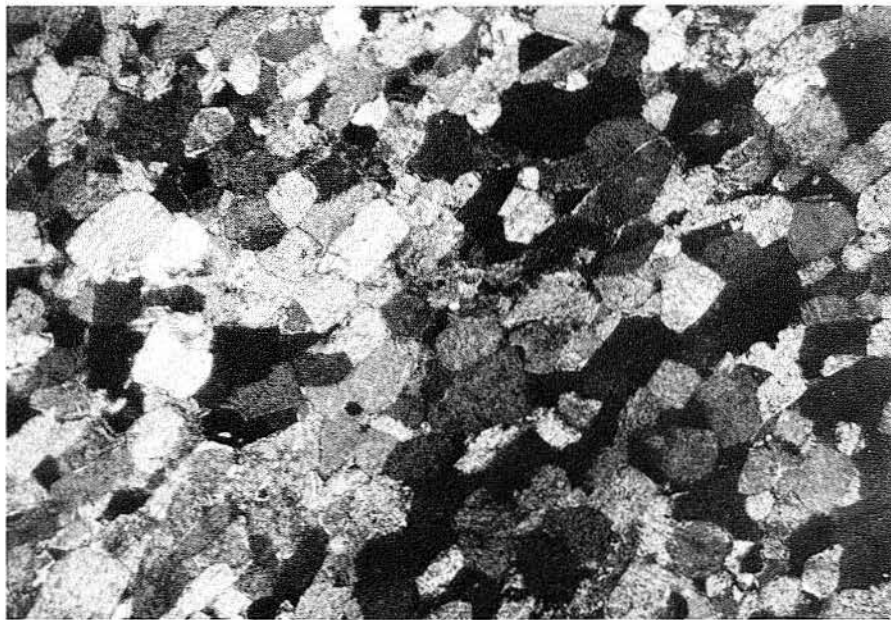
0 1 mm

Figure 10. Photomicrograph of anhydrite crystal from the coarse-grained unfoliated rock salt showing pitted and unpitted areas on the (100) crystallographic plane. Unpitted part is area of former contact with another anhydrite crystal. Plane-polarized light, R-3 zone, depth 354.6 m.



0 0.5 mm

Figure 11. Photomicrograph of irregular network of unpitted areas on the finely pitted (100) face of an anhydrite crystal. Pattern suggests pitting by a liquid influenced by surface tension. Plane-polarized light, depth 354.6 m.



0 1 2 mm

Figure 12. Photomicrograph showing preferred orientation in anhydrite-rich layer on the limb of a microfold. Thin section, crossed nicols, depth 397.2 m.

Unfoliated Rock Salt

The contact between foliated and unfoliated rock salt is 2 m below the cap rock (Appendix). The transition zone is less than 2 cm wide and the contact is parallel to the foliation, having a dip of $+20^\circ$ (fig. 13). Unfoliated rock salt comprises two zones. A lower R-2 zone comprises 140 cm of medium-grained (mean grain size 5 to 10 mm) halite, which contains a disseminated-anhydrite layer. Its texture is granoblastic, equigranular, and interlobate (consisting of a mosaic of equant xenoblastic grains with smooth but irregular contacts). An upper 60-cm-thick R-3 zone consists of coarse-grained (up to 50 mm in diameter) granoblastic halite containing three anhydrite layers, two of which are indistinct. An indistinct, disseminated-anhydrite layer also crosses the contact between the R-2 and R-3 zones.



Figure 13. Contact (dashed line) dipping at $+20^\circ$ between the foliated R-1 zone below and the unfoliated R-2 zone above. Pale horizontal line above contact is saw cut. 10-cm-wide thick section, transmitted light, depth 356.4 m.

Medium-Grained R-2 Zone

Halite grain size in this interval coarsens slightly from 6 mm at the base to 9 mm at the top (based on 120 measurements). The disseminated-anhydrite layer shows transposed layering on a millimeter scale (fig. 14, Appendix). Transposition can take place when a layer is greatly shortened subparallel to its length and surrounded by a matrix of much lower viscosity. As deformation

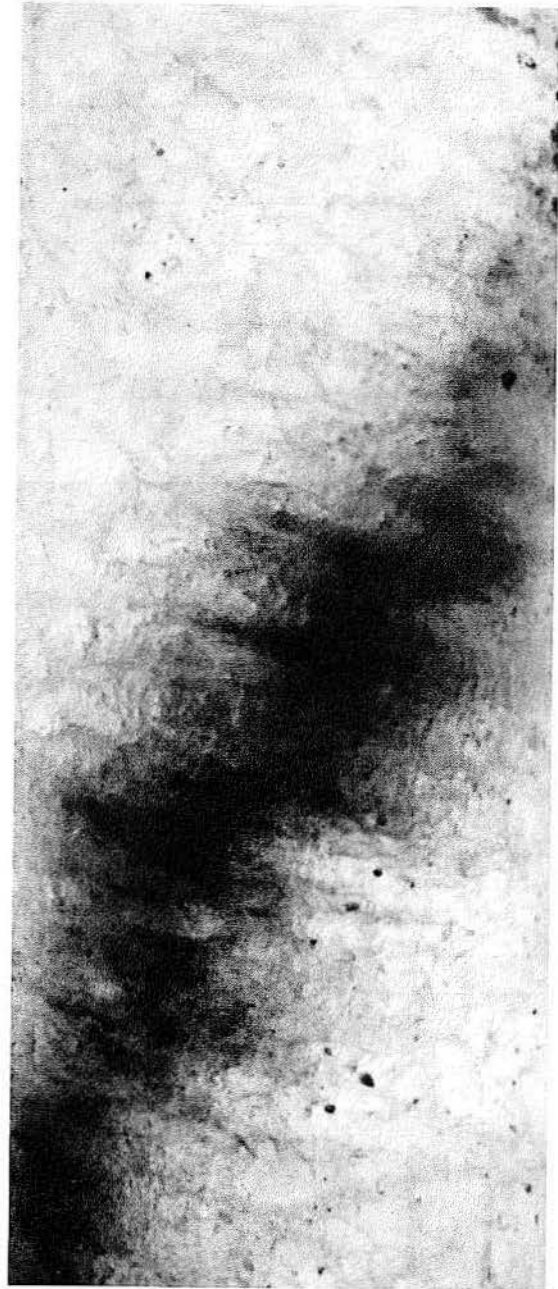


Figure 14. Millimeter-scale transposition of a disseminated-anhydrite layer (dark) in the medium-grained unfoliated R-2 zone. 10-cm-wide unslabbed core, transmitted light, depth 355.9 m.

MESOSCOPIC FORM OF
DISSEMINATED-ANHYDRITE
LAYER

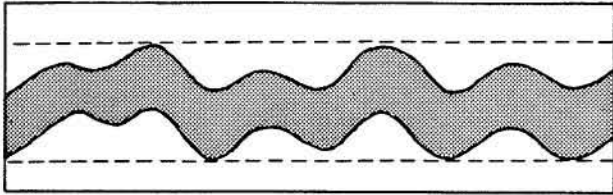
■ Disseminated anhydrite
□ Halite

ANHYDRITE
MICROSTRUCTURE

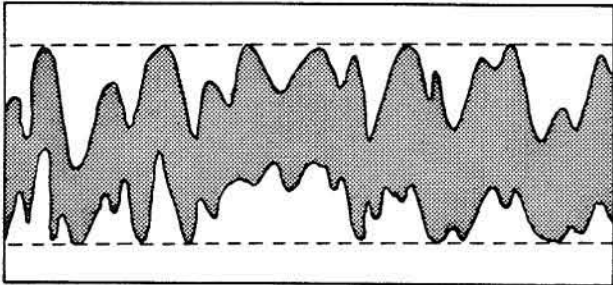
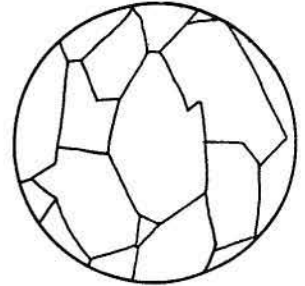
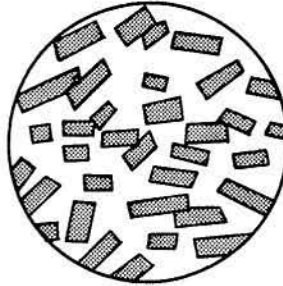
HALITE
MICROSTRUCTURE

└───┘ 2 mm

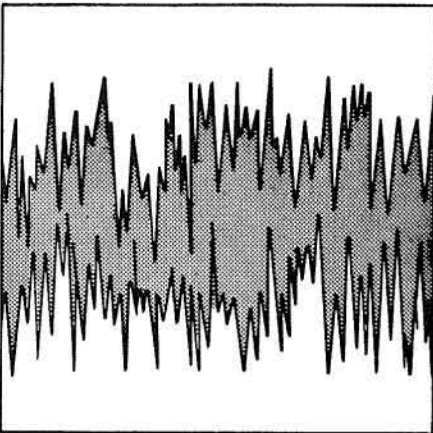
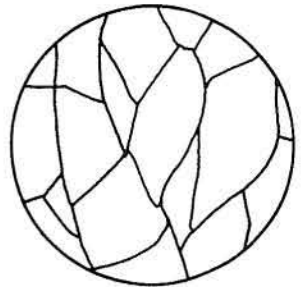
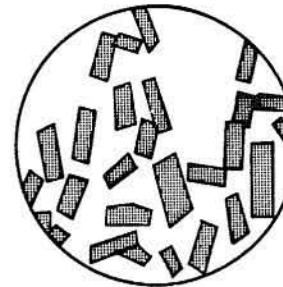
└───┘ 10 mm



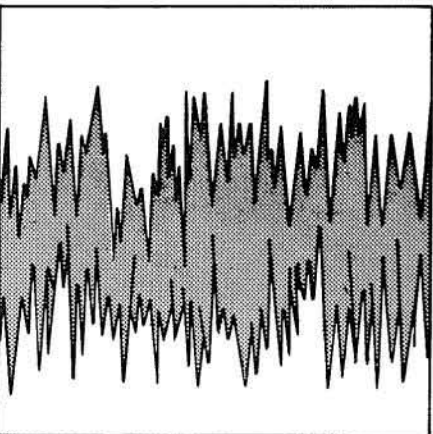
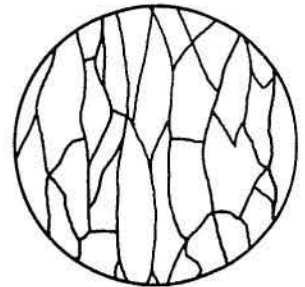
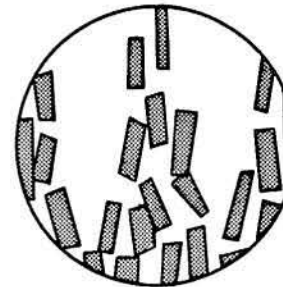
A



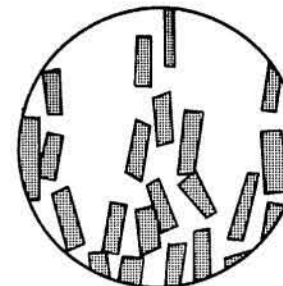
B



C



D



proceeds, folds are initiated (fig. 15, A) and become progressively tighter (fig. 15, B and C). This process produces an axial-plane foliation, which, in the case of rock salt, is defined by elliptical halite crystals aligned parallel to the fold axial surface (fig. 15, B and C). In the case of advanced transposition, grains may become oriented at angles of up to 90° from their original orientation. This type of millimeter-scale transposition is probably also present in many of the anhydrite-bearing layers in the R-1 zone, but is difficult to detect because of the diffuse nature of the layering. Recrystallization of halite in the R-2 zone obliterated the axial-plane foliation in the rock salt (fig. 15, D).

A transposed and tightly folded anhydrite layer in virtually unfoliated rock salt indicates, first, that a strong foliation existed before halite recrystallized under stable conditions of low differential stress. Second, recrystallization was a solid-state, in situ process of grain-boundary adjustment without much reprecipitation from solution, because the latter process would have destroyed the layering. The abrupt upward transition from the R-1 to R-2 zones (less than 2 cm) suggests that recrystallization was promoted by intercrystalline fluids, rather than by pressure or temperature gradients, which would produce a far more gradual transition.

Recrystallization of deformed grains involves the processes of recovery and primary recrystallization (Spry, 1969, p. 115; Vernon, 1976, p. 166). Deformed crystals contain a variety of planar and linear lattice defects, which are thermodynamically unstable. During recovery, stored strain energy from deformation is reduced by, for example, migration of dislocation tangles to grain boundaries, thereby forming subgrains. Primary recrystallization releases the remaining strain energy; high-angle boundaries form and migrate to produce strain-free new grains (Bell and Etheridge, 1973; Hobbs and others, 1976, p. 107-108).

In the R-2 zone, a finer grained granoblastic texture has replaced the previous fabric by these

recrystallization processes. Strain analysis indicates a weak fabric in the R-2 zone, although it is not detectable by the naked eye (Jackson, in preparation). The halite crystals vary greatly in grain size; their grain boundaries are more regular than those in the foliated rock salt of the R-1 zone (compare figs. 8A and 8B).

Coarse-Grained R-3 Zone

The abrupt contact between the medium-grained R-2 rock salt and the coarse-grained R-3 granoblastic rock salt dips at -30° (fig. 16, Appendix). Disseminated-anhydrite layers indicate that recrystallization of the R-3 rock salt was also an in situ process. Absence of growth bands (for example, lines of fluid inclusions) is further evidence that this halite was not precipitated from solution (see Schlichta, 1968).

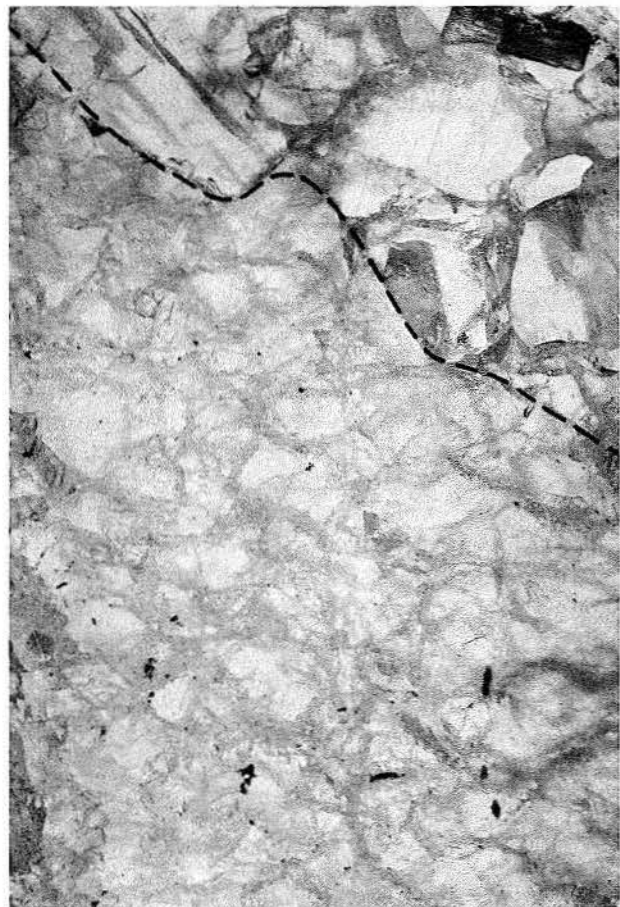


Figure 16. Abrupt contact (dashed line) between medium-grained, unfoliated rock salt in the R-2 zone below and coarse-grained unfoliated rock salt in the R-3 zone above. 10-cm-wide thick section, transmitted light, depth 355.1 m.

Figure 15. Schematic diagram showing inferred anhydrite and halite microstructure in a disseminated-anhydrite layer during successive stages of transposition. A. Mild folding. B. Tight folding, incipient transposition of anhydrite fabric, moderate axial-plane schistosity defined by halite. C. Isoclinal folding, advanced transposition of anhydrite fabric, strong axial-plane schistosity defined by halite. D. Recovery, recrystallization, and new grain growth of halite when directed stress ceases.

Halite grain boundaries are smoother and more planar in the R-3 zone than in the R-2 zone. Furthermore, grain size is markedly coarser because larger halite grains grew at the expense of smaller ones. These observations suggest that recrystallization in the R-3 zone resulted from normal grain growth. This growth lowered interfacial free energy of crystals by (1) increasing grain size, (2) forming more equant crystals, (3) smoothing grain boundaries, and (4) reducing the number of nonrational high-angle grain boundaries (Spry, 1969, p. 20-21; Hobbs and others, 1976, p. 110-112).

Normal grain growth in the R-3 zone is attributed either to the presence of more abundant intercrystalline fluids or OH^- ions, or to a longer period of recrystallization. Assuming the source of the liquids to be the rock-salt - cap-rock contact, recrystallization would be more advanced nearer the cap rock. Nevertheless, a more gradational change in grain size than that observed would also be expected. Alternatively, the coarse- and medium-grained halite could represent two distinct stages of recrystallization. This is feasible if dissolution of rock salt were not simultaneous over the entire crest of the diapir, but was localized by, for example, differential movement of rock salt. Inhomogeneous recrystallization and dissolution is evidenced by the fact that boreholes drilled into the crest of other salt domes have intersected a cavity, in places with anhydrite sand, at the top of the rock salt, and elsewhere in the same dome have passed directly from cap rock into rock salt (Judson and Stamey, 1933; O'Donnell, 1935). Halite within the Oakwood core recrystallized within 200 cm of the cap-rock contact. Suppose that a new phase of dissolution removed 140 cm of rock salt from the top of the core and that halite again recrystallized within 200 cm of the new plane of dissolution (fig. 17). The upper 60 cm of unfoliated rock salt therefore could have recrystallized again by normal grain growth, whereas the lower 140 cm of foliated rock salt could have undergone recovery and primary recrystallization (fig. 17). This hypothetical process accounts for the coarse-grained nature of halite within the R-3 zone and the sharp contact between the R-3 and R-2 zones.

Contact Between Rock Salt and Cap Rock

The contact between rock salt of the R-3 interval and the overlying cap rock is subhorizontal, sharp, and undulating (fig. 18, Appendix) and comprises two zones:

(1) A lower transition zone (in contact with the R-3 interval) is 1 to 4 mm thick (fig. 19) and

contains 60 to 70 percent anhydrite as idioblastic to subidioblastic, prismatic crystals within a matrix of halite (fig. 20A). The upper and lower contacts of this lamina are abrupt. This zone is similar to the lower transition zone in Hockley Dome (Goldman, 1933, p. 87).

(2) An upper transition zone, which is 3 to 5 mm thick, contains about 95 percent anhydrite, also largely in the form of idioblastic to subidioblastic, prismatic crystals (fig. 20B). This zone grades over a distance of 1 mm into the overlying cap rock, which consists almost entirely of xenoblastic to subidioblastic anhydrite in an equigranular granoblastic-polygonal texture (fig. 21).

About half of the anhydrite crystals within these two zones display weak to moderate undulose extinction, which is confined almost entirely to the subidioblastic and xenoblastic crystals. This is also true of anhydrite in rock salt below the contact. However, the proportion of xenoblastic crystals increases sharply from about 15 percent in the rock salt immediately below the cap-rock contact to 50 percent in the cap rock itself. Associated with this trend is a decrease in the proportion of idioblastic crystals, from 45 percent to 5 percent (fig. 22). These changes reflect grain-boundary impingement with increasing concentration of anhydrite; crowding of anhydrite grains interfered with grain growth, resulting in the formation of nonrational adjustment boundaries (oblique to the lattice structure of one or both of the crystals in contact). Nevertheless, 120° dihedral angles are scarce (fig. 21), and undulose extinction, subgrains, and deformation bands are still present in many crystals; lattice strains have therefore not been completely neutralized. Furthermore, the mean size and the axial ratio of anhydrite crystals remain constant from the rock salt up into the cap rock, indicating negligible grain enlargement (fig. 22).

Cap rock within 80 cm of the rock-salt contact contains vertical halite-filled extension fractures up to 1 cm wide and up to at least 10 cm long (fig. 23). Halite within the fractures has grown perpendicular to the fracture walls and, unlike halite of the R-3 interval, does not contain fluid inclusions or anhydrite crystals. Absence of anhydrite suggests that the mechanism responsible for transporting sodium chloride into the fractures was incapable of transporting or precipitating calcium sulfate. Two extension-fracture arrays in the cap rock extend downward to the rock-salt contact (fig. 24). The lower transition zone is continuous across the openings of the fractures, indicating that anhydrite was accreted from below against the base of the cap rock after fracturing and extension. The lower

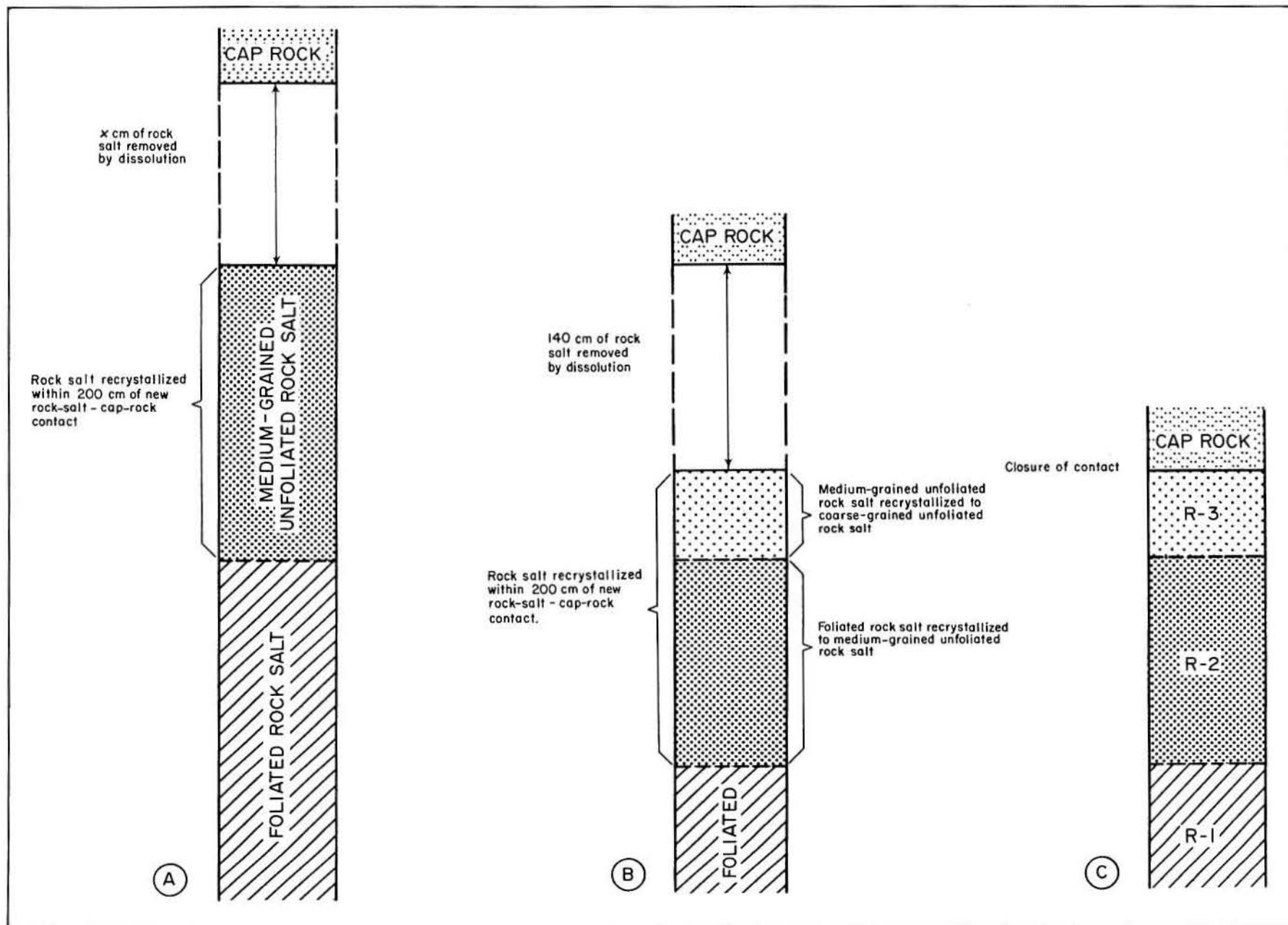


Figure 17. Schematic diagram showing possible evolution of the R-2 and R-3 zones (diagram C) of unfoliated rock salt as the result of two periods of dissolution and recrystallization (diagrams A and B).



Figure 18. Abrupt contact between cap rock and rock salt of the coarse-grained unfoliated R-3 zone; contact is smooth but undulating. Note horizontal laminae and halite-filled extension fractures in cap rock. Dark color of halite near contact and in fractures is due to internal reflection. 10-cm-wide unslabbed core, reflected and transmitted light, depth 355.5 m.

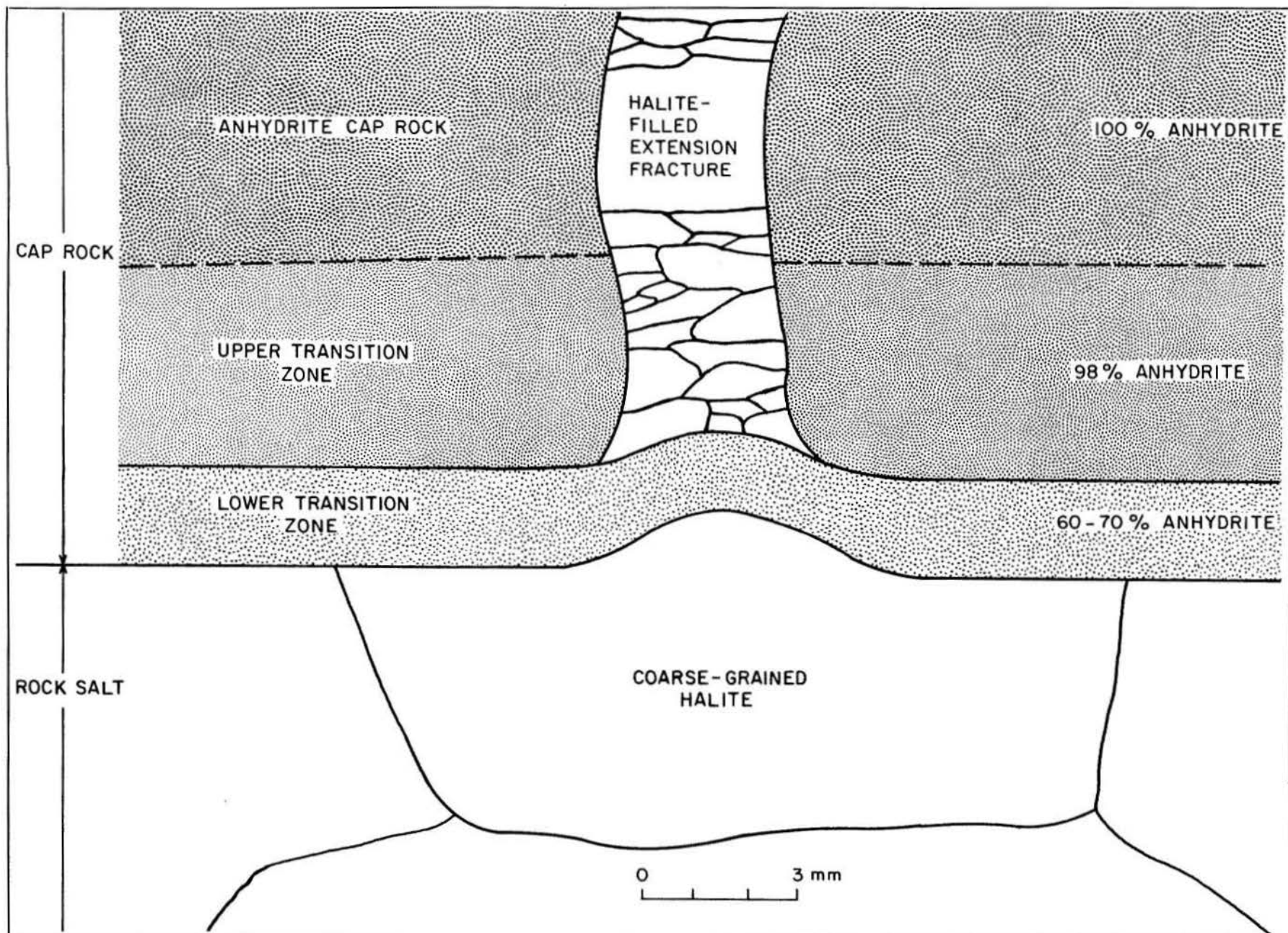


Figure 19. Schematic diagram of the rock-salt - cap-rock contact zone, showing the upper and lower transition zones. The lower transition zone extends across the mouth of the extension fracture. Note preferential orientation of halite perpendicular to the walls of the fracture.

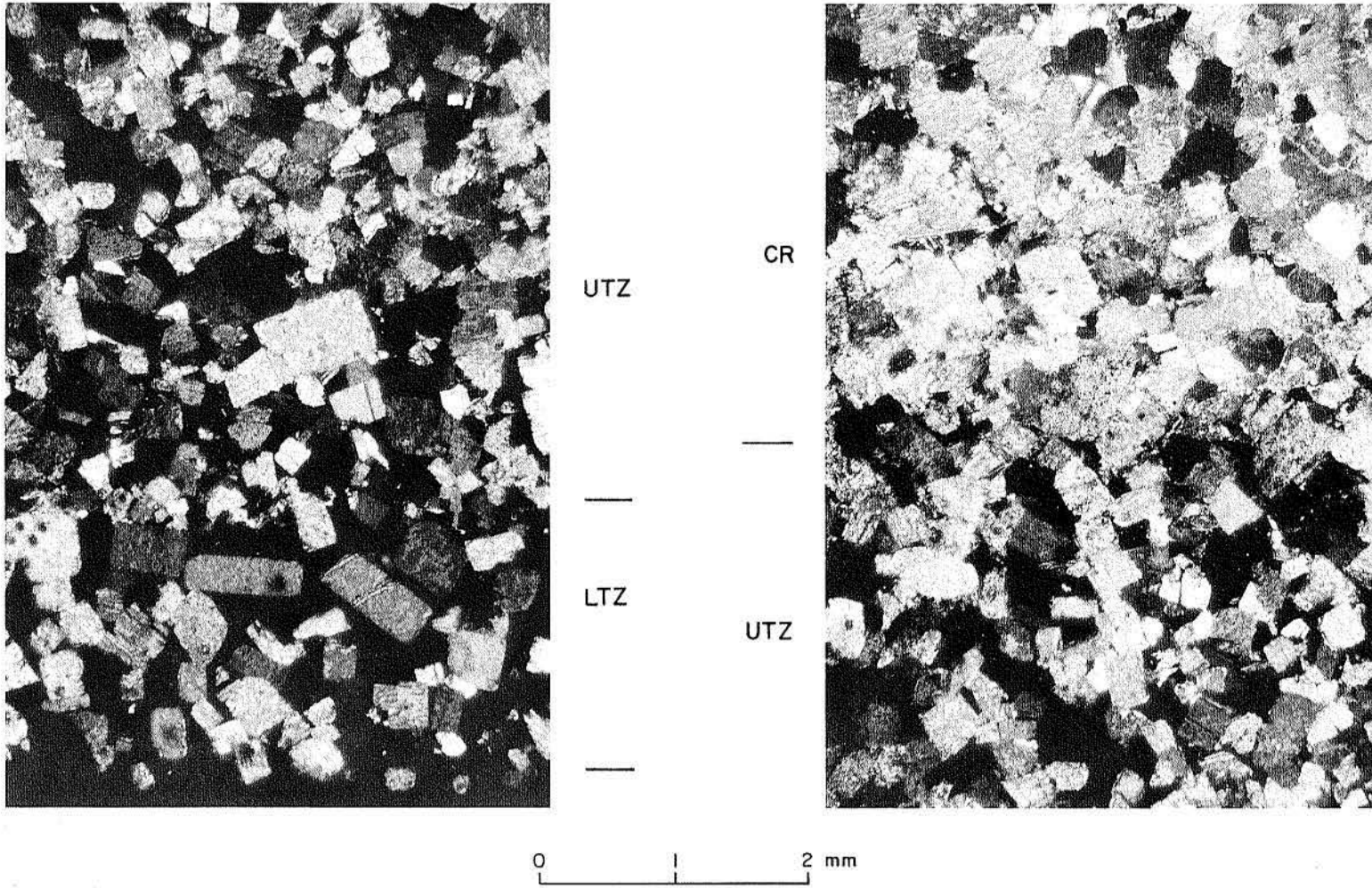
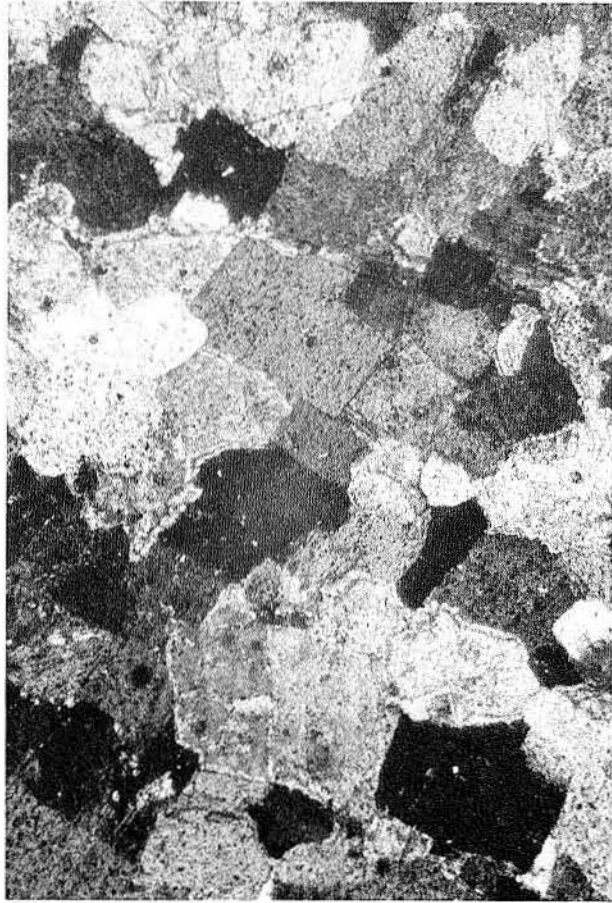


Figure 20A. Photomicrograph showing idioblastic to subidioblastic grains of anhydrite surrounded by halite (black) in the lower transition zone (LTZ). The LTZ is overlain by rock salt (black) and overlain by the transition zone (UTZ). Thin section, crossed nicols, depth 355.5 m.

Figure 20B. Photomicrograph showing idioblastic to subidioblastic grains of anhydrite surrounded by halite (black) in the upper transition zone (UTZ). The UTZ is overlain by granoblastic anhydrite cap rock (CR), visible in the upper half of the photograph. Thin section, crossed nicols, depth 355.5 m.



0 | mm

Figure 21. Photomicrograph of the base of the cap rock consisting of xenoblastic to subidioblastic equant anhydrite grains in an equigranular granoblastic-polygonal texture. No halite is present. Thin section, crossed nicols, depth 355.5 m.

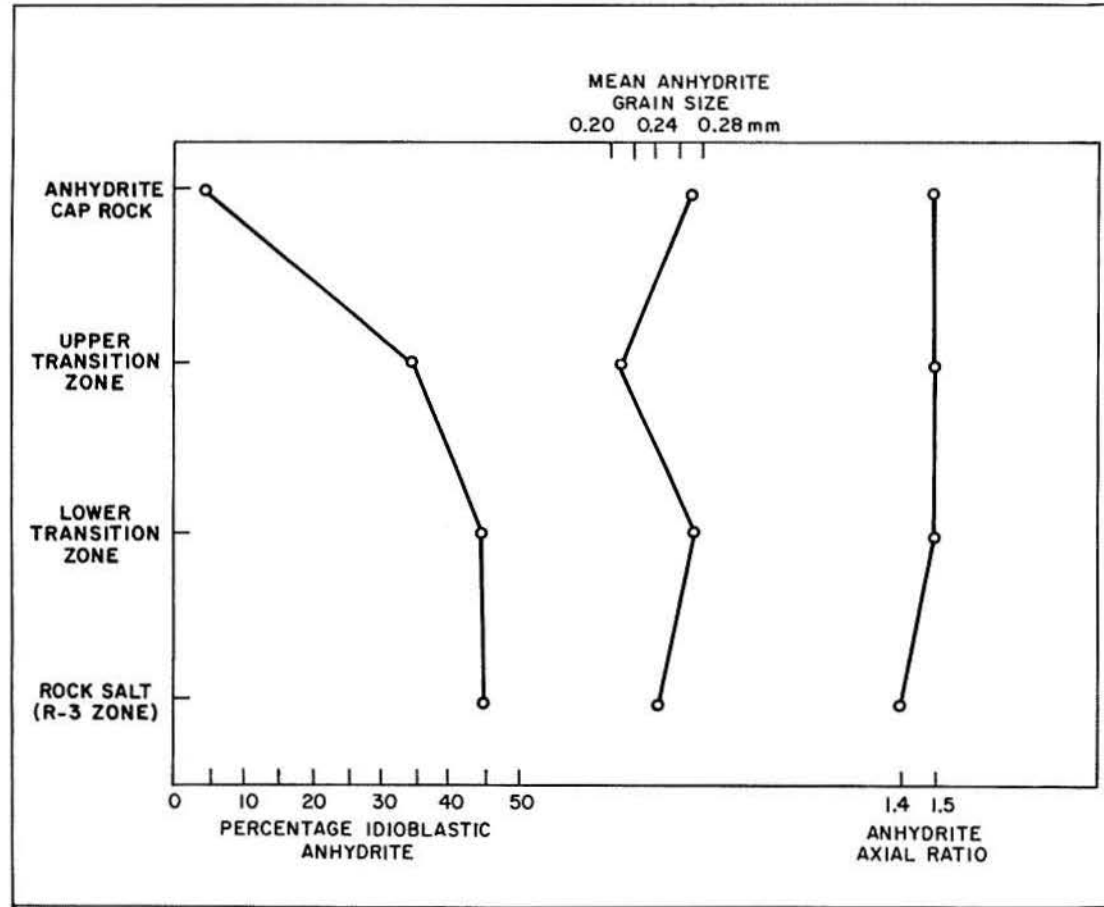


Figure 22. Graph showing changes in percentage of idioblastic anhydrite, mean anhydrite grain size, and anhydrite axial ratios across the rock-salt - cap-rock contact. Idioblastic crystals become rarer upward, whereas their sizes and axial ratios show little variation. One hundred grains in each zone were measured.

transition zone thins across the fractures and is convex upward into them, possibly as a result of further opening of the fracture.

At one location along the larger of the two extension fractures, the upward convexity is more pronounced and is considerably wider than the fracture itself (fig. 24). This feature is circular in plan and may be the result of local truncation by erosion or of primary thinning of anhydrite laminae before accretion against the base of the cap rock. One possible sequence of events for the lower 15 mm of cap rock at this location can be termed the "erosion hypothesis." This hypothesis infers (1) uninterrupted basal accretion of anhydrite onto the base of the cap rock; (2) truncation of the lower part of lamina A, together with laminae B and C, by erosion from below; (3) fracturing and vein dilation during formation of lamina D; (4) continued accretion of lamina D across the fracture; (5) accretion of lamina E across the fracture; (6) erosional thinning of lamina E below the dilation vein; and (7) rise of lamina E into the dilation vein.

According to this hypothesis, two periods of secondary truncation are superposed and coincident with the dilation vein. This suggests a relationship between the extension fracture and the irregularities in the laminae, a situation difficult to explain by secondary erosive truncation. The circular shape of the thinned zone in plan is also at variance with the erosion hypothesis.

Another explanation, termed the "drip hypothesis," holds that these thickness variations in anhydrite laminae are primary and were present before the laminae were accreted against the base of the cap rock. Brine may have dripped from the base of dilation fractures at various points. Falling drops would have splashed out anhydrite sand on top of the rock salt, producing small, circular impact craters (fig. 25A). Subsequent accretion of the sand against the base of the cap rock would have resulted in conical projections of rock salt into the cap rock (fig. 25B). According to the drip hypothesis, brine started dripping from the fractures during accumulation of lamina A. No new anhydrite would have been added to the splashed-out area during accretion of laminae B and C, and only a thin layer of anhydrite would have been added during accretion of lamina E. Lamina D is thicker at the fracture; it is necessary to postulate that anhydrite sand accumulated in a splashed-out cavity between episodes of dripping and subsequently became accreted against the base of the cap rock as a locally thickened layer after rise of rock salt. In both hypotheses discussed above, closure of the



Figure 23. Contact between rock salt and cap rock. See figure 24 for explanation. 4.5-cm-wide thick section, transmitted light, depth 355.5 m.

dissolution cavity and accretion of anhydrite sand against the base of the cap rock is thought to have resulted from diapiric rise of the salt stock rather than from collapse of the overlying cap rock; no breccia or other collapse features are present near the base of the anhydrite cap rock.

Lamination in the Contact Zone

The following observations refer to lamination in the transition zones and in the anhydrite cap rock a few centimeters above. Because the 77 m of cap rock above the transition zone is similar to the base of the cap rock, the conclusions made here may well apply to the entire anhydrite cap rock described by Dutton and Kreidler (1981).

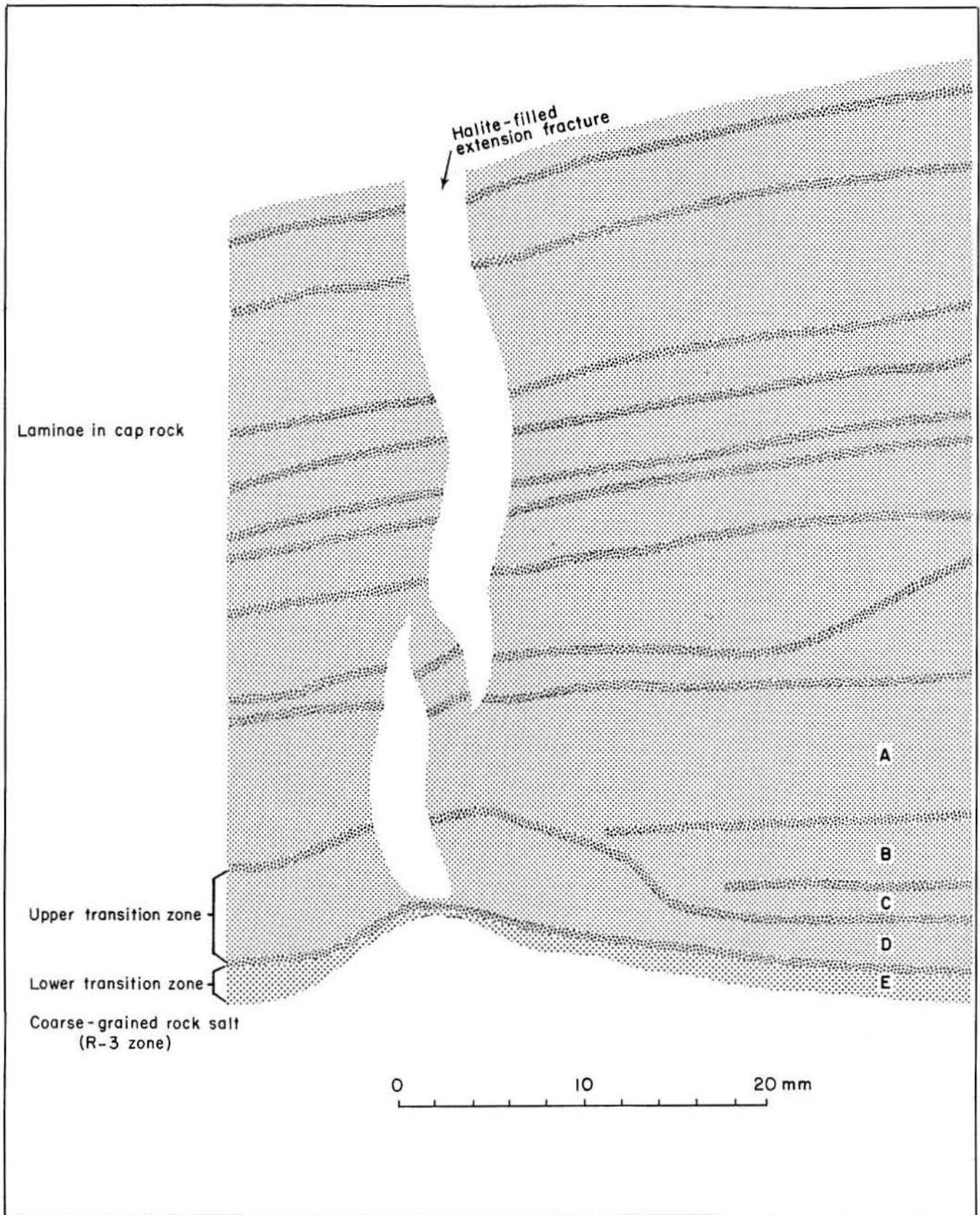


Figure 24. Explanatory diagram of specimen in figure 23 showing continuation of lower transition zone across halite-filled extension fracture, apparent truncation of laminae A, B, and C, and slight buckling of the en echelon extension fractures.

In the contact zone and above, laminae 2 to 5 mm wide are conspicuous in thick section, but are not generally recognizable in thin section. They are defined largely by varying concentrations of dark, very fine grained intercrystalline impurities. Two samples of cap rock within centimeters of the cap-rock contact were analyzed for TOC. The sample with abundant dark matter contains 0.052 percent TOC, and the sample with very little dark matter contains 0.042 percent. Because of the small difference in TOC concentration in the two samples, we conclude that the darkness of the layers is not primarily controlled by organic matter. Samples of the dark and light layers contained FeS_2 concentrations of 110 ppm and 65

ppm, respectively, suggesting that pyrite may be the darkening agent. Hanna (1934) identified pyrite in similar dark layers of cap rock in Hockley Dome. Grain-size determinations of dark layers and pale layers revealed no difference in anhydrite grain size (table 1).

All the layers are subhorizontal and vary from diffuse laminae up to 4 cm thick to very thin, sharply defined, dark layers (fig. 26). The alternation between contorted laminae and apparently undisturbed, horizontal laminae (fig. 27) suggests that the former were disrupted before they were accreted against the cap rock. This disruption could result from moving brines or granular flow of anhydrite sand on top of the rock salt.

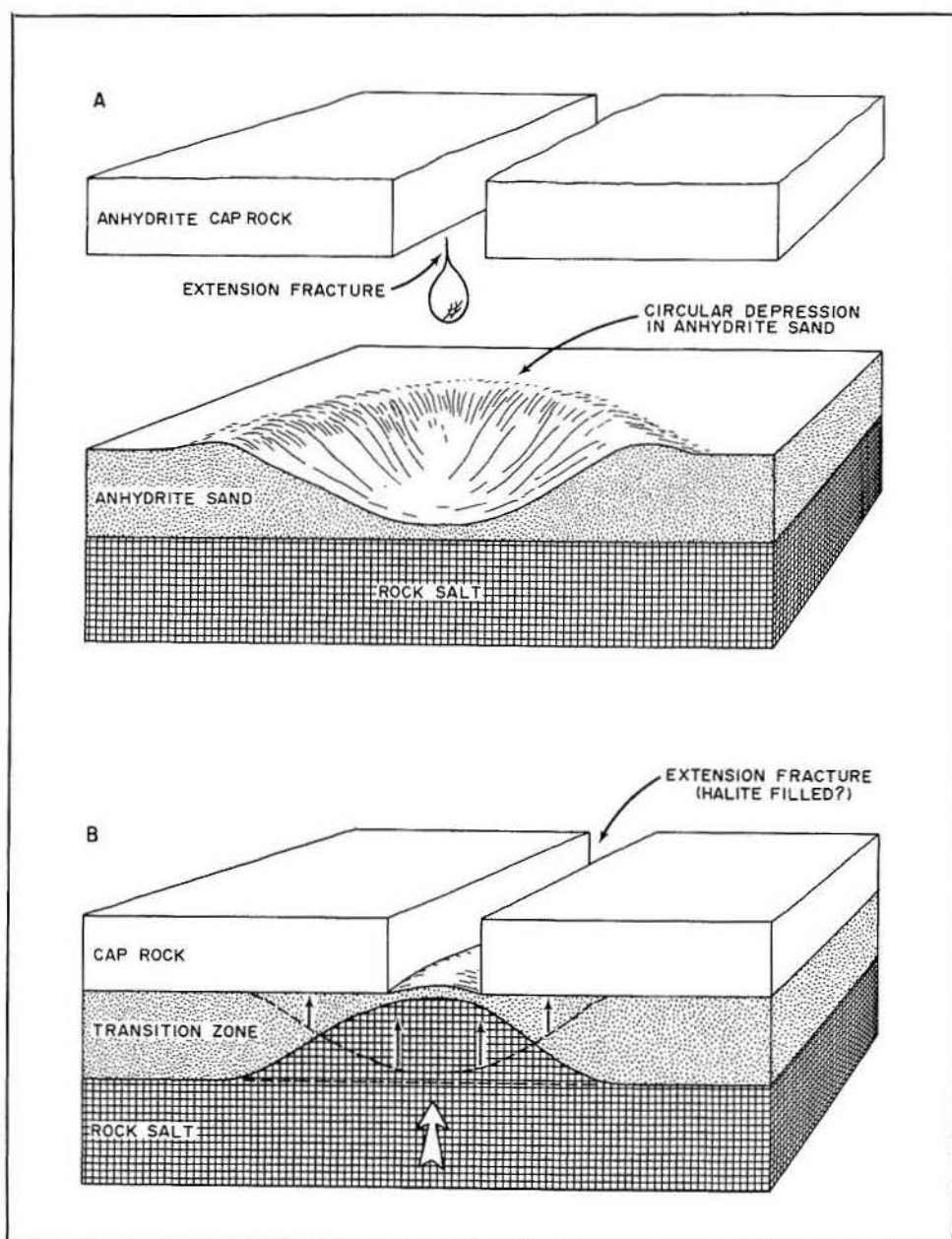


Figure 25. Block diagram of the drip hypothesis. (A) Circular splash crater in anhydrite sand is formed by brine dripping from an extension fracture. (B) Dissolution cavity between rock salt and cap rock is closed by diapiric rise of rock salt; anhydrite sand is accreted against the base of cap rock, forming a transition zone.

Table 1. Grain-size data for laminae* at the base of the anhydrite cap rock in Oakwood Dome core.

	PALE LAMINA		DARK LAMINA	
	Sample 1	Sample 2	Sample 3	Sample 4
Number of grains measured	100	100	100	100
Mean maximum dimension (mm)	0.36	0.39	0.37	0.39
Standard deviation (mm)	0.13	0.21	0.17	0.23
	⏟		⏟	
Number of grains measured	200		200	
Mean maximum dimension (mm)	0.38		0.38	
Standard deviation (mm)	0.18		0.20	

*Each lamina was sampled in two places to assess its uniformity.



0 40 mm

Figure 26. Two different thicknesses of layers at the base of the anhydrite cap rock. A 4-cm-wide pale zone is sandwiched between two darker layers containing a greater proportion of dark impurities. All three layers contain 1-mm-wide dark laminae, some of which (arrowed) crosscut larger, more diffuse structures. The thin, dark laminae are interpreted as being stylolitic solution cleavages, sometimes referred to as tectonic stripes. White blebs are zones of pure anhydrite. Thick section, transmitted light, depth 353.5 m.

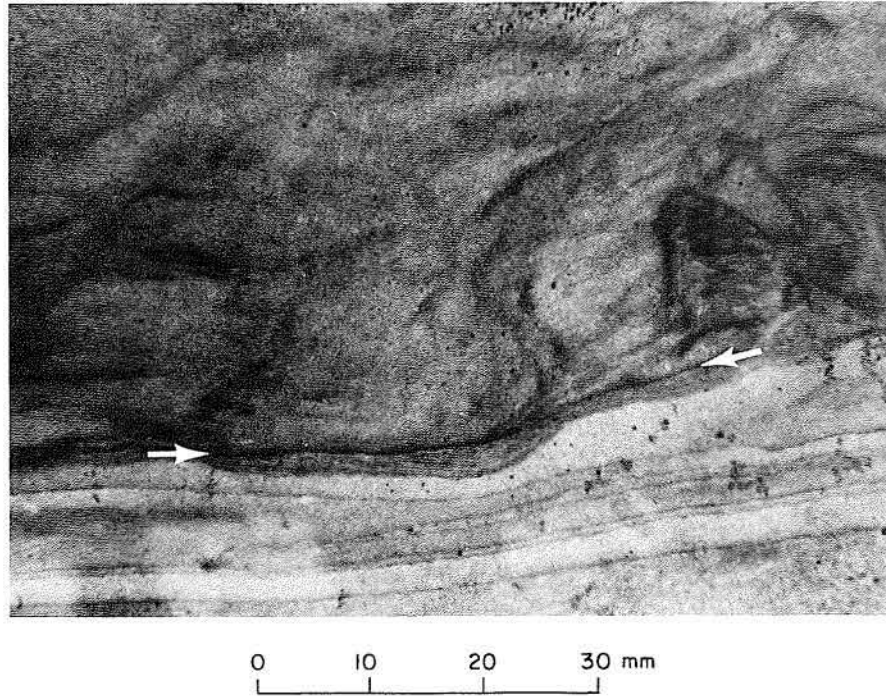


Figure 27. Thin, dark, stylolitic solution cleavage (arrowed) cutting across contorted laminae in the base of the anhydrite cap rock. Thick section, transmitted light, depth 354.2 m.

In places, very thin (<1 cm thick), secondary, dark layers cut across the laminae (figs. 26 and 27). These dark, discordant layers resemble stylolitic pressure stripes and probably resulted from localized pressure solution of anhydrite along planar zones statistically perpendicular to the vertical σ_1 principal stress axis (Durney, 1976, 1978). Solution mass transfer would have taken place by diffusion of ions along grain boundaries toward zones of lower differential stress and lower chemical potential, where the dissolved mineral would have been redeposited (Gray and Durney, 1979; Ramsey, 1980). The undissolved minerals in the thin zones of pressure solution would have accumulated as a dark residue. These stylolitic zones appear to represent a type of spaced solution cleavage, typically observed in limestones, or terrigenous clastic sediments that have undergone low- or medium-grade metamorphism. The discrete nature, strong preferred orientation, and low amplitude/wavelength ratio of the stylolitic cleavage all suggest moderate shortening strains, whereas their broad spacing (>1 cm) indicates that these strains were not high (compare Alvarez and others, 1978). Analogy with similar cleavages in pelagic limestones (Alvarez and others, 1978) suggests that the cap rock shortened vertically by 5 to 25 percent during stylolite formation. Assuming plane strain (Hobbs and others, 1976, p. 27), the cap rock would have extended laterally

by 5 to 33 percent. Assuming axially symmetric shortening (Hobbs and others, 1976, p. 27) rather than plane strain, lateral extension of the cap rock would have been 2.5 to 15 percent.

This inferred phase of lateral extension was followed by further extension during formation of the halite-filled fractures, which postdate the stylolitic cleavage; plane-strain extension by fissure dilation across the width of the core at the cap-rock base varied between a minimum of 3 and 7 percent. Vertical shortening during this second phase of lateral extension is reflected by slight buckling of the vertical halite veins (fig. 23) and by the formation of shear fractures that dip from 30° to 50° and offset the dilation veins. Similar geometric relations between stylolites and extension veins in carbonate rocks have been documented by Nelson (1981).

Two layers of rock salt are isolated in the cap rock at depths of 318.8 m and 317.7 m (fig. 28). In both layers, the contact with anhydrite cap rock is sharp and concordant with laminae in the cap rock. No transition zones are present. The lower rock-salt layer is 3 cm thick and resembles an incompletely exposed fold hinge with a horizontal hinge line. The upper layer is at least 7 cm thick. Only the upper contact is preserved; it is subhorizontal and undulate with downward projecting ribs of anhydrite (relief about 5 mm) along the contact surface (fig. 28).

Halite within the rock salt has an equigranular granoblastic-interlobate texture and a mean grain size of about 4 mm. Grain boundaries are irregular, as are those of the R-2 rock salt. Halite from both rock-salt layers contains abundant inclusions of compressed gas (see section entitled "Compressed-Gas Inclusions"). Similar inclusions have been reported from rock salt within other Gulf Coast salt domes (Roedder and Belkin, 1979). The halite also contains minor anhydrite, which displays little or no undulose extinction.

Similar occurrences of rock salt in cap rock have been reported at other domes (Hager and Stiles, 1925; Teas, 1931; Wendlandt and Knebel, 1936). Teas (1931) described a horizontal lens of rock salt with dimensions of 300 by 150 by 25 cm within the cap rock of Hockley Dome. There, too, the rock salt is in sharp contact with the cap rock

but contains no anhydrite. The large size of that halite lens and its horizontal attitude suggest that it is not filling an extension fracture; vertical extension could only take place during collapse, for which there is no other lithologic or structural evidence.

Rock-salt inclusions in the Oakwood cap rock could conceivably have originated at the cap-rock contact and been subsequently isolated from further dissolution after enclosure in anhydrite cap rock. However, this is a rather elaborate hypothesis, and it is much more likely that the rock salt precipitated from brine that percolated into a cavity; such brine-filled cavities are common in cap rock (Van der Gracht, 1925). The latter hypothesis is strongly supported by the low bromine content of halite in Oakwood Dome (see section entitled "Geochemistry").



Figure 28. Undulating upper contact of a rock-salt layer enclosed in anhydrite cap rock. Note anhydrite ribs projecting down from contact. Inclined shear fracture passes downward into an array of halite-filled extension fractures. Outer part of rock salt was dissolved during drilling. 10-cm-wide unslabbed core, transmitted and reflected light, depth 317.7 m.

FLUID INCLUSIONS

Brine Inclusions

Intracrystalline brine inclusions in cuboid negative crystals (fig. 29) are abundant within halite in the R-3 zone, but have not been identified in the R-1 and R-2 zones. Irregular intercrystalline inclusions attached to one or more anhydrite crystals are also present (fig. 30). Both intracrystalline and intercrystalline types have been identified in rock salt from Rayburn's and Vacherie salt domes in northern Louisiana (Roedder and Belkin, 1979).

Study of the intracrystalline brine inclusions in the Oakwood R-3 zone involved the following steps:

(1) Preparation of small cleavage fragments and determination of their volume by gauging how much liquid they displaced.

(2) Measurement of the dimensions of the inclusions.

(3) Measurement of the bubble diameter where the inclusion was large enough and where the inclusion size was known in three dimensions.

(4) Use of the water-dissolution technique (Roedder and Belkin, 1979) to assess volume changes on release of gas inclusions.

The cuboid inclusions range in size from less than 0.02 mm to more than 1.0 mm. About 55 percent are orthorhombic, 40 percent are tetragonal, and 5 percent are cubic in shape. The mean ratio of the three axes, as determined from 100 inclusions measured in three dimensions, is 1.00:1.25:1.50. All inclusions in halite grains, except the smallest, contain a gas bubble (fig. 29). About 5 percent of the cuboid inclusions contain small, black particles, which are possibly organic, attached to their enclosed bubble (compare Roedder and Belkin, 1979). An additional 5 percent of brine inclusions contain one or more euhedral crystals resembling anhydrite.

The bubbles in the intracrystalline fluid inclusions expanded eightfold to tenfold (800 to 1,000 percent) on experimental breaching of the inclusions at room temperature after the enclosing halite was dissolved in water. This expansion was noted by Roedder and Belkin (1979) in 95 percent of the brine inclusions they studied and was attributed to the presence of pressurized gas (probably CO_2 or CH_4) in the bubbles. The mean volume of the Oakwood bubbles is less than 0.1 percent of the total inclusion volume. These bubbles therefore have about one tenth the relative

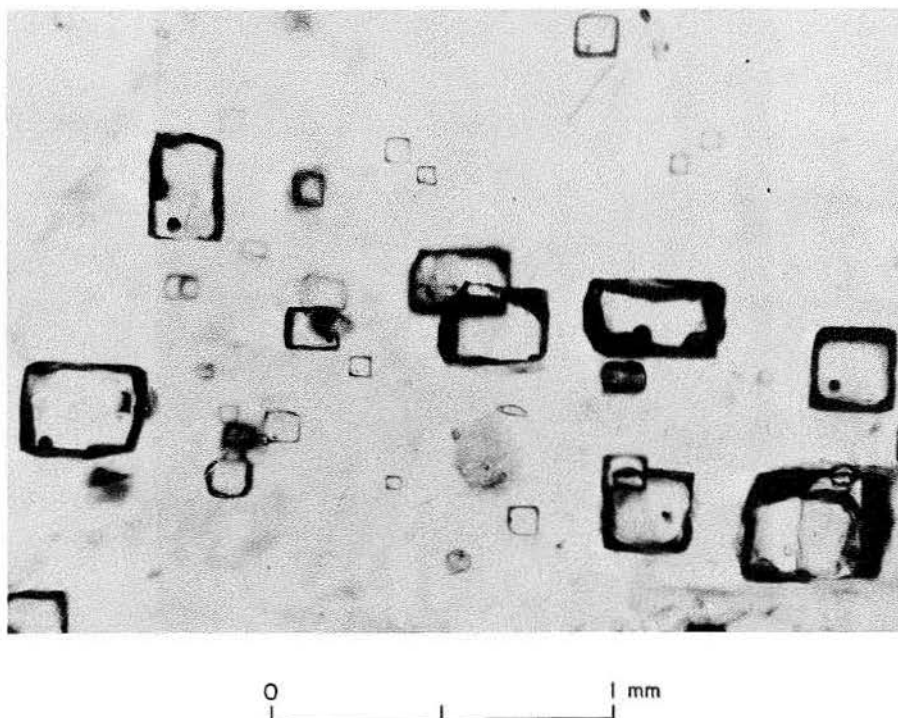


Figure 29. Photomicrograph of brine inclusions in cuboid negative crystals within halite from the R-3 zone of recrystallized rock salt. Note small gas bubbles occupying less than 0.1 percent of the inclusion volume. Cleavage fragment, plane-polarized light, depth 354.7 m.

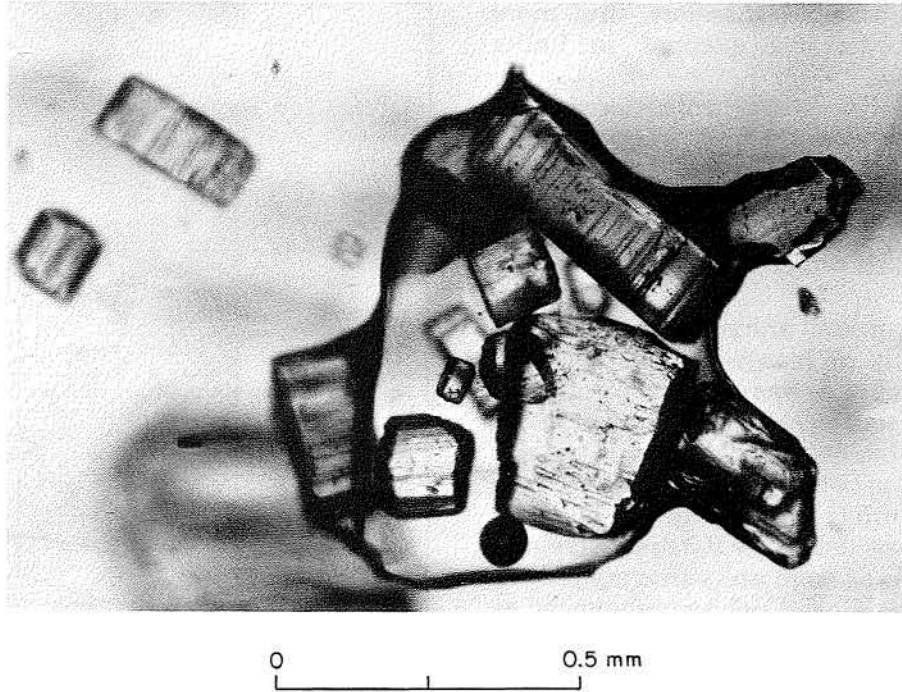


Figure 30. Photomicrograph of an irregular brine inclusion in halite grain from the R-3 zone; inclusion contains numerous anhydrite crystals. Plane-polarized light, depth 354.6 m.

volume of bubbles in brine inclusions from Rayburn's and Vacherie Domes (Roedder and Belkin, 1979). A minority of brine inclusions attached to the surface of anhydrite crystals also contain a bubble.

To determine the distribution of brine inclusions within the R-3 zone, 30 samples of rock salt were taken at 2-cm intervals throughout this zone. The upper 25-cm interval contains approximately 20 cuboid inclusions per cm^3 , whereas the lower 35-cm interval contains only 2 inclusions per cm^3 (fig. 31 and table 2); maximum recorded concentration is 36 inclusions per cm^3 . The volume of brine contained in cuboid inclusions in the upper interval is 0.05 percent, as compared with 0.0005 percent in the lower interval. Roedder and Belkin (1979) estimated a comparable range of 0.001 to 0.01 volume percent in rock salt from Louisiana salt domes. The distribution of cuboid brine inclusions is erratic, particularly in the lower 35-cm interval. Here, large, isolated crystals of halite (generally containing very few anhydrite grains) enclose numerous brine inclusions, whereas surrounding halite crystals contain only a few inclusions.

Three possible explanations exist for these differing quantities of intracrystalline cuboid inclusions in the upper and lower sections of the

R-3 zone. We consider the second and third to be more plausible.

(1) The upper 25-cm interval contains an average of only 0.2 percent anhydrite, as compared with 4.9 percent in the lower 35 cm of rock salt. Abundant disseminated anhydrite in the lower interval may have inhibited recrystallization of halite, which may in turn have influenced the amount of brine that was trapped. A negative correlation coefficient for volume-percent anhydrite versus number of cuboid inclusions per cm^3 for all 30 samples from the R-3 zone is significant at the 99-percent level of confidence, which supports this hypothesis. However, the negative correlation coefficient for the upper part of the R-3 zone is barely significant at the 90-percent level of confidence. For the lower part of the interval, the correlation is positive, but not statistically significant. It appears, therefore, that the negative correlation between volume percent anhydrite and frequency of cuboid brine inclusions for the entire R-3 zone is not meaningful, so the control of disseminated anhydrite on the trapping of cuboid fluid inclusions cannot be substantiated.

(2) The upper 25 cm, containing most of the cuboid inclusions, is nearer the cap-rock contact, which is inferred to be a former site of rock-salt

dissolution. It is possible, therefore, that more intracrystalline brine was trapped in halite nearest this contact.

(3) Roedder and Belkin (1979) noted that most of the brine in their samples was trapped along halite-anhydrite grain boundaries. It is possible that the lower interval contains as much brine as the upper 25-cm interval, but in the form of intercrystalline films rather than intracrystalline cuboid inclusions.

Films of liquid around anhydrite inclusions in halite are difficult to recognize (fig. 32), and measurement of volumes was not possible. Liquid fillets connecting two or more anhydrite crystals are easily visible, but determination of volumes is difficult because of their irregular shape. The frequency of the fillets is 3 per cm^3 for both the upper and lower intervals of the R-3 zone. Elongate fillets between two or more anhydrite crystals in halite are rare (fig. 33) and not as pronounced as those reported by Roedder and Belkin (1979). Those authors attributed the elongation to stretching during deformation of the rock salt, followed by recrystallization of the halite. This is an unlikely mechanism for the elongate inclusions in Oakwood Dome because they have not been previously identified within deformed halite. Oakwood inclusions appear to have formed after deformation, during normal grain growth. Twelve fluid inclusions were found in anhydrite crystals from the upper 25-cm interval of the R-3 zone (fig. 34). All of these inclusions contain a bubble, and one contains an unidentified crystal.

Origin of Brine Inclusions

Brine trapped within halite crystals, notably in the R-3 zone, could represent connate seawater, deep formation water, or shallow ground water (Roedder and Belkin, 1979). If the brine was derived from connate seawater or deep formation water, it would be present throughout the salt core, including the foliated R-1 zone. However, this fluid would be difficult to recognize. First, the brine might well be present as intercrystalline films between halite grains rather than as intracrystalline inclusions; Parrish (1979) has shown experimentally that brine in deformed rock salt is apparently confined to grain boundaries and only becomes incorporated as intracrystalline inclusions after high-temperature annealing of the foliated rock salt. Second, intercrystalline brine films are present in the foliated Oakwood salt, but it is difficult to determine whether water was trapped naturally at depth, introduced from drilling fluid, or hygroscopically absorbed during transportation and storage of the core.

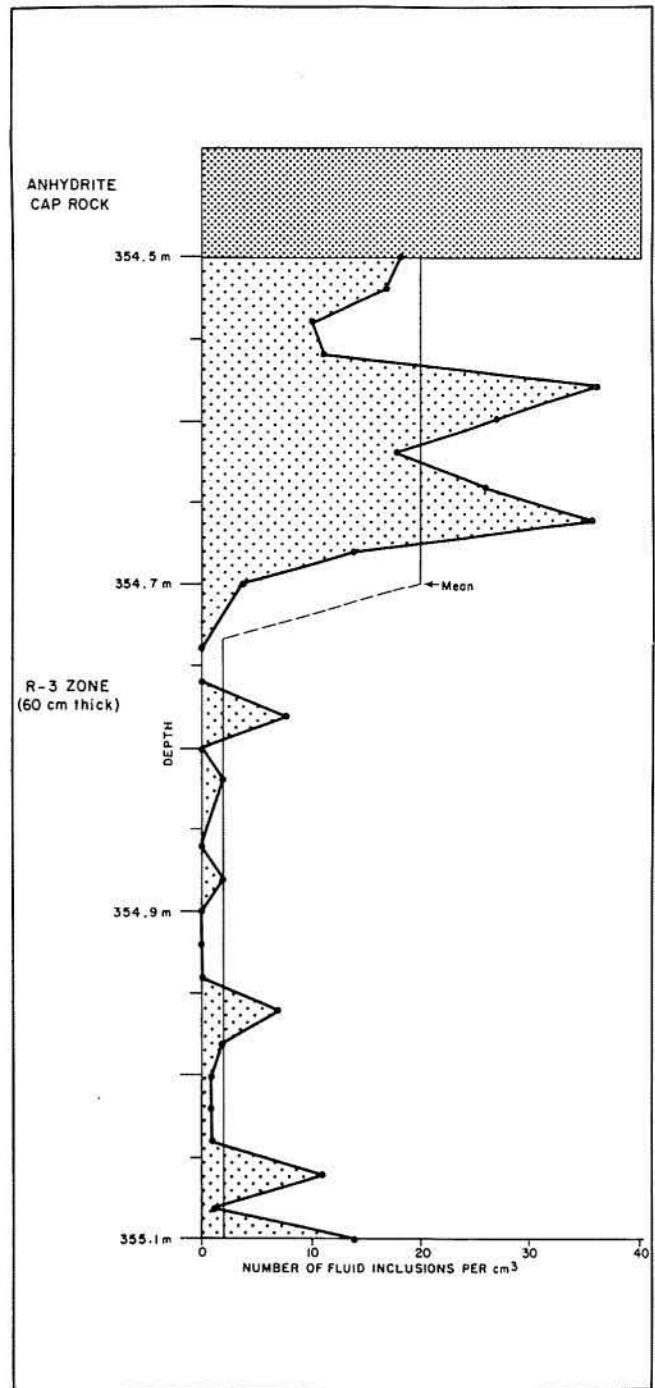


Figure 31. Graph showing the concentration of cuboid brine inclusions in rock salt of the R-3 zone.

If the water was derived largely from surrounding shallow aquifers, it could have entered from the margins of the dome along the cap-rock contact, or it may have moved down through the porous calcite cap rock and fractures in the underlying anhydrite zone. The upward increase in the proportion of intracrystalline cuboid brine inclusions in the recrystallized R-3 zone (fig. 31) toward the cap rock suggests that the brines moved down from the base of the cap rock. However, as discussed previously, it is probable that some brine is present along anhydrite grain boundaries in the lower part of the R-3 zone, so the

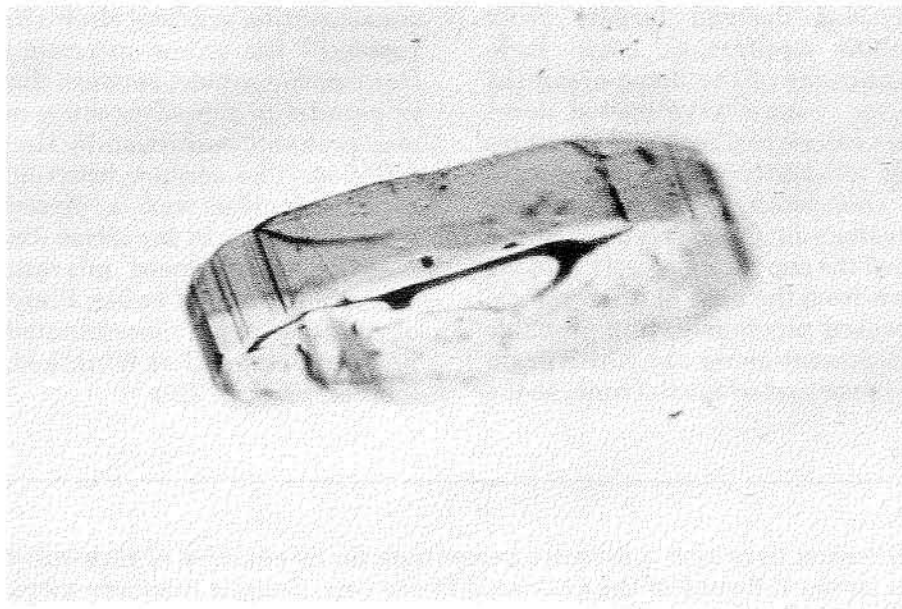
concentration gradient shown in figure 31 does not represent the entire spectrum of trapped brine. Because the contact between the R-1 and R-2 zones is parallel to the schistosity, migration of brine was probably controlled by the anisotropy of the foliation. The contact between the R-2 and R-3 zones coincides with a disseminated-anhydrite layer and dips in the same direction. Anhydrite may have influenced migration of water and recrystallization of halite. Preferential movement of moisture along disseminated-anhydrite layers has been reported at Winnfield Dome, Louisiana (Huner, 1939, p. 219).

Table 2. Fluid-inclusion data and anhydrite percentage for 30 samples of rock salt collected at 2-cm vertical intervals in the R-3 zone of the Oakwood Dome core. Sample numbers increase with depth.

Sample number	Sample volume (cm ³)	Number of inclusions (in sample) (cm ⁻³)		Mean diameter (mm)	Percentage fluid inclusions as fillets	Weight percent anhydrite*
1	3.1	57	18	0.22	10	0.10
2	1.5	25	17	0.19	19	0.08
3	3.2	32	10	0.27	9	0.05
4	2.4	26	11	0.25	16	0.07
5	2.4	86	36	0.21	0	0.08
6	2.4	65	27	0.19	3	0.07
7	2.7	48	18	0.27	28	0.16
8	2.5	66	26	0.17	11	0.14
9	2.7	96	36	0.21	6	0.08
10	2.5	35	14	0.14	19	0.45
11	2.3	9	4	0.26	61	1.17
12 [†]						
13	1.6	0	0	----	0	3.63
14	2.4	0	0	----	0	6.32
15	2.2	17	8	0.11	0	5.34
16	2.5	0	0	----	0	5.18
17	2.4	5	2	0.09	0	2.00
18	2.1	2	1	0.06	33	3.83
19	2.6	0	0	----	0	1.85
20	2.4	5	2	0.08	0	1.34
21	2.7	0	0	----	100	0.67
22	1.7	0	0	----	0	1.38
23	2.2	0	0	----	0	5.04
24	2.6	18	7	0.06	42	3.60
25	2.0	4	2	0.08	60	4.34
26	1.4	2	1	0.18	83	14.25
27	1.5	2	1	0.06	87	10.23
28	2.2	2	1	0.11	87	5.35
29	1.5	16	11	0.10	47	8.75
30	1.8	2	1	0.06	93	4.88
31	1.7	22	14	0.13	63	4.54

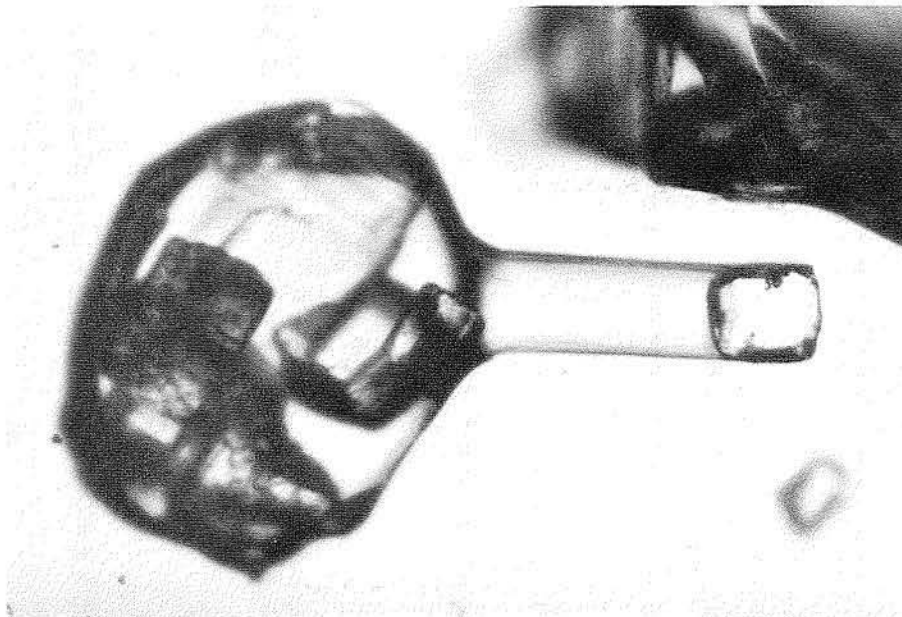
*Determined by weighing cleavage fragments of halite, dissolving the halite, and weighing the insoluble residue of anhydrite.

[†]Missing core interval.



0 0.5 mm

Figure 32. Photomicrograph showing irregular film of liquid on an anhydrite crystal enclosed in halite. Dark appearance of liquid is due to internal reflection. Cleavage fragment, plane-polarized light, depth 354.6 m.



0 0.2 mm

Figure 33. Photomicrograph showing elongate fillet of brine between two anhydrite crystals in halite. Cleavage fragment, plane-polarized light, depth 354.6 m.

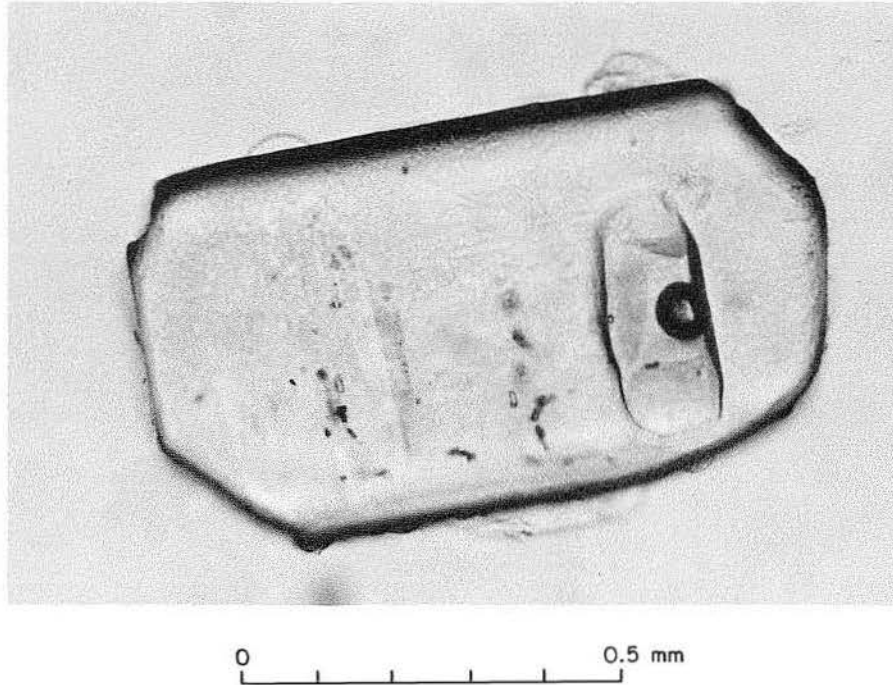


Figure 34. Photomicrograph of anhydrite grain containing a bubble-bearing fluid inclusion. The grain was dissolved out of R-3 rock salt. Plane-polarized light, depth 354.6 m.

Compressed-Gas Inclusions

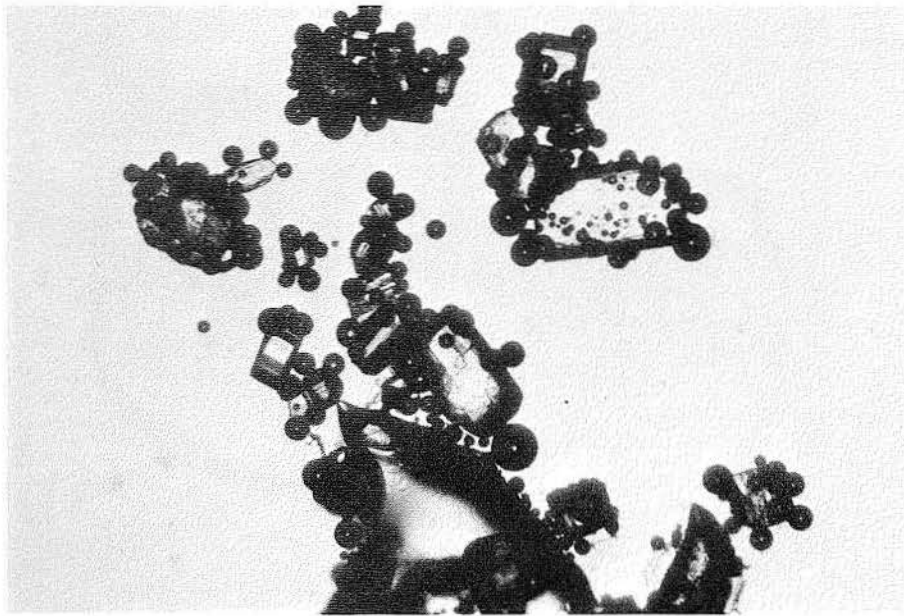
Inclusions consisting entirely or largely of compressed gas are present on most halite-anhydrite grain boundaries throughout the rock-salt core. They form either numerous discrete bubbles and blebs on the grain boundaries or thin films that are not optically detectable (compare Roedder and Belkin, 1979). The films were identified by experimental dissolution of small fragments of rock salt in fresh water. As dissolution fronts moved along halite-anhydrite grain boundaries, small bubbles (about 0.02 mm in diameter) formed rapidly at the boundary. These coalesced within seconds to produce large bubbles (fig. 35).

Compressed-gas inclusions in negative crystals (without recognizable brine) are most common in rock-salt layers in the cap rock but are also present in the R-3 rock salt. These, too, were identified by experimental dissolution of the enclosing halite. Inclusions range in size from less than 0.01 mm to more than 0.40 mm; local concentrations range as high as hundreds or thousands of gas inclusions per cm^3 (fig. 36). On breaching of the inclusions, volume of the colorless gas increased with a dilation, Δ , of 50 to 150. Compressed-gas inclusions similar to these have been reported from domes in Louisiana (Hoy and others, 1962; Roedder and Belkin, 1979).

Pressures and Temperatures During Halite Recrystallization

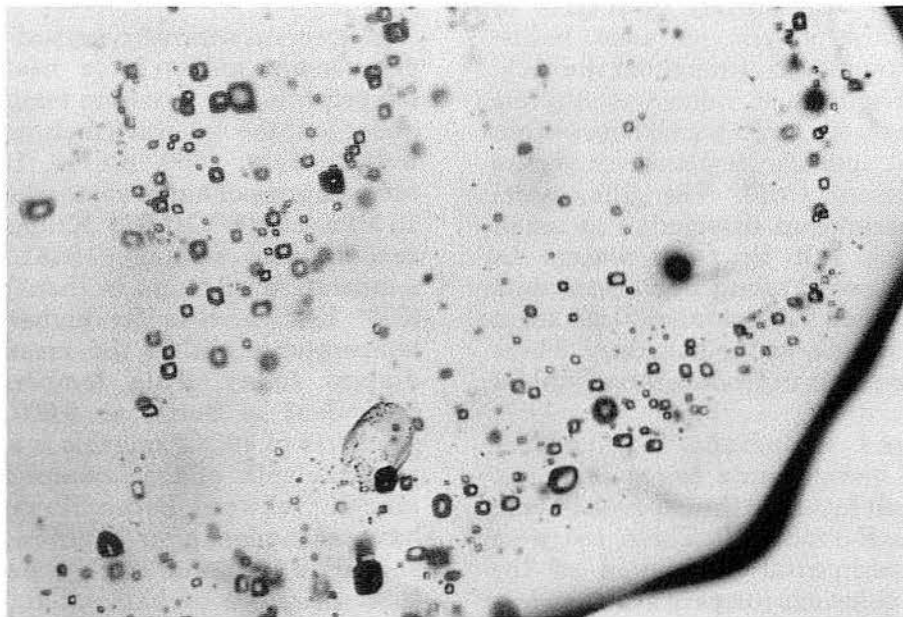
A mineral will not recrystallize in the absence of solvents unless it is heated to a critical temperature (the Tamman temperature), which is about half the mineral's melting point, in degrees Kelvin (Spry, 1969, p. 116, 123). The melting temperatures of halite at standard pressure and at 15 MPa are 800° C (1,073° K) and 803° C (1,076° K), respectively (Clark, 1966). The Tamman temperature of halite is therefore about 265° C (538° K), which is far higher than maximum temperatures within the crests of East Texas diapirs today. This temperature would be equivalent to burial at 6,600 m with a high geotherm of 40° C/km; this is approximately the present depth of the Louann Salt source layer around Oakwood Dome. Recrystallization must have taken place after diapiric emplacement of the salt, or all the halite would show evidence of flow. It is therefore probable that, given the lower temperatures and pressures in the diapiric crest, recrystallization of halite in the R-2 and R-3 zones was promoted by intercrystalline brines that migrated down from the rock-salt - cap-rock contact.

Assuming that the eightfold to tenfold expansion by bubbles in cuboid inclusions of the R-3 zone represents expansion of gas without a



0 1 mm

Figure 35. Photomicrograph showing bubbles of decompressed gas released from anhydrite-halite grain boundaries during experimental dissolution of halite in water. Largest crystal is remnant of partially dissolved halite; other grains are insoluble anhydrite released during halite dissolution. Plane-polarized light, depth 403.3 m.



0 0.5 mm

Figure 36. Photomicrograph of compressed-gas inclusions in negative crystals in rock salt isolated within the anhydrite cap rock. Note apparent banding defined by a zone of inclusions parallel to the grain boundary. Cleavage fragment, plane-polarized light, depth 317.7 m.

phase change (compare Roedder and Belkin, 1979), we calculated the pressure at which the inclusions were trapped to be 0.8 to 1.0 MPa. The gas inclusions in rock salt from the cap rock contain no liquid, so their 50- to 150-dilation on rupturing did not involve a phase change. Consequently these inclusions were trapped at pressures between 5 and 15 MPa.

Depth equivalents of these pressures were calculated by assuming that the gas pressure was in equilibrium with the hydrostatic and lithostatic pressure. Estimating average overburden densities of between 2.0 and 2.4 g/cm³, the corresponding pressure gradient is between 0.0196 MPa/m and 0.0235 MPa/m (Gretener, 1979, p. 12). For the cuboid brine inclusions located at an actual depth of 355 m, anomalously low trapping depths of 35 m and 50 m were calculated. In

contradistinction, the gas inclusions located at an actual depth of 315 m are calculated to have been trapped in a depth range of between 213 and 765 m.

Inclusions were sealed either in the crest of the salt stock during recrystallization or in the fractured anhydrite cap rock during precipitation of halite from solution. Without positive identification of the gas, its source cannot be identified. Cooling of the brine inclusions from a high temperature of formation to room temperature reduced the pressure of the gas bubbles to some extent by allowing them to expand as the fluid contracted; however, contraction of the liquid would be insufficient to account fully for the low gas pressures. It is also possible that gas pressure was lowered by leakage through microfractures during coring.

GEOCHEMISTRY

Selected aspects of the rock-salt geochemistry have been used to determine the anhydrite content of the rock salt and to elucidate the crystallization history of the halite. Thirty-eight samples of rock salt were taken from the core at intervals of approximately 1.5 m. Inductively Coupled Plasma Atomic Emission Spectroscopy (ICP) enabled simultaneous analysis for the elements beryllium, sodium, magnesium, aluminum, calcium, titanium, vanadium, chromium, manganese, iron, cobalt, nickel, copper, zinc, arsenic, selenium, strontium, molybdenum, cadmium, tin, antimony, barium, and lead. Samples were dissolved in dilute HNO₃ and fused at high temperature with Li₂B₄O₇. Sulfate contents were determined by digestion with dilute HCl and by turbidimetric analysis. Bromine contents were determined by digestion with dilute HCl, oxidation with Ca(OCl)₂, addition of Na₂MoO₄·2H₂O, KI, and H₂SO₄, and titration with Na₂S₂O₃.

To calculate the anhydrite content of the rock salt directly from the chemical analyses, it was necessary to assume that all the sulfate ions were derived from anhydrite. Table 3 shows the calculated anhydrite contents of the 39 samples of Oakwood rock salt. The mean anhydrite content and error for the entire 57.3-m section of rock-salt core was calculated to be 1.3 ± 0.7 percent at the 95-percent level of confidence. For comparative purposes, the mean anhydrite content was calculated by a second method, using both geochemical data and the core log. The core was divided into "pure" rock salt (<0.5 percent anhydrite) and anhydrite-rich rock salt. Because

the darkness of a layer is proportional to the concentration of disseminated anhydrite, the layers were subdivided into three categories: pale layers (2 percent anhydrite), dark layers (9 percent anhydrite), and the anhydrite-rich layer (60 percent anhydrite). Mean anhydrite contents of the three types of layers were calculated from geochemical analyses. Anhydrite content of the entire salt core was then calculated by adding the thicknesses of each layer determined by core logging. This method gave a mean anhydrite content of 1.9 percent, which is comparable to results obtained by the first method.

The distribution coefficient of bromine in halite is well established by observation and experimentation on natural and artificial salt ponds (Holser, 1966; Herrmann, 1972; Herrmann and others, 1973). Distribution coefficients depend on the relative ease with which a trace element, such as bromine, can replace chlorine during precipitation of halite. Because the distribution coefficient for bromine in halite is much less than 1, this element is not easily incorporated into the growing halite crystals (Holser, 1979). The normal concentration of bromine in sea water is 65 to 75 ppm, a concentration that rises to about 510 ppm when water has evaporated to the point where halite begins to crystallize. Because of the distribution coefficient, initially formed halite contains only 65 to 75 ppm of bromine, a concentration that rises to about 200 ppm in the most concentrated brines just before precipitation of potassium salts. If this first-cycle halite is subsequently redissolved in marine water, it

contributes a very small amount of bromine, compared with sodium chloride, to the brine, which therefore becomes relatively depleted in bromine. Governed by the distribution coefficient, second-cycle halite that begins to precipitate from this modified brine has less than 20 ppm bromine. Such depletion of bromine in halite therefore indicates chemically recycled halite (Holser, 1979).

Halite samples from the Oakwood rock-salt core have a range of 37 to 50 ppm bromine and a mean value of 45 ppm (table 3). This mean is intermediate between first-cycle and second-cycle halite. These bromine contents suggest chemical modification by partial re-resolution of halite and later homogenization of bromine in mixtures of first- and second-cycle halite; it is also possible that brine containing redissolved halite became sufficiently concentrated by evaporation to raise the bromine contents to an intermediate level of 45 ppm. The time of this chemical recycling is not known but it must have been before the R-2 zone of rock salt recrystallized because halite from this zone has a bromine content of 50 ppm (table 3). If this halite had been redissolved to a greater extent than the foliated rock salt, it would have had a below-average bromine content. This suggests that the R-2 halite recrystallized in the presence of very small amounts of water, a situation that is also indicated by the survival of discrete layers of disseminated anhydrite exhibiting transposition on a millimeter scale. The R-3 zone of rock salt just below the cap-rock contact has the lowest bromine content (37 ppm); significantly, this zone is thought to have been in contact with more water than the R-2 zone because of the coarser grain size and more abundant intracrystalline brine inclusions.

The rock-salt inclusion 318.97 m deep in the cap rock was also analyzed. This halite contains only 23 ppm bromine, indicative of complete re-resolution of first-cycle halite and reprecipitation from brine in a cavity in the cap rock; the 1.5 percent disseminated anhydrite present could have been derived from the cap rock.

In summary, the bromine contents of halite are compatible with conclusions reached on the basis of textural and structural relations. Conclusions are that most rock salt (R-1 and R-2 zones) consists of metamorphosed evaporites that have undergone partial re-resolution before or during diapirism; that the uppermost unfoliated rock salt (R-3 zone) has undergone more advanced chemical recycling by recrystallization in the presence of some water; and that the rock-salt inclusion in the cap rock precipitated from solution in a cavity.

Table 3. Anhydrite contents* of rock salt and bromine contents† of halite in Oakwood Dome core.

Sample	Depth (m)	Petrologic zone	Anhydrite in rock salt (%)	Bromine in halite (ppm)
ODG-39	354.70	R-3	0.03	37
ODG-1	355.37	R-2	0.25	50
ODG-2	356.92	R-1	0.39	47
ODG-3	358.51	R-1	0.83	48
ODG-4	360.03	R-1	1.94	46
ODG-5	361.46	R-1	0.14	45
ODG-6	363.14	R-1	0.51	44
ODG-7	365.24	R-1	0.03	45
ODG-8	366.06	R-1	0.78	48
ODG-9	367.53	R-1	1.22	44
ODG-10	369.08	R-1	1.28	45
ODG-11	370.67	R-1	0.20	44
ODG-12	372.25	R-1	1.16	44
ODG-13	374.57	R-1	0.22	46
ODG-14	375.33	R-1	1.40	45
ODG-15	376.85	R-1	0.20	47
ODG-16	378.35	R-1	0.61	44
ODG-17	379.75	R-1	1.37	44
ODG-18	380.79	R-1	0.29	43
ODG-19	382.74	R-1	0.08	45
ODG-20	384.14	R-1	7.33	42
ODG-21	385.94	R-1	0.23	44
ODG-22	387.46	R-1	1.20	44
ODG-23	388.99	R-1	1.14	46
ODG-24	390.54	R-1	0.03	42
ODG-25	392.06	R-1	0.03	42
ODG-26	393.53	R-1	0.81	42
ODG-27	395.45	R-1	0.50	44
ODG-28	396.42	R-1	0.13	45
ODG-29	398.10	R-1	1.93	42
ODG-30	399.68	R-1	0.18	43
ODG-31	401.21	R-1	10.80	50
ODG-32	402.82	R-1	1.68	43
ODG-33	404.26	R-1	5.31	44
ODG-34	405.38	R-1	0.40	45
ODG-35	407.18	R-1	0.47	45
ODG-36	409.01	R-1	1.56	45
ODG-37	410.17	R-1	1.33	43
ODG-38	410.81	R-1	0.96	45
Standard deviation			2.10	2.3
Standard error			0.34	0.4
Mean and error at 95% confidence level			1.26 ± 0.67	44.5 ± 0.7

*Weight percent calculated from whole-rock analyses by assuming all SO_4^{2-} ions are derived from anhydrite.
†Calculated from whole-rock analyses by assuming all Na^+ ions are derived from halite.

ORIGIN OF ANHYDRITE CAP ROCK

Three hypotheses were advanced early in this century to explain cap rock overlying salt domes:

(1) *Original strata hypothesis*: All or part of the cap rock was derived from sedimentary anhydrite beds that originally overlay bedded rock salt. The anhydrite was pushed up by the rising salt stock and was brecciated, recemented, and altered in the presence of ground water.

(2) *Deposition from solution hypothesis*: Gypsum or anhydrite was precipitated when ground water containing calcium sulfate mixed with highly saline water above salt domes (Barton, 1925), or meteoric water containing calcium carbonate mixed with sulfate-bearing waters associated with salt domes (Stuart, 1931). Walker (1976) proposed that halite and anhydrite were dissolved from the flanks of a dome by rising ground water and reprecipitated at the diapiric crest.

(3) *Residual accumulation hypothesis*: Formulated by German geologists in the early 1900's, this hypothesis was subsequently applied to Gulf Coast salt domes (Barton, 1925; Van der Gracht, 1925). Rock salt was dissolved at the crest of the diapir, and the insoluble residue (mainly anhydrite) was recrystallized or cemented to form cap rock. Alteration of the anhydrite cap rock is thought to have produced the gypsum, sulfur, and calcite zones. This hypothesis has received the most support in recent years (Goldman, 1933; O'Donnell, 1935; Taylor, 1938, p. 91; Bodenlos, 1970; Halbouty, 1979, p. 45; Dutton and Kreitler, 1980).

In evaluating these three hypotheses, certain characteristics of Gulf Coast salt stocks are pertinent:

(1) The anhydrite content of rock salt is generally less than 5 percent (Huner, 1939, p. 291; Kupfer, 1963), somewhat less than that of the Zechstein salt stocks in Germany (DeGolyer, 1925). If all the anhydrite was derived from the salt stock, dissolution of great thicknesses of rock salt has to be postulated. In the case of Oakwood Dome, about 6 km of salt would have had to be dissolved to yield a 120-m-thick anhydrite residue. This is comparable to estimates of salt loss based on calculation of the volume of the salt-withdrawal basin around Oakwood Dome (S. Seni, personal communication, 1981).

(2) About 55 percent of the domes have a cap rock (Hawkins and Jirik, 1966), ranging from less than 3 m to more than 450 m thick (Walker, 1974). Below the Five Islands of Louisiana, the domes with little or no cap rock (Jefferson Island, Weeks

Island, and Avery Island Domes) have little anhydrite in the rock salt, but Belle Isle Dome rock salt is overlain by relatively thick cap rock and contains substantially more impurities than that of other domes (Vaughan, 1925).

(3) Disseminated-anhydrite layers in the rock salt of the diapir crest generally have a steep to vertical dip (Vaughan, 1925; Balk, 1949, 1953; Eargle, 1962; Hoy and others, 1962; Muehlberger and Clabaugh, 1968; Nance and others, 1979).

(4) The upper limit of the rock salt is generally planar and horizontal (Bowman, 1925; Kelley, 1925; Hoy and others, 1962). This "salt table" truncates layers and folds within the rock salt (Taylor, 1938, p. 91).

(5) Contact between the rock salt and cap rock is of two basic types, both of which can be present within a single dome. The first type is an abrupt transition from rock salt to anhydrite cap rock. Examples are Oakwood, Hockley, Tatum, and Vacherie Domes (Teas, 1931; Goldman, 1933; Eargle, 1962; Nance and others, 1979). The second type of contact is marked by a cavity with or without anhydrite sand. Examples are Gyp Hill, Winnfield, Jefferson Island, and Lake Washington Domes (O'Donnell, 1935; Taylor, 1938, p. 53-54; Hoy and others, 1962; Dutton and Kreitler, 1980). Active flow of ground water has been documented within some of these cavities (Huner, 1939, p. 221; Hoy and others, 1962).

Many of these features are entirely compatible with the residual-accumulation hypothesis. In the case of Oakwood Dome, this hypothesis is supported by the following findings:

(1) Geometric analysis (Jackson and Dix, 1981) indicates that at least 50 m, and possibly as many as thousands of meters, of rock salt have been truncated in Oakwood Dome.

(2) At the rock-salt - cap-rock contact, the presence of an anhydrite-rich lamina across the openings of extension fractures within the cap rock proves that at least some of the cap rock formed by basal accretion of anhydrite. Because most of the overlying laminae are similar in appearance to the basal lamina, the anhydrite cap rock may have been produced by this mechanism. It may also be significant that the transition-zone lamina at the Oakwood Dome cap-rock contact is approximately as thick as laminae within the overlying cap rock (fig. 37). This relationship also holds for Hockley Dome (Goldman, 1933, his fig. 8); however, both the transition zone and the laminae of Hockley Dome are seven times as thick as those of Oakwood Dome (fig. 37).

Formation of cap rock in Oakwood Dome clearly involved complex interaction between dissolution and recrystallization of both halite and anhydrite. Table 4 outlines inferred processes in the rock salt, contact zone, and adjacent cap rock.

Approximately half the anhydrite crystals in the two transition zones of the rock-salt - cap-rock contact at Oakwood Dome show evidence of strain in the form of undulose extinction. The ratio of strained to unstrained anhydrite grains in the base of the cap rock is higher than in the rock salt; grain impingement during anhydrite concentration may be the cause. The origin of the unstrained, generally idioblastic anhydrite crystals is debatable: they could have been derived from rock salt in the diapiric crest, which contains both strained and unstrained anhydrite crystals; they may have been precipitated in the transition zone by circulating ground water (Barton, 1925; Stuart, 1931; Walker, 1976); or they may represent strained grains that subsequently underwent primary recrystallization after incorporation in the cap rock.

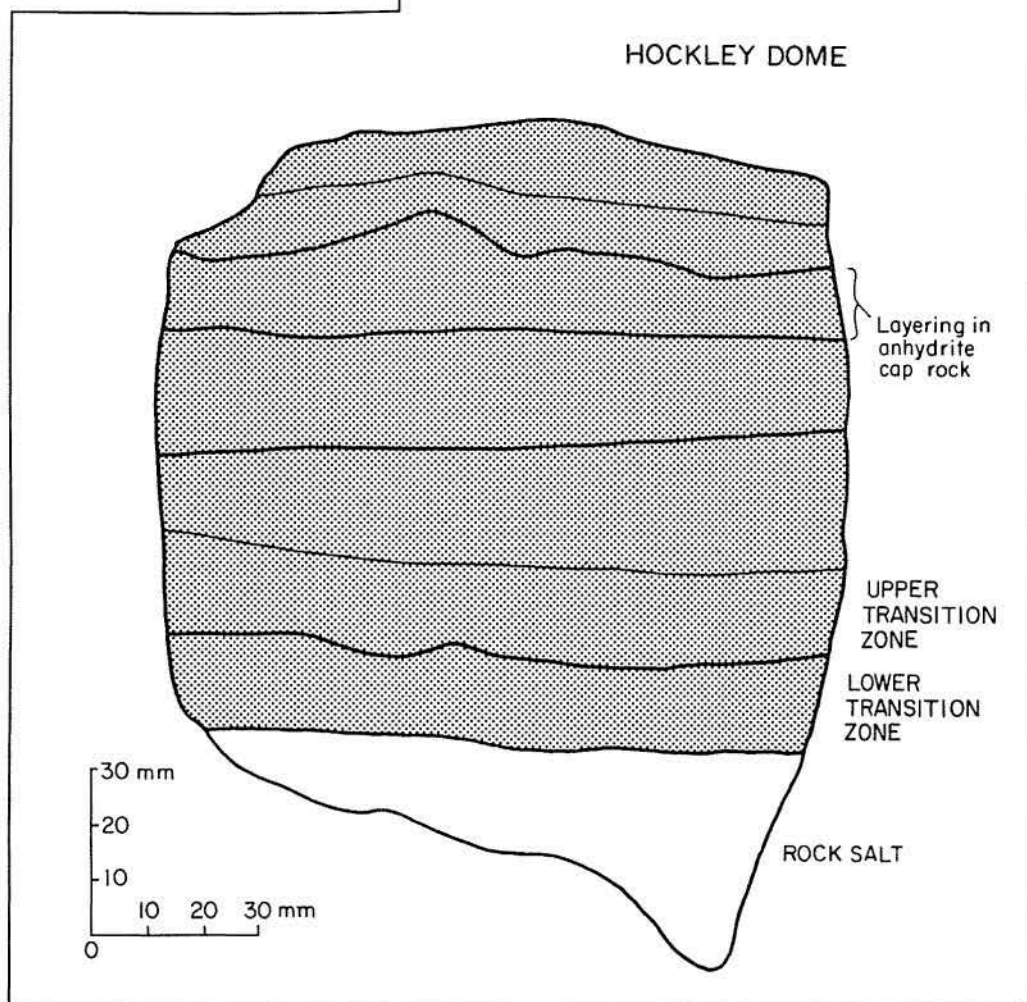
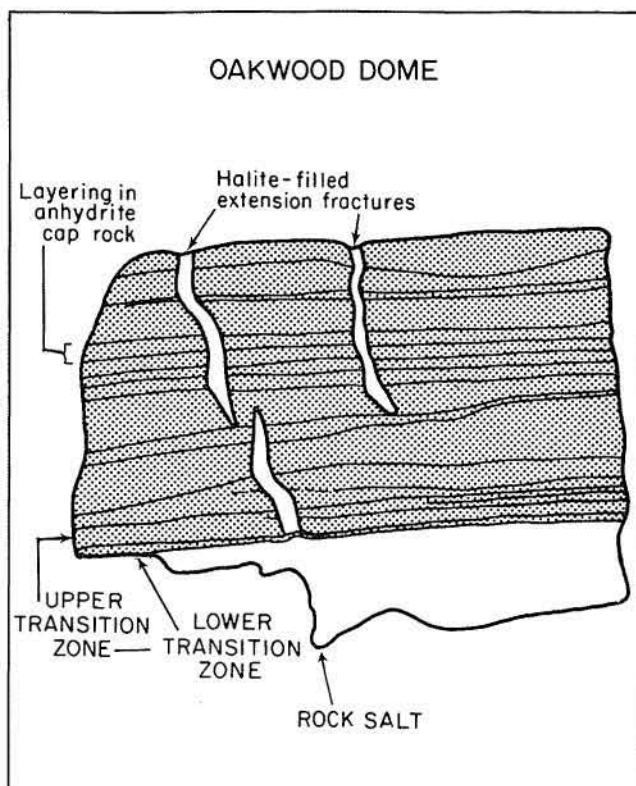


Figure 37. Cross sections showing laminae in lowermost cap rock from Oakwood and Hockley Domes. The ratio between thickness of the transition zone and mean thickness of laminae in the cap rock is similar for each dome, although the Hockley Dome layers are seven times as thick as those in Oakwood. Data for Hockley Dome from Goldman (1933, his fig. 8).

Table 4. Sequence of events in rock salt and base of cap rock in Oakwood Dome. Correlation of events between columns is tentative.

ROCK SALT	ROCK-SALT - CAP-ROCK CONTACT	BASE OF ANHYDRITE CAP ROCK
<p>Formation of schistosity in foliated rock salt (R-1 zone).</p>	<p>Concentration of the insoluble residue from dissolved rock salt (mainly anhydrite) at rock-salt - cap-rock contact.</p>	
<p>Localized cyclic dissolution of rock salt at top of salt stock.</p>	<p>Movement of brines in the solution cavity to produce structures in the anhydrite sand and possibly cause erosional truncation of laminae in cap rock.</p>	
<p>Recrystallization of foliated rock salt within 2 m of cap-rock contact by recovery and by primary recrystallization to produce medium-grained unfoliated rock salt (R-2 zone).</p>	<p>Concentration of finely disseminated intercrystalline (?) pyrite near base of anhydrite sand.</p>	
<p>Further recrystallization of unfoliated rock salt within 0.6 m of cap-rock contact by normal grain growth to produce coarse-grained unfoliated rock salt (R-3 zone). Trapping of fluids in cuboid negative crystals.</p>	<p>Rise of salt stock to form transition zone of anhydrite sand in matrix of recrystallized halite at rock-salt - cap-rock contact.</p>	
	<p>Removal of halite in the transition zone and reconcentration of anhydrite at top of salt stock during further dissolution of rock salt.</p>	<p>Removal of halite matrix from transition zone; limited recrystallization of anhydrite. Lamina of anhydrite accretes against base of preexisting cap rock.</p>
		<p>Localized pressure solution of anhydrite along horizontal planar zones to produce spaced pressure-solution cleavage (stylolites). Filling of intergranular extension voids and pressure shadows by mass transfer of pressure-dissolved anhydrite.</p>
		<p>Formation of vertical extension fractures; fracture filling by halite during extension.</p>
		<p>Further vertical shortening reflected in (1) slight buckling of the vertical, halite-filled extension fractures and (2) formation of steeply inclined, conjugate, shear fractures that offset stylolites.</p>

SUMMARY

Table 4 summarizes the inferred sequence of events in the rock-salt - cap-rock contact. All but the upper 2 m of rock-salt has strong penetrative schistosity and parallel cleavage dipping at 30° to 40°. This fabric was produced by deformation of the rock salt during diapirism. Recrystallization of the foliated rock salt produced a granoblastic-polygonal texture in the upper 2 m of core. Recrystallization was probably promoted by downward movement of intercrystalline brine from the rock-salt - cap-rock contact. Bromine concentrations in halite suggest that the rock salt of the recrystallized R-3 zone has been chemically recycled by limited re-solution to a greater degree than has the remainder of the rock salt. The amount of brine trapped as fluid inclusions in the rock salt is minute (less than 0.05 percent). Maximum concentration is directly below the cap-rock contact, which we infer to have acted as a path enabling brines to reach the center of the salt-stock crest. The absence of a cavity at the contact between rock salt and cap rock indicates that the salt stock is not being dissolved in the zone intersected by the borehole, and that past dissolution has been compensated for by diapiric rise of rock salt.

The presence of an anhydrite-rich lamina across halite-filled extension fractures at the base

of the cap rock indicates that anhydrite lamina have accreted against the base of the cap rock. Horizontal lamination throughout the anhydrite cap rock is thought to reflect this process. The 57.3 m of rock-salt core from Oakwood Dome contains an average of 1.3 ± 0.7 percent anhydrite. If all the cap rock was derived by residual accumulation of such low concentrations of anhydrite, dissolution of more than 6 km of rock salt would be required (slightly more than the present height of the salt stock). This value is comparable to estimates based on calculation of the volume of the salt-withdrawal basin around Oakwood Dome.

Upward force from the rising salt stock probably induced the observed vertical shortening in the cap rock just above the contact. This strain resulted in horizontal, spaced, stylolitic cleavage formed by pressure solution and mass transfer of anhydrite. The stylolitic cleavage, which is marked by a dark, insoluble pyritic residue, transects the older lamination that we believe results from cycles of anhydritic accretion against the base of the cap rock. Further lateral extension and vertical shortening in the base of the cap rock resulted in halite-filled vertical extension fractures and inclined shear fractures that postdate both the cap-rock lamination and the stylolitic cleavage.

SIGNIFICANCE FOR STORAGE OF NUCLEAR WASTES

The internal structure of Oakwood Dome was studied principally to reveal how rock salt flows during the emplacement of a diapir and to allow assessment of the probability and nature of solid flow in the future. Such predictions are vitally important for the safe containment of high-level nuclear wastes that require long periods of isolation. Early observations of the contact zone between rock salt and cap rock supplied abundant evidence of the importance of fluids in almost every process inferred to have taken place: recrystallization of rock salt, dissolution of rock salt, diapiric rise of the salt stock, the formation of laminated anhydrite cap rock, and deformation and self-sealing of the cap rock. Processes such as these serve both to breach waste repositories and to geologically isolate them. Knowledge of these processes is therefore vital for any project designed to geologically contain wastes in a salt

stock; thus, most of the study has been directed toward these fluid-related processes.

The gross internal structure of Oakwood Dome, to be described in a future Bureau report, shows that the crest of the salt stock has been truncated, almost certainly by dissolution. As much as 6 km of salt may have been dissolved during numerous episodes to form the overlying cap rock. It follows that rock salt presently at the crest of the dome has been diapirically uplifted 6 km to its present level. Oakwood Dome and all other domes in the East Texas Basin have shown a decline in uplift rates over the last 80 Ma (Seni and Jackson, in preparation); consequently, the threat of exposure due to differential uplift of salt stocks is also declining.

Water has reached the crest of the salt stock by traveling either from the flanks of the dome along the base of the cap rock or down through fractures

in the cap rock. Ingress of water initiates processes at the cap-rock contact whereby destruction of the salt stock is balanced by formation of cap rock and addition of sodium chloride to the ground water. These processes include those that are detrimental to waste isolation and those that are favorable; some processes can even be interpreted as being

both detrimental and favorable. Tables 5 and 6 summarize processes significant to isolation of nuclear wastes in domal salt. Despite the strong evidence for repeated attrition and uplift of the salt stock, the geologic system of rock salt and cap rock has the ability to offset, at least partially, these negative processes by self-sealing and recovery.

Table 5. Inferred processes within Oakwood Dome that are detrimental to storage of nuclear wastes in salt diapirs.

PROCESS OR OBSERVATION	DETRIMENTAL SIGNIFICANCE
1. Structural truncation of diapiric crest.	Considerable diapiric uplift.
2. Water-induced recrystallization of uppermost 2 m of rock salt. Greater abundance of fluid inclusions in rock salt close to cap-rock contact. Accretion of anhydrite lamina against base of cap rock. Similar appearance of lamination throughout anhydrite cap rock.	Introduction of water to diapiric crest and destruction of up to 6 km of rock salt by repeated episodes of dissolution.
3. Tight seal between rock salt and anhydrite cap rock.	Renewed uplift of salt diapir after most recent episode of dissolution.
4. Vertical extension fractures in anhydrite cap rock.	Fracturing and dilation of cap rock because of rise of salt stock, creating further avenues for ground water to enter and wastes to escape.
5. Low bromine content of halite in lens of rock salt in anhydrite cap rock.	Passage of brines through fractures in cap rock, precipitation of halite in cavities, and possible escape of brines from cap rock into surrounding strata.

Table 6. Inferred processes within Oakwood Dome that are favorable for storage of nuclear wastes in salt diapirs.

OBSERVATION	FAVORABLE SIGNIFICANCE
1. Tight seal between rock salt and anhydrite cap rock. Extension fractures and spaced cleavage in anhydrite cap rock.	Ability of salt flow driven by diapirism to close cavities and apply upward pressure on cap rock to keep cavity closed.
2. Halite-filled extension fractures in anhydrite cap rock.	Ability of halite to grow in opening fractures, thereby sealing them.
3. Horizontal, stylolitic spaced cleavage in anhydrite cap rock.	Ability of anhydrite aggregates to respond to stresses by migrating in solution to nearby pressure shadows and pore spaces, thereby reducing porosity and enhancing sealing properties of the cap rock.

ACKNOWLEDGMENTS

This study is part of the East Texas Nuclear Waste Isolation Feasibility Project, which was funded by the National Waste Terminal Storage (NWTS) Program of the U.S. Department of Energy under Contract No. DE-AC97-80ET-46617 (formerly Contract No. DE-AC97-79ET-46605). The ETWI Project of the Bureau of Economic Geology is integrated with others outside Texas by the Office of Nuclear Waste Isolation, Battelle Memorial Institute. The TOG-1 core was supplied by Law Engineering and Testing Company under the NWTS Program. TOC analyses were provided by GeoStrat, Inc.

We would like to thank the following people for their contributions to this study: A. Bein, L. F. Brown, Jr., T. E. Ewing, A. G. Goldstein, C. W. Kreitler, R. L. Bassett, and A. Kolker for reviewing the manuscript; Ginger C. Zeikus and Barbara A. Dudgeon for typing; Dorothy C. Johnson and Margaret Chastain for word processing and Fannie M. Sellingsloh for typesetting the publication, under the direction of Lucille C. Harrell; Michelle Pemberton-Gilson for editing the manuscript; Mark T. Bentley, Thomas M. Byrd, Richard P. Flores, and Jamie McClelland, under the direction of J. W. Macon, for drafting; J. A. Morgan and D. M. Stephens for photographic printing; Eva Hardeman for designing the publication; C. L. Ho, S. W. Tweedy, N. Bui, and C. Mahan for geochemical analyses; and H. J. Madsen and M. K. Plowman for preparation of thin sections.

REFERENCES

- Alvarez, W., Engelder, T., and Geiser, P. A., 1978, Classification of solution cleavage in pelagic limestones: *Geology*, v. 6, no. 5, p. 263-266.
- Balk, R., 1949, Structure of Grand Saline salt dome, Van Zandt County, Texas: *American Association of Petroleum Geologists Bulletin*, v. 33, no. 11, p. 1791-1829.
- 1953, Salt structure of Jefferson Island salt dome, Iberia and Vermilion Parishes, Louisiana: *American Association of Petroleum Geologists Bulletin*, v. 37, no. 11, p. 2455-2474.
- Barton, D. C., 1925, The salt domes of South Texas: *American Association of Petroleum Geologists Bulletin*, v. 9, no. 3, p. 536-589.
- 1933, Mechanics of formation of salt domes with special reference to Gulf Coast salt domes of Texas and Louisiana: *American Association of Petroleum Geologists Bulletin*, v. 17, no. 9, p. 1025-1083.
- Bell, T. H., and Etheridge, M. A., 1973, Microstructure of mylonites and their descriptive terminology: *Lithos*, v. 6, no. 4, p. 337-348.
- Bodenlos, A. J., 1970, Cap-rock development and salt stock movement, in Kupfer, D. H., ed., *Geology and technology of Gulf Coast salt—a symposium*: Louisiana State University, School of Geoscience, p. 73-86c.
- Bowman, W. F., 1925, The South Dayton salt dome, Liberty County, Texas: *American Association of Petroleum Geologists Bulletin*, v. 9, no. 3, p. 655-666.
- Brown, L. S., 1931, Cap-rock petrography: *American Association of Petroleum Geologists Bulletin*, v. 15, no. 5, p. 509-529.
- Clark, S. P., 1966, High-pressure phase equilibria, in Clark, S. P., ed., *Handbook of physical constants (revised edition)*: Geological Society of America Memoir 97, p. 345-370.
- DeGolyer, E., 1925, Origin of North American salt domes: *American Association of Petroleum Geologists Bulletin*, v. 9, no. 5, p. 831-874.
- Durney, D. W., 1976, Pressure-solution and crystallization deformation, in Ramsay, J. G., and Wood, D. S., eds., *A discussion on natural strain and geological structure: Philosophical Transactions of the Royal Society, London*, v. A283, p. 229-240.
- 1978, Early theories and hypotheses on pressure-solution-redeposition: *Geology*, v. 6, no. 6, p. 369-372.
- Dutton, S. P., and Kreitler, C. W., 1980, Cap rock formation and diagenesis, Gyp Hill salt dome, South Texas: *Gulf Coast Association of Geological Societies Transactions*, v. 30, p. 333-339.
- 1981, Cap rock studies in Oakwood Dome, in Kreitler, C. W., and others, *Geology and hydrology of the East Texas Basin: a report on the progress of nuclear waste isolation feasibility studies (1980)*: The University of Texas at Austin, Bureau of Economic Geology Geological Circular 81-7, p. 162-166.
- Eargle, D. H., 1962, Geology of core hole WP-1, Tatum Dome, Lamar County, Mississippi: U. S. Geological Survey Open-File Report 474-278, 50 p.
- Flinn, D., 1969, Grain contacts in crystalline rocks: *Lithos*, v. 2, no. 4, p. 361-370.
- Giles, A. B., and Wood, D. H., in preparation, Oakwood salt dome, East Texas: geologic framework and growth history: The University of Texas at Austin, Bureau of Economic Geology Geological Circular.
- Goldman, M. I., 1933, Origin of anhydrite cap rock of American salt domes: U.S. Geological Survey Professional Paper 175-D, p. 83-114.

- 1952, Deformation, metamorphism, and mineralization in gypsum-anhydrite cap-rock, Sulphur salt dome, Louisiana: Geological Society of America Memoir 50, 169 p.
- Gray, D. R., and Durney, D. W., 1979, Crenulation cleavage differentiation: implications of solution-deposition processes: *Journal of Structural Geology*, v. 1, no. 1, p. 73-80.
- Gretener, P. E., 1979, Pore pressure: fundamentals, general ramifications and implications for structural geology: American Association of Petroleum Geologists, Continuing Education Course Note Series No. 4 (revised ed.), 131 p.
- Hager, D. S., and Stiles, E., 1925, The Blue Ridge salt dome, Fort Bend County, Texas: *American Association of Petroleum Geologists Bulletin*, v. 9, no. 2, p. 304-316.
- Halbouty, M. T., 1979, Salt domes, Gulf Coast region, United States and Mexico: Houston, Gulf Publishing Company, 561 p.
- Hanna, M. A., 1934, Geology of Gulf Coast salt domes, in Wrather, W. E., and Lahee, F. H., eds., *Problems of petroleum geology*: Tulsa, American Association of Petroleum Geologists, p. 629-678.
- Hawkins, M. E., and Jirik, C. J., 1966, Salt domes in Texas, Louisiana, Mississippi, Alabama and offshore tidelands—a survey: U.S. Bureau of Mines Information Circular 8313, 78 p.
- Herrmann, A. G., 1972, Bromine distribution coefficients for halite precipitated from modern sea water under natural conditions: *Contributions to Mineralogy and Petrology*, v. 37, p. 249-252.
- Herrmann, A. G., Knake, D., Schneider, J., and Peters, H., 1973, Geochemistry of modern seawater and brines from salt pans: main components and bromine distribution: *Contributions to Mineralogy and Petrology*, v. 40, p. 1-24.
- Hobbs, B. E., Means, W. D., and Williams, P. E., 1976, *An outline of structural geology*: New York, John Wiley, 571 p.
- Holser, W. T., 1966, Bromide geochemistry of salt rocks, in Rau, J. L., ed., *Second symposium on salt*: Cleveland, Ohio, Northern Ohio Geological Society, v. 1, p. 248-275.
- 1979, Trace elements and isotopes in evaporites, in Burns, R. G., ed., *Marine minerals: Mineralogical Society of America Short Course Notes 6*, p. 295-336.
- Hoy, R. B., Foose, R. M., and O'Neill, B. J., Jr., 1962, Structure of Winnfield salt dome, Winn Parish, Louisiana: *American Association of Petroleum Geologists Bulletin*, v. 46, no. 8, p. 1444-1459.
- Huner, J., Jr., 1939, Geology of Caldwell and Winn Parishes: *Louisiana Geological Survey Bulletin* 15, 356 p.
- Jackson, M. P. A., in preparation, Natural strain in rock salt from Oakwood Dome, East Texas: implication for structural stability: The University of Texas at Austin, Bureau of Economic Geology Report of Investigations.
- Jackson, M. P. A., and Dix, O. R., 1981, Geometric analysis of macroscopic structures in Oakwood salt core, in Kreitler, C. W., and others, *Geology and geohydrology of the East Texas Basin: a report on the progress of nuclear waste isolation feasibility studies (1980)*: The University of Texas at Austin, Bureau of Economic Geology Geological Circular 81-7, p. 177-182.
- Judson, S. A., and Stamey, R. A., 1933, Overhanging salt on domes of Texas and Louisiana: *American Association of Petroleum Geologists Bulletin*, v. 17, no. 12, p. 1492-1520.
- Kelley, P. K., 1925, The Sulphur salt dome, Louisiana: *American Association of Petroleum Geologists Bulletin*, v. 9, no. 3, p. 479-496.
- Kreitler, C. W., Wermund, E. G., Guevara, E. H., Giles, A. B., and Fogg, G., 1978, Preliminary evaluation of salt domes in East Texas for the National Waste Terminal Storage Program: U.S. Department of Energy, Interim Contract Report, 16 p.
- Kupfer, D. H., 1963, Structure of salt in Gulf Coast domes, in Bersticker, A. C., ed., *Symposium on salt*: Cleveland, Ohio, Northern Ohio Geological Society, p. 104-123.
- 1970, Mechanism of intrusion of Gulf Coast salt, in Kupfer, D. H., ed., *Geology and technology of Gulf Coast salt: a symposium*: Louisiana State University School of Geoscience, p. 25-66.
- Martin, R. G., 1978, Northern and eastern Gulf of Mexico continental margin: stratigraphic and structural framework, in Bouma, A. H., Moore, G. T., and Coleman, J. M., eds., *Framework, facies, and oil-trapping characteristics of the upper continental margin*: American Association of Petroleum Geologists Studies in Geology, no. 7, p. 21-42.
- 1980, Distribution of salt structures in the Gulf of Mexico: map and descriptive text: U. S. Geological Survey Map MF-1213, 8 p.
- Muehlberger, W. R., 1959, Internal structure of Grand Saline salt dome, Van Zandt County, Texas: University of Texas, Austin, Bureau of Economic Geology Report of Investigations No. 38, 22 p.
- Muehlberger, W. R., and Clabaugh, P. S., 1968, Internal structure and petrofabrics of Gulf Coast salt domes, in Braunstein, J., and O'Brien, G. B., eds., *Diapirism and diapirs*: American Association of Petroleum Geologists, Memoir 8, p. 90-98.


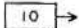

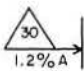

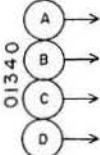
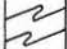

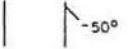
- Nance, D., Rovik, J., and Wilcox, R. E., 1979, Lithology of the Vacherie salt dome core: Louisiana State University, Institute for Environmental Studies, 343 p.
- Nance, D., and Wilcox, R. E., 1979, Lithology of the Rayburn's Dome salt core: Louisiana State University, Institute for Environmental Studies, 307 p.
- Nelson, R. A., 1981, Significance of fracture sets associated with stylolite zones: American Association of Petroleum Geologists Bulletin, v. 65, no. 11, p. 2417-2425.
- O'Donnell, L., 1935, Jefferson Island salt dome, Iberia Parish, Louisiana: American Association of Petroleum Geologists Bulletin, v. 19, no. 11, p. 1602-1644.
- Parrish, D., 1979, Transient creep in rock salt, *in* Technical progress report for the quarter 1 October to 31 December, 1979: Battelle Memorial Institute, Office of Nuclear Waste Isolation, p. 27-31.
- Ramsay, J. G., 1980, Pressure solution and tectonic deformation in limestone, *in* Cristallisation, déformation, dissolution des carbonates. Symposium organized by Université de Bordeaux III Institut de Géodynamique, Bordeaux, November 17-18, 1981, p. 389-397.
- Roedder, E., and Belkin, H. E., 1979, Fluid inclusions in salt from the Rayburn and Vacherie Domes, Louisiana: U.S. Geological Survey Open-File Report 79-1675, 26 p.
- Schlichta, P. J., 1968, Growth, deformation, and defect structure of salt crystals, *in* Mattox, R. B., ed., Saline deposits: Geological Society of America Special Paper 88, p. 597-617.
- Seni, S. J., and Jackson, M. P. A., in preparation, Sedimentary record of Cretaceous to Tertiary salt movement in the East Texas Basin: the key to patterns and rates of salt flow: The University of Texas at Austin, Bureau of Economic Geology.
- Seni, S. J., and Kreitler, C. W., 1981, Evolution of the East Texas Basin, *in* Kreitler, C. W., and others, Geology and geohydrology of the East Texas Basin: a report on the progress of nuclear waste isolation feasibility studies (1980): The University of Texas at Austin, Bureau of Economic Geology Geological Circular 81-7, p. 12-20.
- Smith, C. S., 1948, Grain phases and interfaces: an interpretation of microstructure: Transactions of the American Institute of Mining and Metallurgical Engineers, v. 175, p. 15-51.
- Spry, A., 1969, Metamorphic textures: New York, Pergamon, 350 p.
- Stuart, M., 1931, A contribution to "salt dome" geochemistry: Institute of Petroleum Technology Journal, v. 17, p. 338-345.
- Taylor, R. E., 1938, Origin of the cap rock of Louisiana salt domes: Louisiana Geological Survey Bulletin 11, 191 p.
- Teas, L. P., 1931, Hockley salt shaft, Harris County, Texas: American Association of Petroleum Geologists Bulletin, v. 15, no. 4, p. 465-469.
- Van der Gracht, W. A. J. M., 1925, The structure of salt domes of northwest Europe as revealed in salt mines: American Association of Petroleum Geologists Bulletin, v. 9, no. 2, p. 326-330.
- Vaughan, F. E., 1925, The Five Islands, Louisiana: American Association of Petroleum Geologists Bulletin, v. 9, no. 4, p. 756-797.
- Vernon, R. H., 1970, Comparative grain-boundary studies of some basic and ultrabasic granulites, nodules and cumulates: Scottish Journal of Geology, v. 6, no. 4, p. 337-351.
- _____, 1976, Metamorphic processes: London, Allen and Unwin, 243 p.
- Walker, C. W., 1974, Nature and origin of caprock overlying Gulf Coast domes, *in* Coogan, A. H., ed., Fourth symposium on salt: Cleveland, Ohio, Northern Ohio Geological Society, p. 169-195.
- _____, 1976, Origin of Gulf Coast salt-dome cap rock: American Association of Petroleum Geologists Bulletin, v. 60, no. 12, p. 2162-2166.
- Wendlandt, E. A., and Knebel, G. M., 1936, Mount Sylvan Dome, Smith County, Texas, *in* Barton, D. C., and Sawtelle, G., eds., Gulf Coast oil fields: Tulsa, American Association of Petroleum Geologists, p. 1041-1049.

APPENDIX

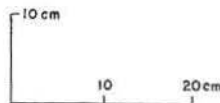
Oakwood Salt-Core Log

Project name: GCSD-Texas
 Project number: MV9620.20
 Location: Oakwood Dome, Freestone-Leon County
 Well number: TOG-1
 Date commenced: 9-27-79
 Date completed: 11-7-79
 Total well depth: 411.8 m (1351 ft)
 Net thickness of rock salt: 57.3 m (188 ft)

Explanation

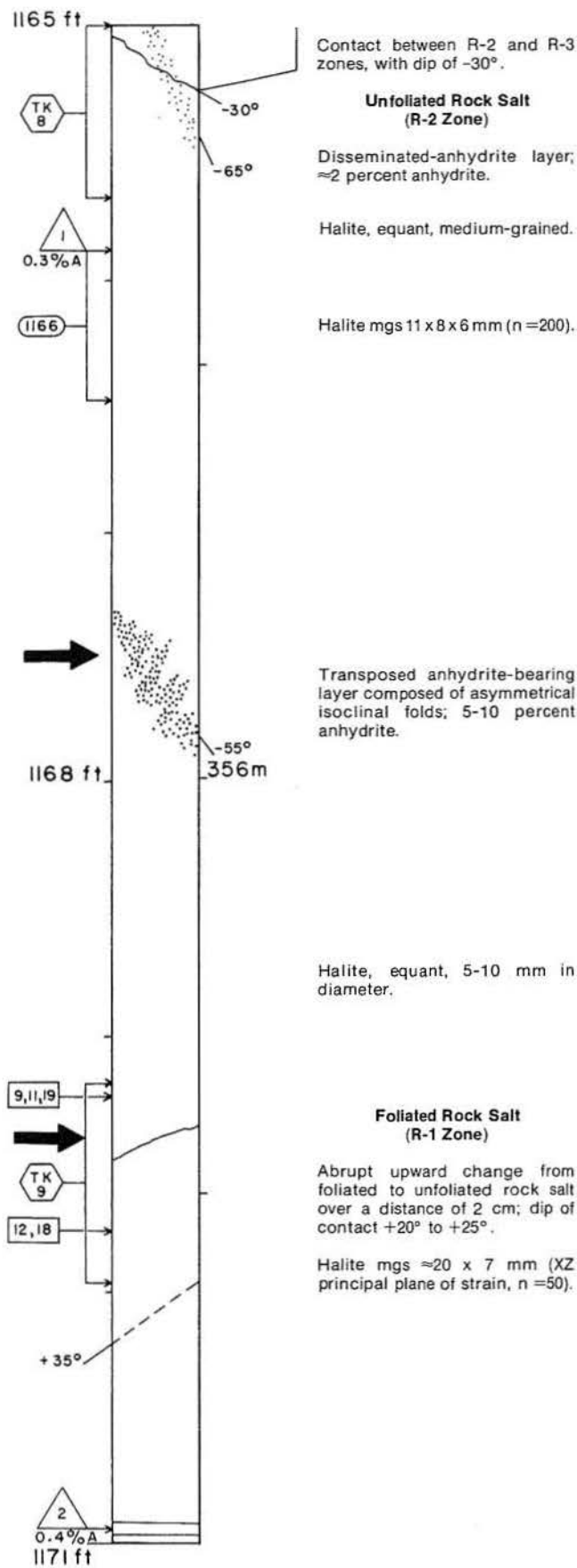
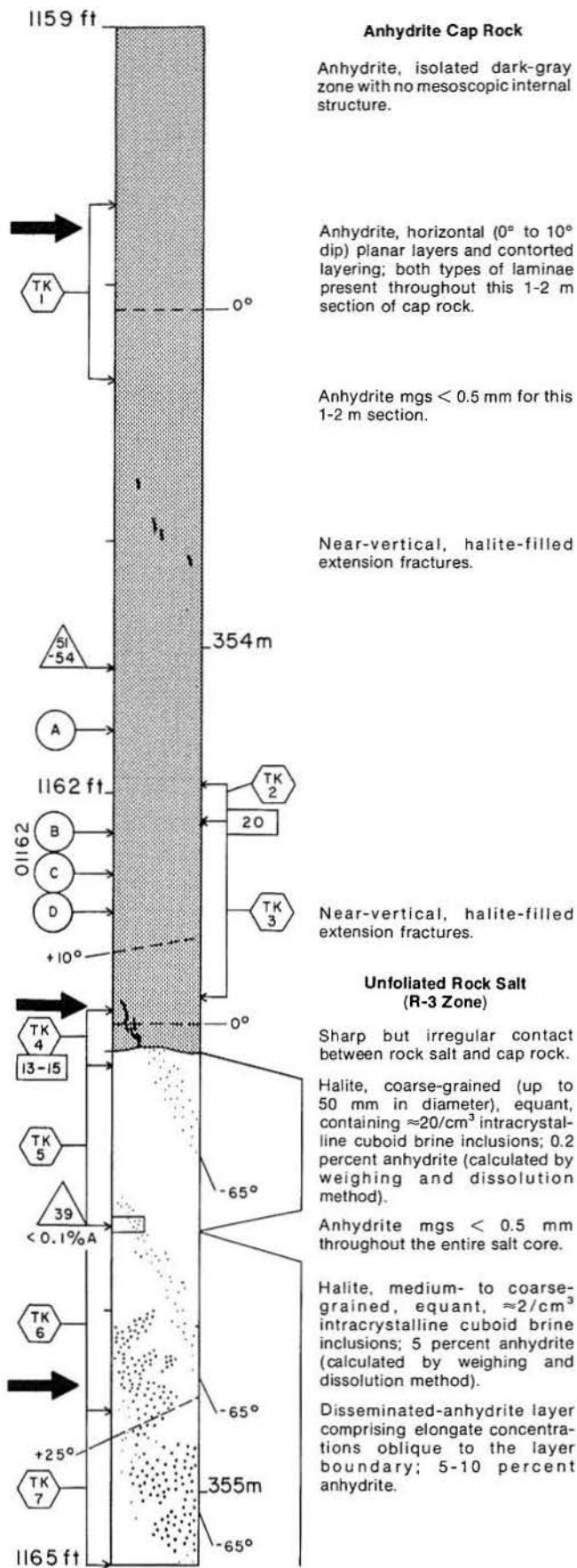
-  Detailed description in text
-  Location and number of thin section (< 1 mm thick)
-  Location and number of thick section (1-10 mm thick)
-  Location and number of sample used for geochemical analysis; exact location and orientation of sample shown on core profile; percentage anhydrite given below triangle
-  Location and number of sample for strain analysis
-  Location and number of plugs for magnetic anisotropy measurements
-  Missing core interval
-  Dip of foliation
-  Dip of contact, anhydrite layer or disseminated anhydrite
- n=50 Number of grains measured for grain-size determination (using only grains clearly visible to the naked eye)
- n=200 Number of grains measured for grain-size determination from strain analysis data (x 10 magnification)
- mgs Mean grain size

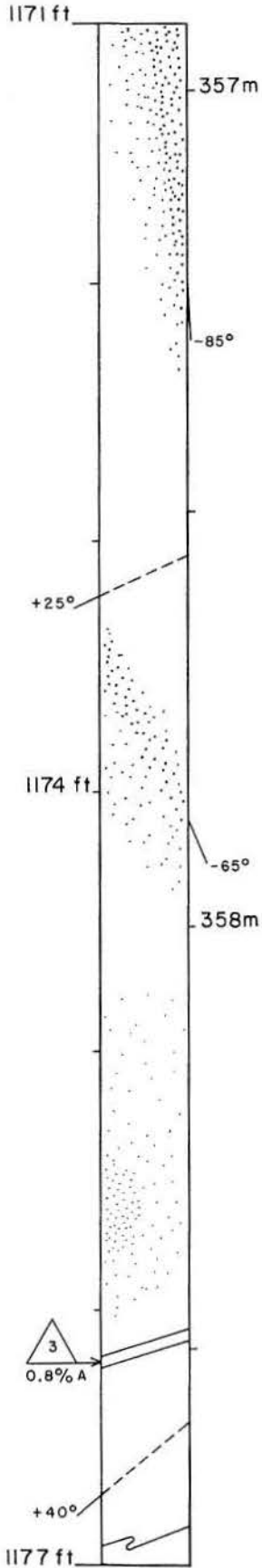
Vertical and horizontal scale:



Halite grain sizes: fine grained < 6 mm
 medium grained 6-20 mm
 coarse grained 21-50 mm

Pure rock salt contains < 1 percent impurities



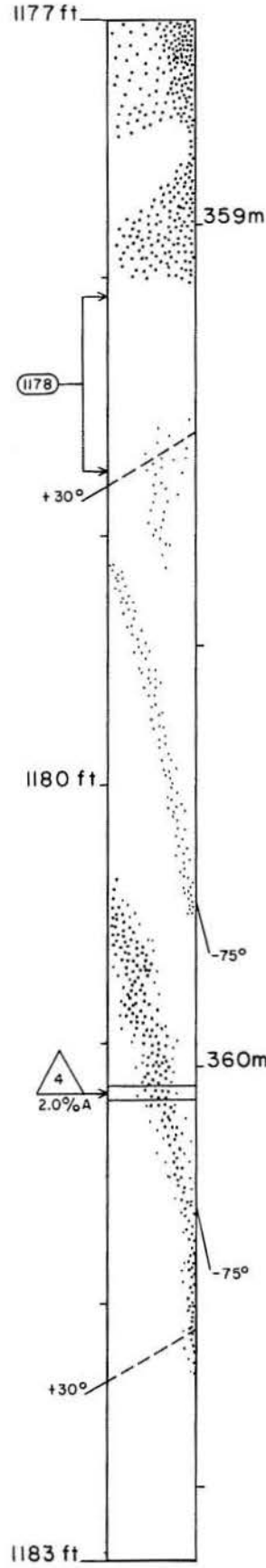


Disseminated-anhydrite layer; 2-5 percent anhydrite; dark concentrations along halite grain boundaries due to some preferred location of anhydrite.

Halite mgs $\approx 20 \times 7$ mm (XZ plane).

Disseminated-anhydrite layer (2-5 percent).

Disseminated anhydrite (≈ 2 percent); orientation not evident.



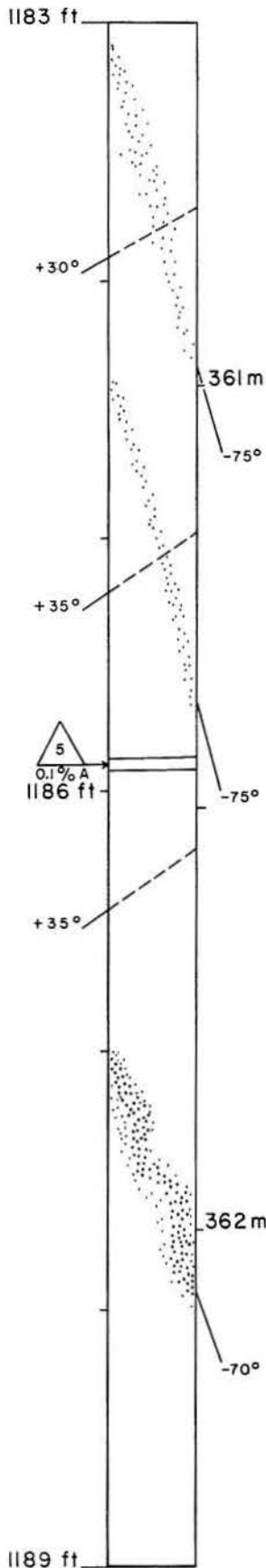
Disseminated anhydrite (5-10 percent); orientation not evident.

Indistinct, disseminated anhydrite (≈ 2 percent); halite mgs $\approx 15 \times 6$ mm (XZ plane).

Indistinct, disseminated-anhydrite layer; ≈ 2 percent anhydrite.

Disseminated-anhydrite layer with mesoscopic folds; 5-10 percent anhydrite.

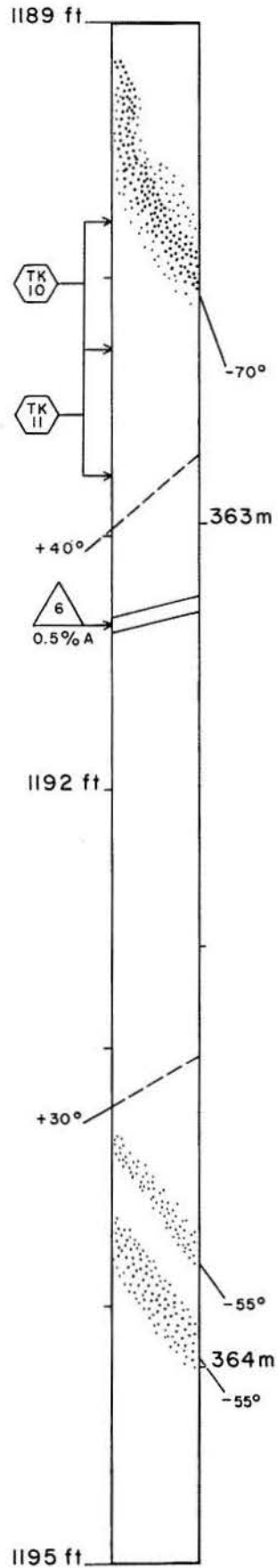
Dip of layer steepens to near vertical.



Indistinct, disseminated-anhydrite layer; ≈ 2 percent anhydrite.

Indistinct, disseminated-anhydrite layer; ≈ 2 percent anhydrite.

Disseminated-anhydrite layer with mesoscopic folds; 5-10 percent anhydrite.

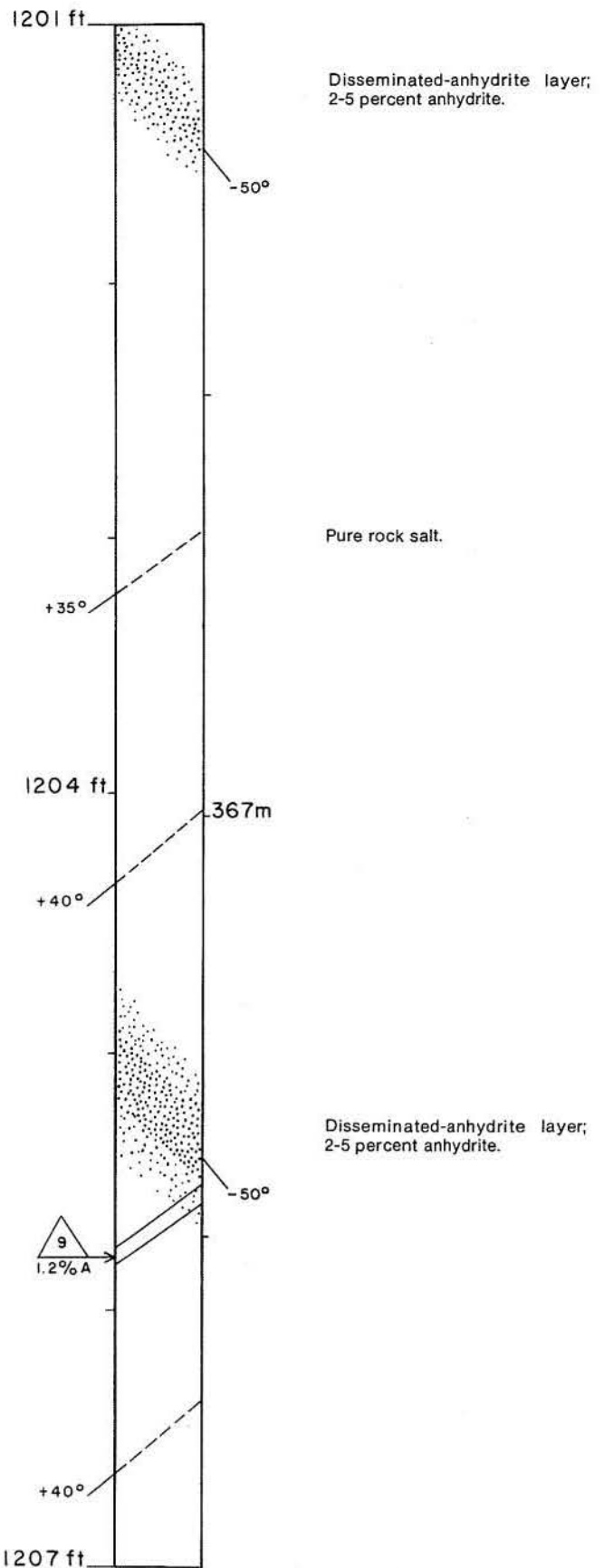
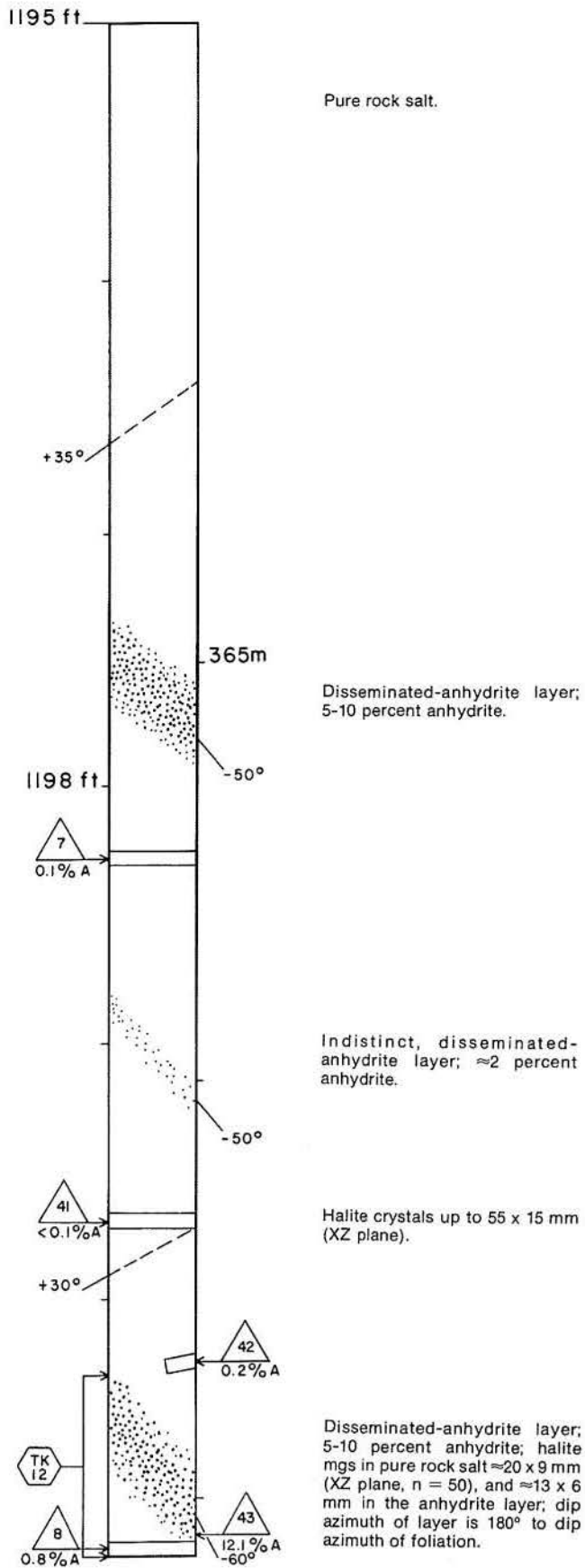


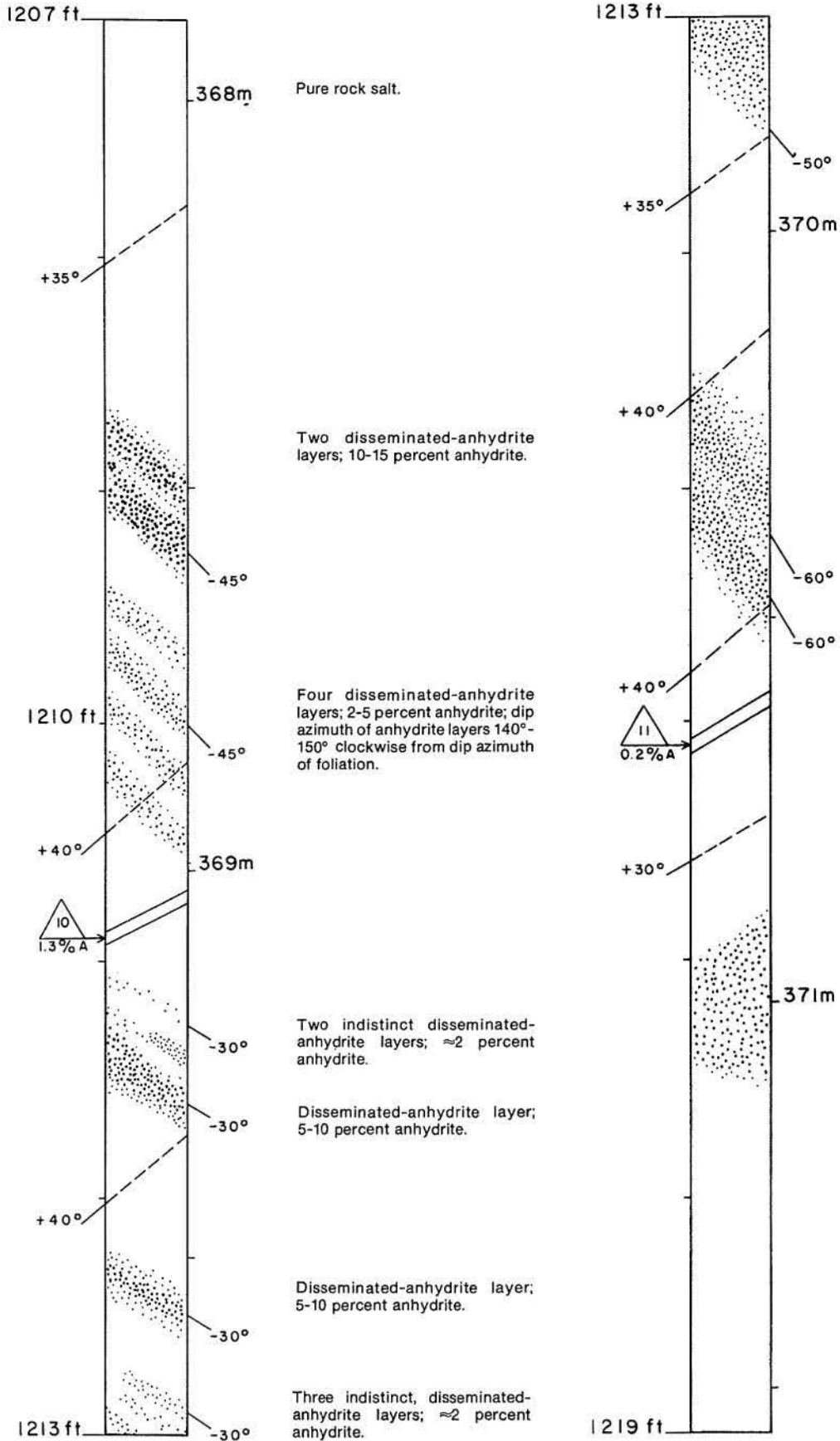
Disseminated-anhydrite layer with mesoscopic folds; 5-10 percent anhydrite; halite mgs $\approx 25 \times 9$ mm in pure rock salt (XZ plane), $\approx 18 \times 7$ mm adjacent to the layer, and $\approx 14 \times 5$ mm within the layering ($n = 50$ for each calculation).

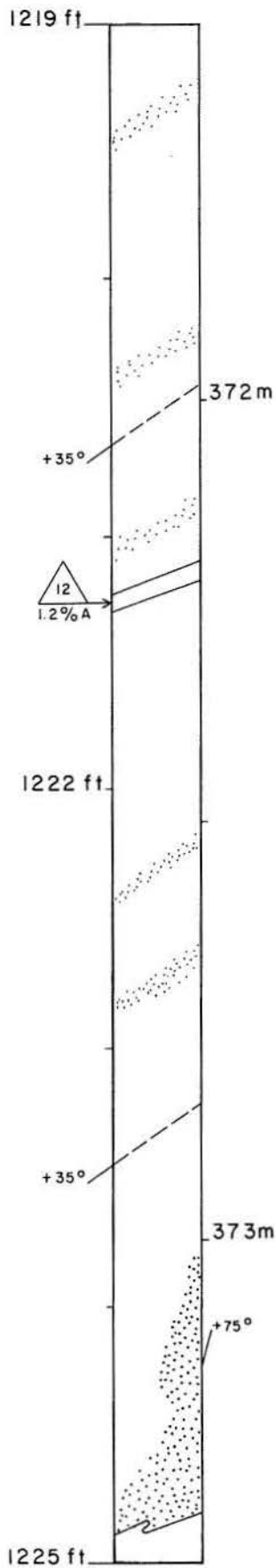
Pure rock salt.

Indistinct, disseminated-anhydrite layer; ≈ 2 percent anhydrite.

Disseminated-anhydrite layer; 2-5 percent anhydrite.







Indistinct, disseminated-anhydrite layer parallel to foliation; ≈2 percent anhydrite.

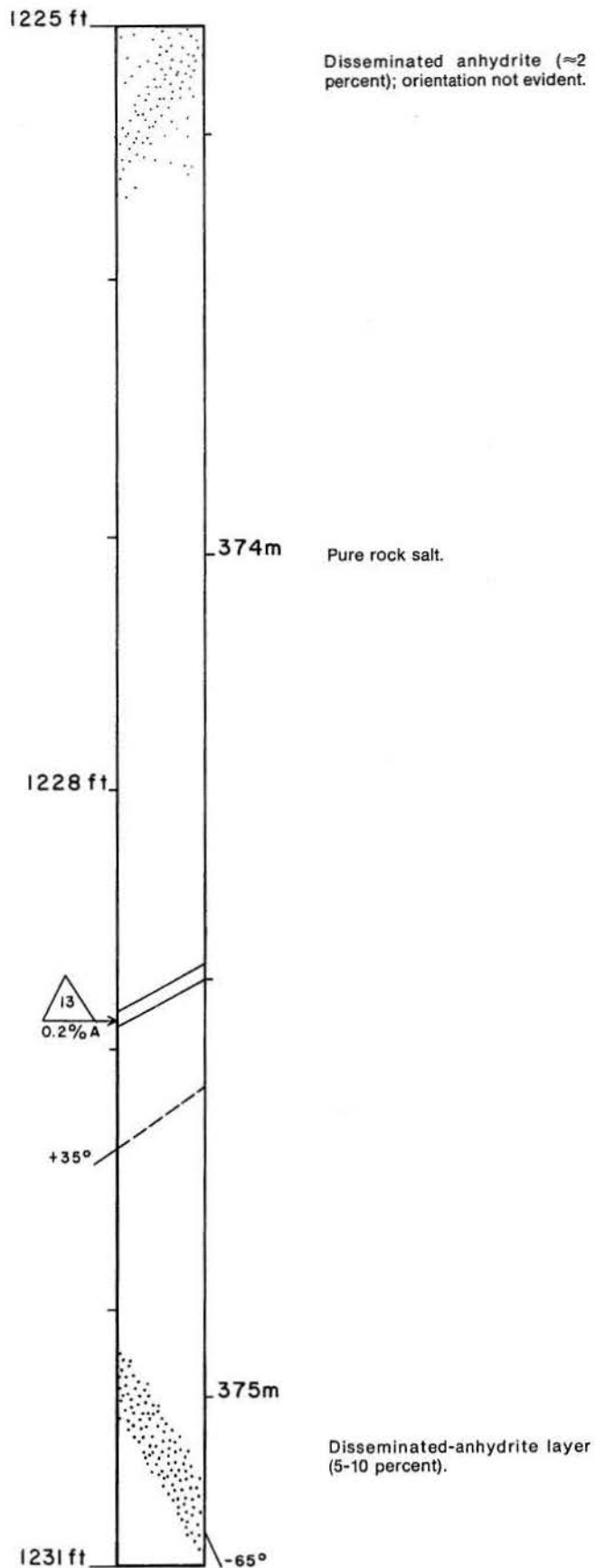
Indistinct, disseminated-anhydrite layer parallel to foliation; ≈2 percent anhydrite.

Indistinct, disseminated-anhydrite layer parallel to foliation; ≈2 percent anhydrite.

Two indistinct, disseminated-anhydrite layers parallel to foliation; ≈2 percent anhydrite.

Disseminated anhydrite (5-10 percent); dark coloration along halite grain boundaries.

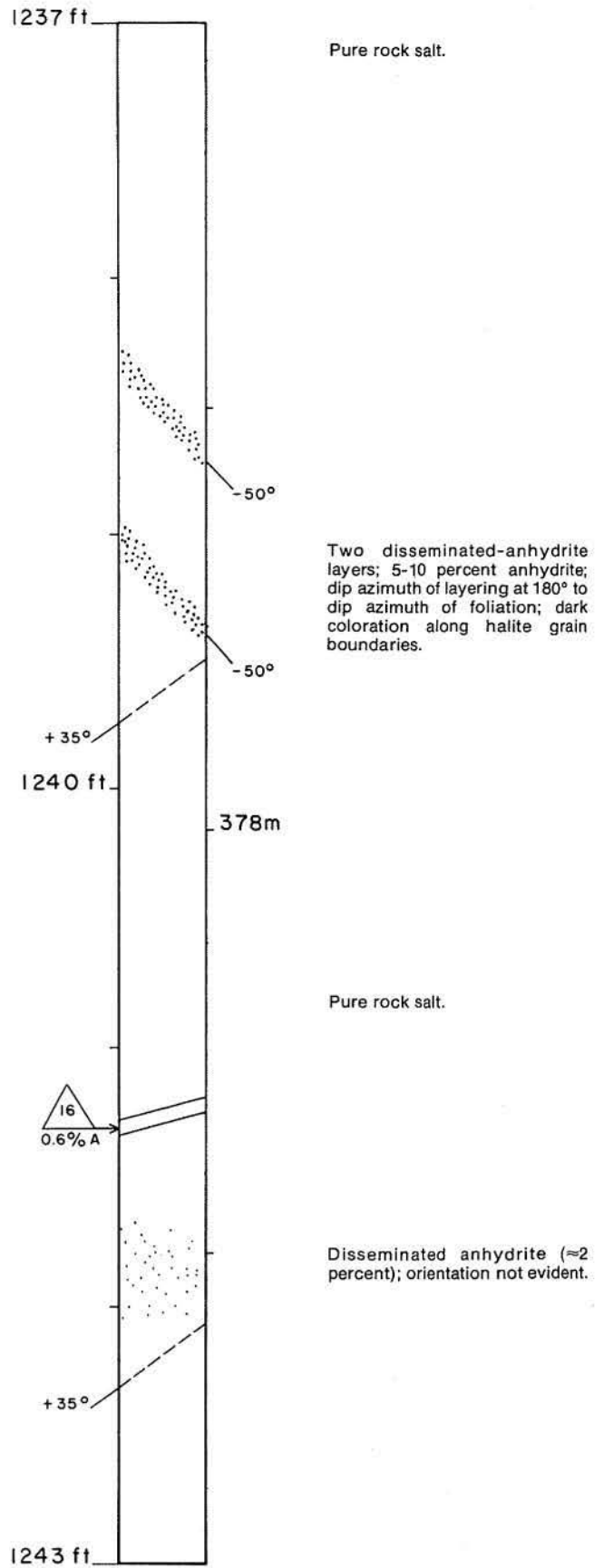
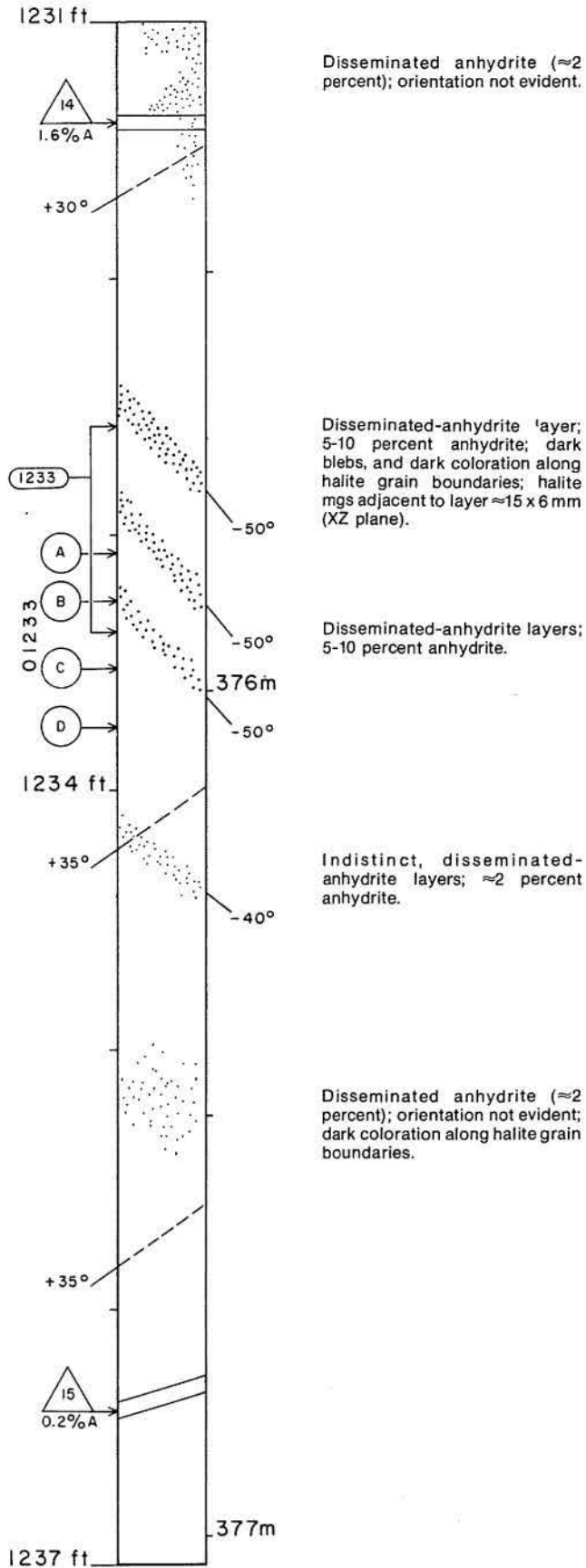
5 cm of core missing.

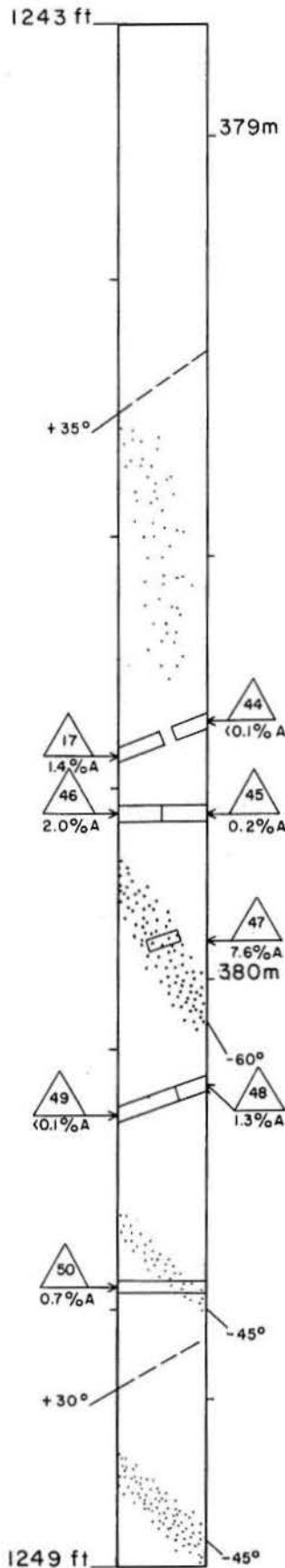


Disseminated anhydrite (≈2 percent); orientation not evident.

Pure rock salt.

Disseminated-anhydrite layer (5-10 percent).





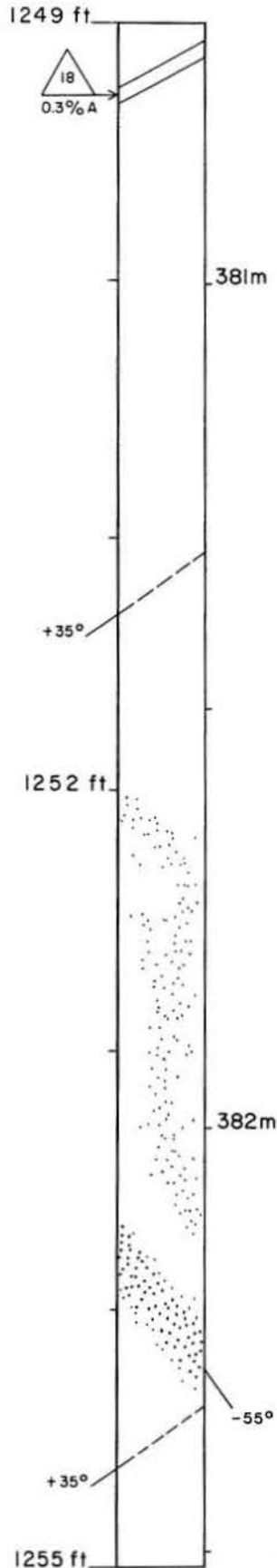
Pure rock salt.

Disseminated anhydrite (≈ 2 percent); orientation not evident.

Disseminated-anhydrite layer, 5-10 percent anhydrite, dark blebs, and dark coloration along halite grain boundaries; dip azimuth of layering 195° clockwise from dip azimuth of foliation.

Disseminated-anhydrite layer; ≈ 2 percent anhydrite.

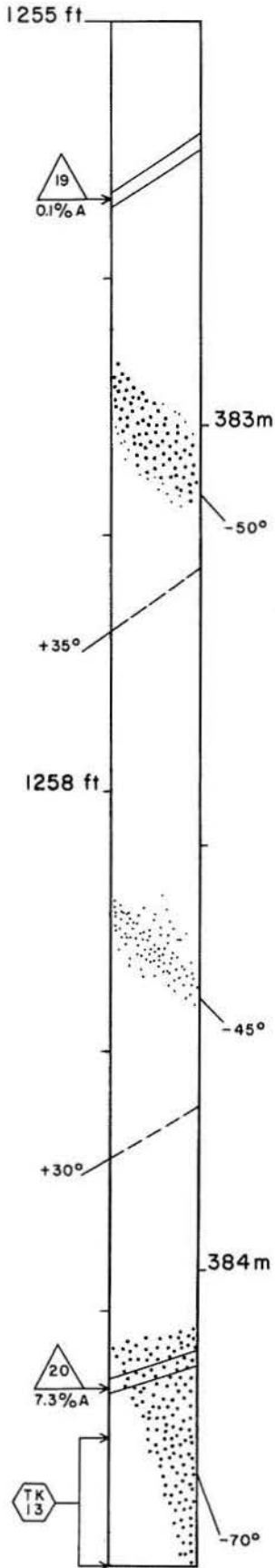
Disseminated anhydrite (≈ 2 percent); dark coloration along halite grain boundaries.



Pure rock salt.

Indistinct, disseminated anhydrite (≈ 2 percent); may represent a folded layer.

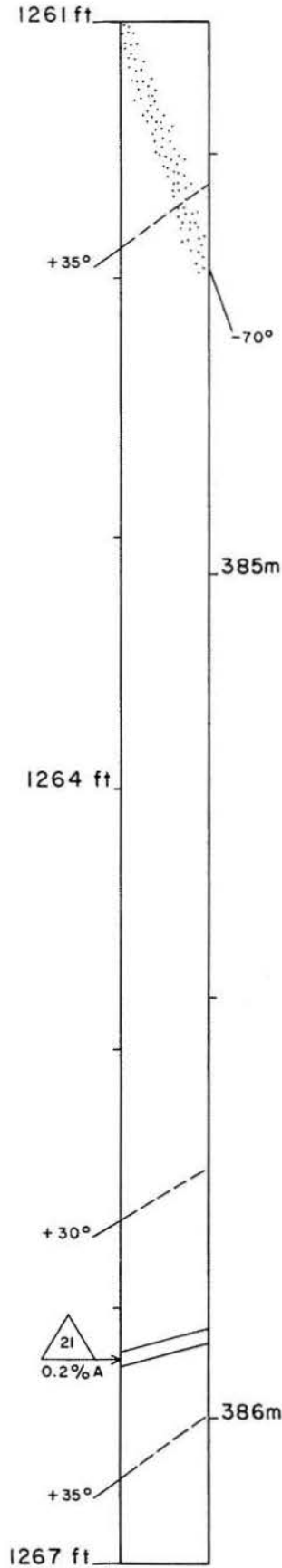
Disseminated-anhydrite layer, 5-10 percent anhydrite; dark coloration along halite grain boundaries; dip azimuth of layer 165° clockwise from dip azimuth of foliation.



Disseminated-anhydrite layer; 5-10 percent anhydrite; dark coloration along halite grain boundaries; dip azimuth of layer 180° to dip azimuth of foliation.

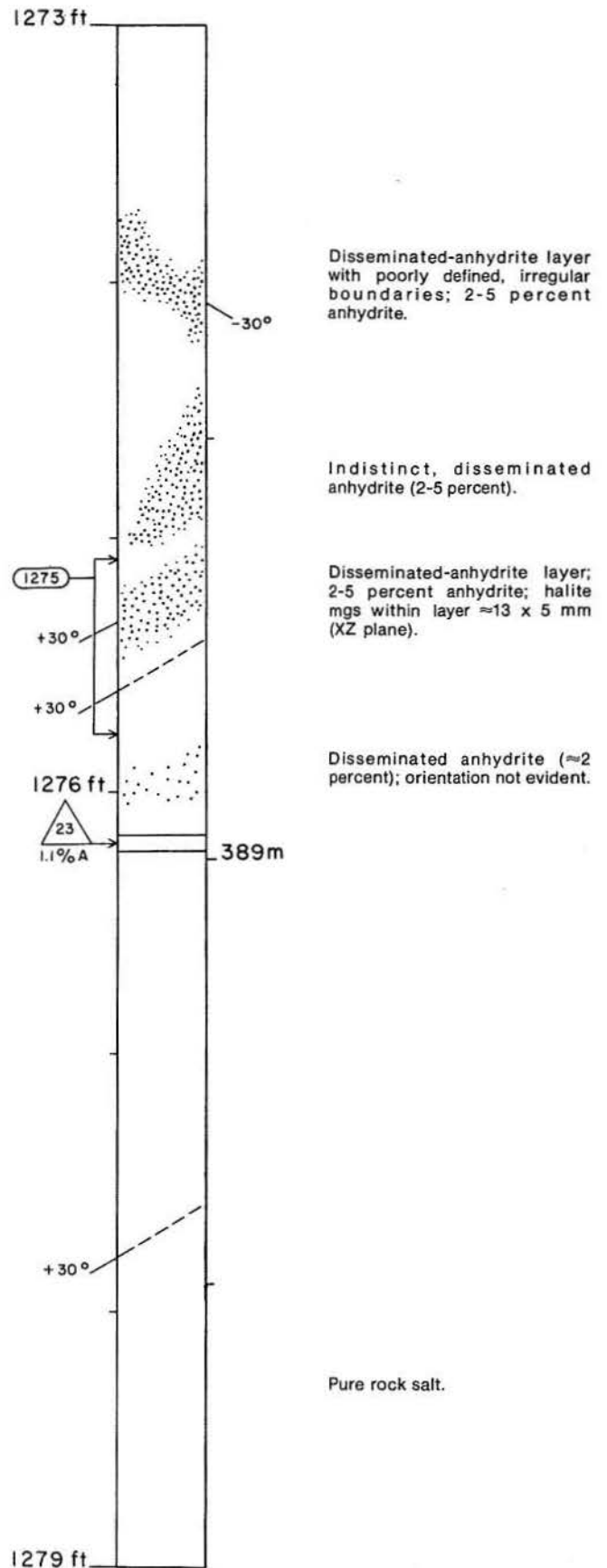
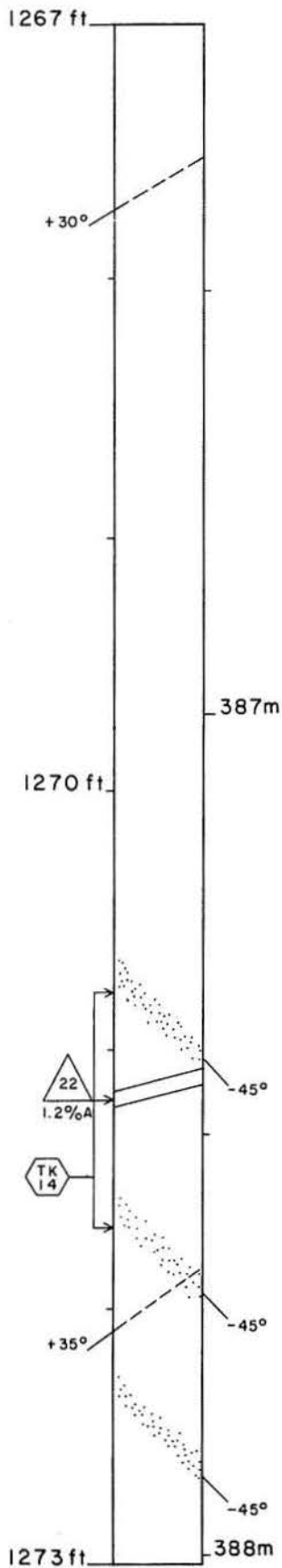
Indistinct, disseminated-anhydrite layer; ≈2 percent anhydrite; dark coloration along halite grain boundaries.

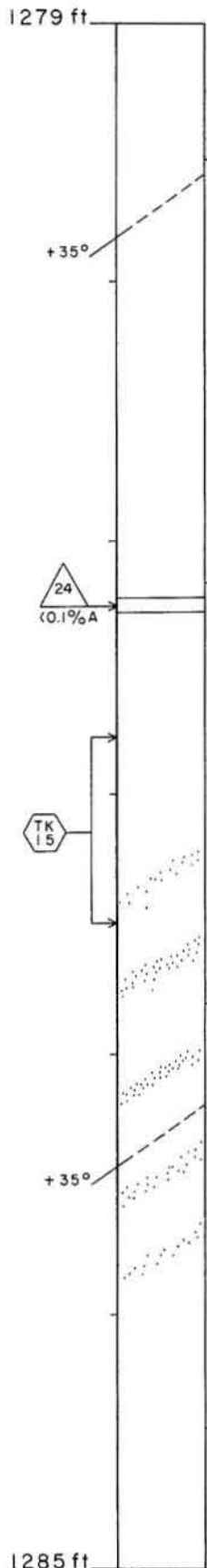
Disseminated anhydrite (5-10 percent).



Disseminated-anhydrite layer; ≈2 percent anhydrite.

Pure rock salt.





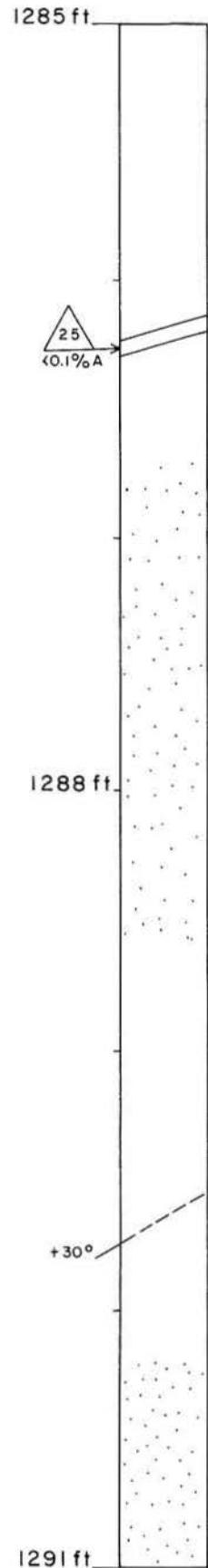
390m
Pure rock salt.

Halite mgs $\approx 25 \times 10$ mm (XZ plane), with a maximum in excess of 50×20 mm.

Disseminated-anhydrite layers (≈ 2 percent) parallel to foliation.

391m

Pure rock salt.



Pure rock salt.

392m

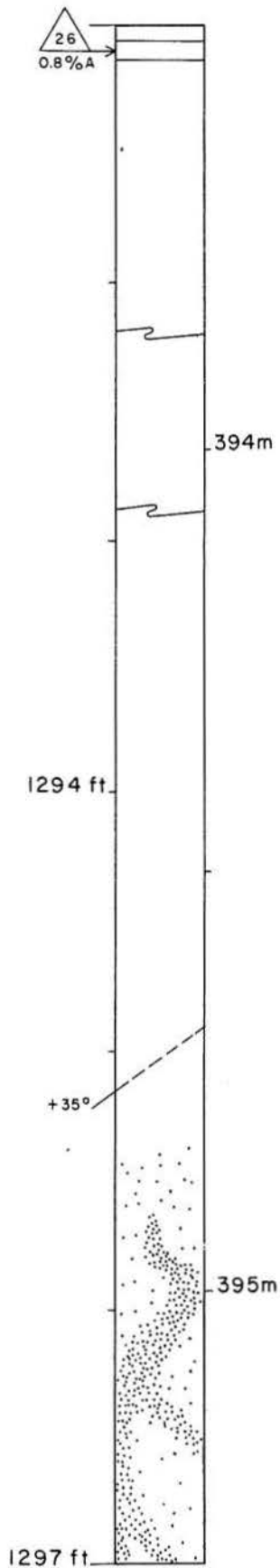
Disseminated anhydrite (≈ 2 percent) from 392.20 m to 392.75 m; orientation not evident.

1288 ft

Pure rock salt.

393m

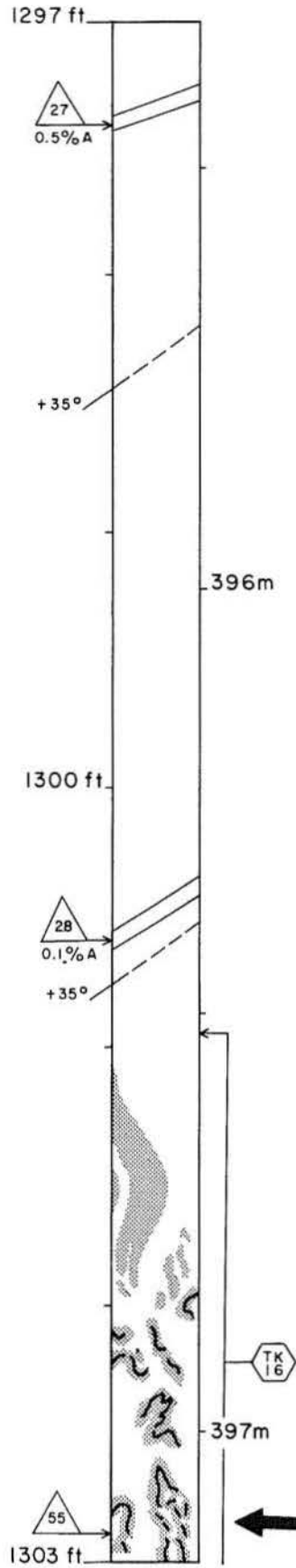
Disseminated anhydrite (≈ 2 percent) from 393.25 m to 393.50 m; orientation not evident.



Core from 393.85 m to 394.05 m missing.

Pure rock salt.

Disseminated anhydrite (5-10 percent); irregularly folded; core dark in reflected light from 394.85 m to 395.35 m due to ≈2 percent disseminated anhydrite.

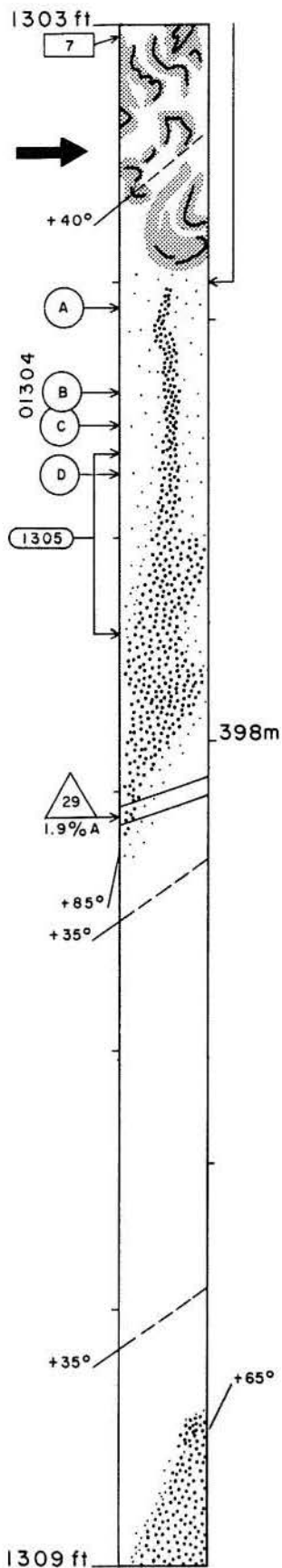


Thin zones of disseminated anhydrite (≈2 percent) parallel to foliation.

Pure rock salt.

Zone of microfolded, anhydrite-rich layering (50-70 percent anhydrite); black line represents finely disseminated intercrystalline organic matter.

← Refolded anhydrite-rich layers.



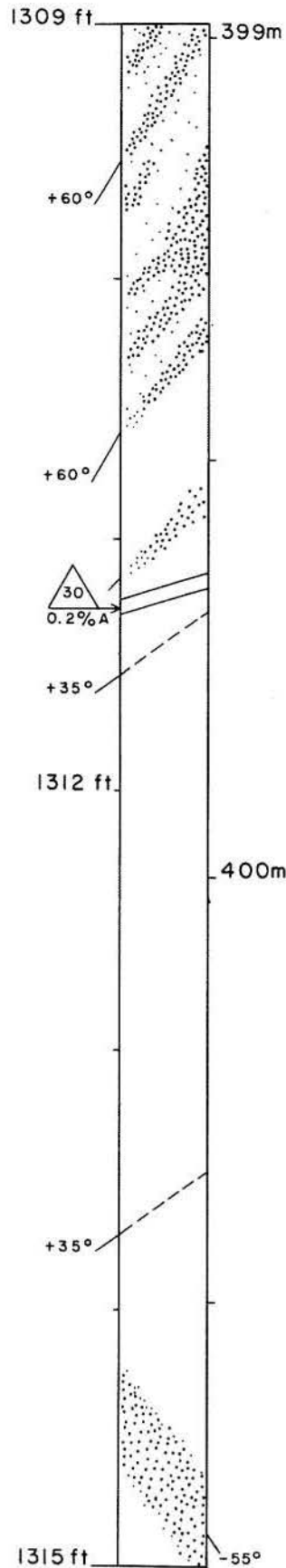
Refolded anhydrite-rich layers.

Lower limit of zone containing anhydrite-rich layers.

Disseminated-anhydrite layer; 10-15 percent anhydrite; halite mgs $\approx 11 \times 4$ mm (XZ plane, $n = 200$).

Pure rock salt.

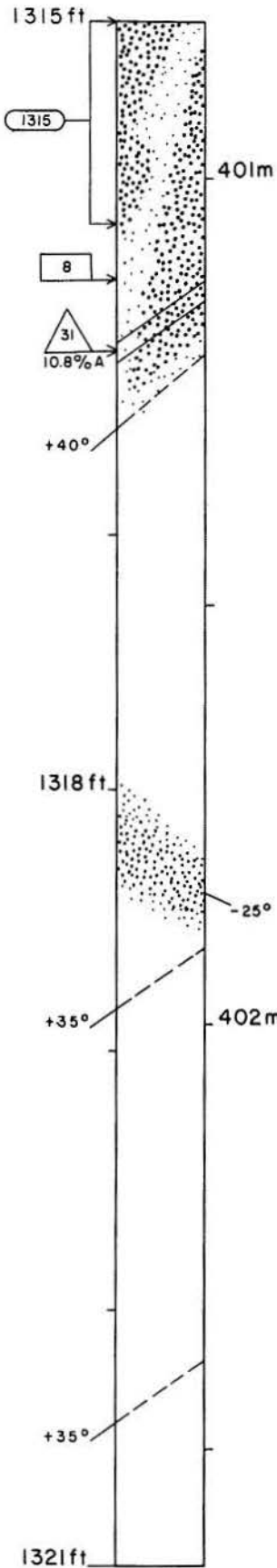
Disseminated-anhydrite layer; 10-15 percent anhydrite; dip azimuth of layer 35° clockwise from dip azimuth of foliation.



More than six disseminated-anhydrite layers; 5-10 percent anhydrite; some layers are discontinuous, others coalesce.

Pure rock salt.

Disseminated-anhydrite layer; 5-10 percent anhydrite; dip azimuth of layer 190° clockwise from dip azimuth of foliation.

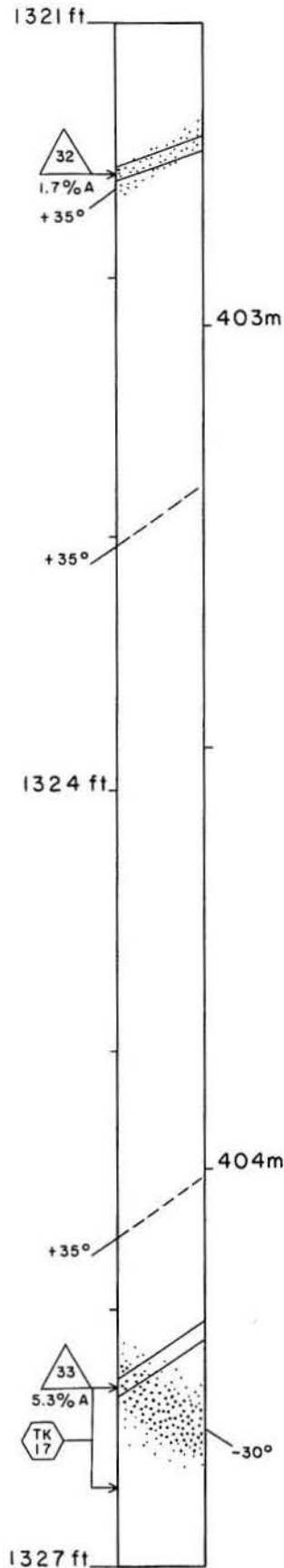


Two irregular disseminated-anhydrite layers; 10-15 percent anhydrite; halite mgs $\approx 12 \times 4$ mm (XZ plane, $n = 200$).

Pure rock salt.

Disseminated-anhydrite layer; 5-10 percent anhydrite.

Pure rock salt.

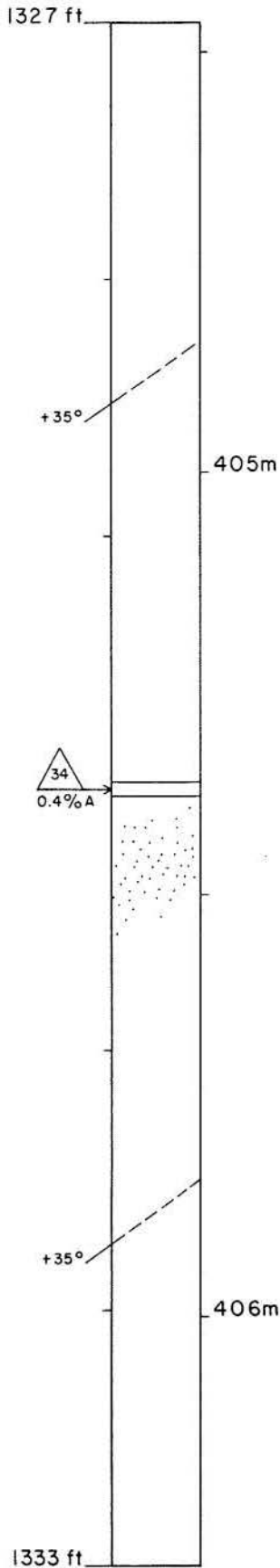


Indistinct, disseminated-anhydrite layer parallel to the foliation; ≈ 2 percent anhydrite.

Pure rock salt.

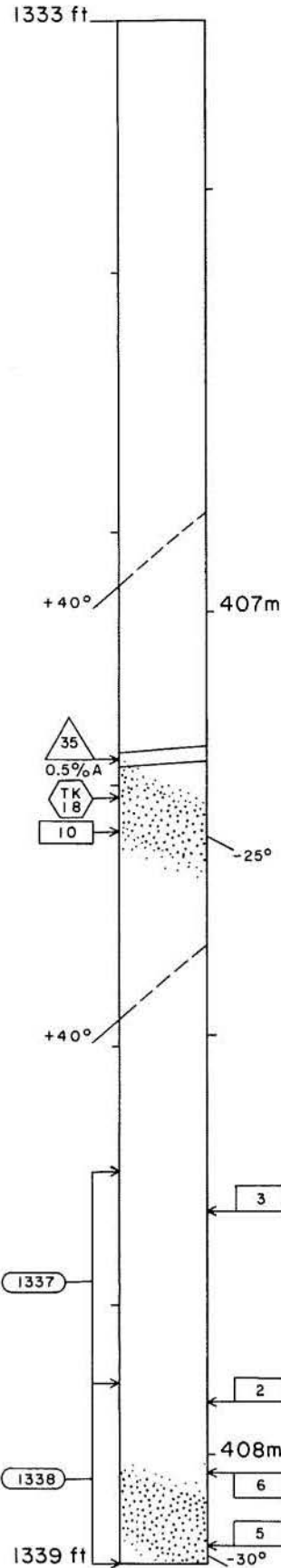
Pure rock salt.

Disseminated-anhydrite layer; 5-10 percent anhydrite.



Pure rock salt.

Disseminated anhydrite (≈2 percent).



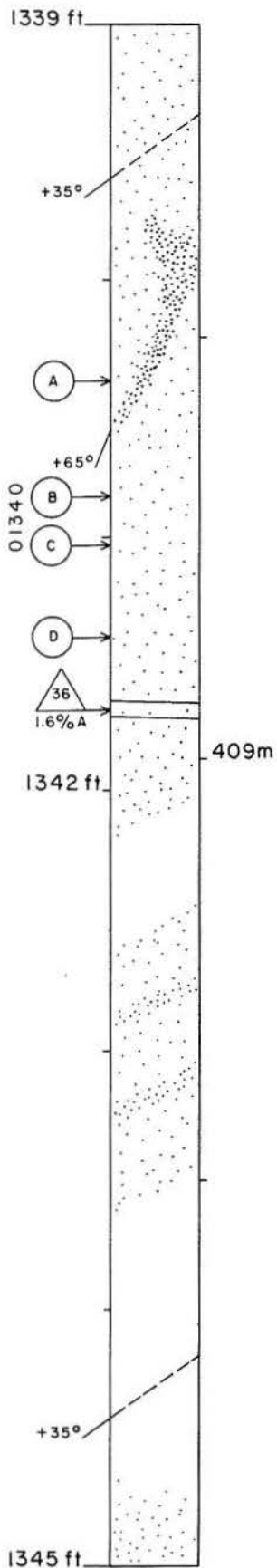
Pure rock salt.

Disseminated-anhydrite layer; 5-10 percent anhydrite; dark coloration along halite grain boundaries.

Pure rock salt.

Halite mgs in pure rock salt ≈19 x 6 mm (XZ plane, n = 100).

Disseminated-anhydrite layer; 5-10 percent anhydrite; layer thins to the left, the thinnest point representing the hinge of a fold; dark coloration along halite grain boundaries; halite mgs ≈11 x 14 mm (XZ plane, n = 100).

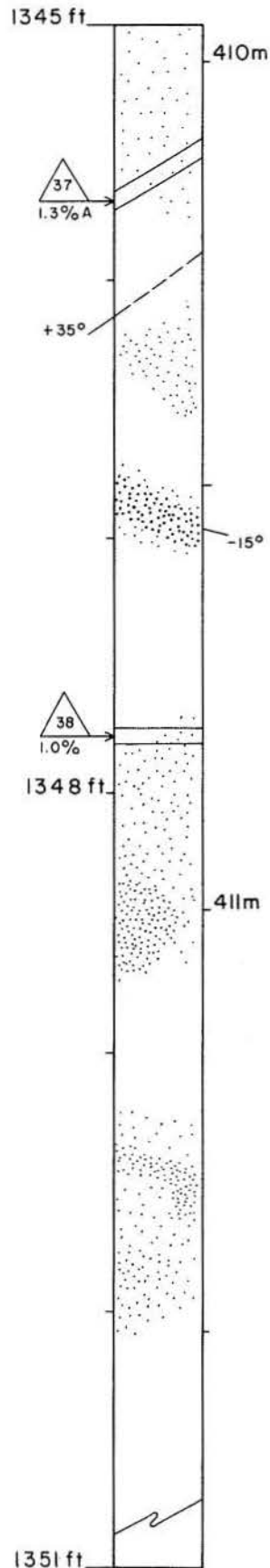


Indistinct, irregular, disseminated-anhydrite layer; 2-5 percent anhydrite.

Disseminated anhydrite (≈2 percent) throughout core from 408.10 m to 409.05 m.

Indistinct, disseminated anhydrite (≈2 percent), in layers parallel to foliation, from 409.20 m to 409.50 m.

Disseminated anhydrite (≈2 percent); orientation not evident.



Disseminated anhydrite (≈2 percent) from 409.95 m to 410.25 m.

Disseminated anhydrite (≈2 percent); orientation not evident.

Disseminated-anhydrite layer; 5-10 percent anhydrite.

Disseminated anhydrite (≈2 percent) from 410.80 m to 411.10 m; orientation not evident; dark coloration along halite grain boundaries.

Disseminated anhydrite (≈2 percent) from 411.25 m to 411.55 m; orientation not evident; dark coloration along halite grain boundaries.

5 cm of core missing.

End of hole.

